EXPLORING NEUROANATOMICAL AND MOLECULAR DISTINCTIONS IN A MATERNAL HYPOTHYROID MOUSE MODEL OF AUTISM SPECTRUM DISORDER

Ronan Tynan BSc (Hons), MSc.

A thesis submitted for the degree:

Doctor of Philosophy

University of Suffolk

School of Engineering, Arts, Science & Technology (EAST)

Submission Date: March 2024

Abstract

This thesis delves into the potential neuroanatomical and molecular characteristics of a maternal hypothyroid model of autism spectrum disorder (ASD) and compares them to those of control mice. We utilise advanced imaging techniques, such as X-absorption micro computed tomography (μCT) scanning and immunohistochemistry (IHC) analysis. Our focus is on examining the effects of maternal hypothyroidism, which is induced by a pharmacological treatment involving 0.1% Methimazole (MMI) in drinking water, administered from the start of gestation (E0) until the 13.5th day of embryonic development (E13.5). Notably, the offspring of MMI-treated mothers exhibit behavioural characteristics associated with autism during neurodevelopment in a sexually dimorphic manner.

Chapter 2 focuses on the use of Micro-computed tomography (μCT) to assess large white matter structures such as the corpus callosum (CC) and fornix, and examines the deep cerebellar nuclei (DCN). However, the findings were inconclusive, with no observable difference between control and MMI-treated mice, highlighting the complex relationship between maternal thyroid function and ASD.

Chapter 3 delves into the molecular landscape of prenatal (E16.5) transient hypothyroid mouse brains. We detected significant changes in T-box, brain, 1 (TBR1) staining of the fastigial nucleus, and RAR-related orphan receptor alpha (RoRα) staining of Purkinje cells. These findings suggest a role for early rhombic lip lineage formation in the role of thyroid hormones (THs) in ASD.

Chapter 4 extends the molecular investigations of juveniles. P30 transient hypothyroid mouse brains. Contrary to expectations, no significant enduring molecular changes were observed, suggesting a differing underlying reason for the observed behavioural changes in the model.

These results demonstrate the complex links between maternal thyroid status and early cerebellar development that may lead to neurodevelopmental disorders such as ASD. This study enhances our understanding of the network of genes potentially involved in ASD and TH disruption, indicating a possible link between THs, ASD-associated gene expression, and neurodevelopment.

TABLE OF CONTENTS

List of Figures and Tables

List of Abbreviations

Atoh1 Atonal1

ASD Autism Spectrum Disorder

BBB Blood-brain barrier

CNS Central nervous system

CC Corpus callosum

Dio1 Type 1 deiodinase

Dio2 Type 2 deiodinase

Dio3 Type 3 deiodinase

DCN Deep cerebellar Nuclei

E1, E2, E3, … embryonic days 1, 2, 3, …

EGL External granule layer

fr Fasciculus retroflex

FMRI Functional magnetic resonance imaging

HPT Hypothalamic-pituitary-thyroid

IHC Immunohistochemistry

IRD Inner ring deiodination

ITGB3 Integrin β3

mt Mammillothalamic tract

MD Mediodorsal thalamic nucleus

µCT Microcomputed tomography

MMI Methimazole

MCT8/10 Monocarboxylate transporters 8 and 10

NTZ Nuclear transitory zone

NAC Nucleus accumbens

OATP1C1 Organic anion-transporting polypeptide 1C1

ORD Outer ring deiodination

PAX6 Paired Box 6

PTA Phosphotungstic acid

PBDE Polybrominated diphenyl ether

PCBs Polychlorinated biphenyls

P30 Postnatal day 30

PFC Prefrontal cortex

PTU Propylthiouracil

PCs Purkinje cells

RR Recurrence risk

RELN- Reelin

RL Rhombic lip

RoRα RAR-related orphan receptor alpha

SFARI Simons Foundation Autism Research Initiative

T3 Triiodothyronine

T4 Thyroxine

TBR1 T-box, brain, 1

TET3tet Methylcytosine dioxygenase 3 gene

TH Thyroid hormone

TR Thyroid hormone receptor

TSH Thyroid-stimulating hormone

TSC1 Tuberous sclerosis complex 1

VTA Ventral Tegmental: ventral tegmental area

VZ Ventricular zone

Acknowledgements

I would like to express my heartfelt gratitude to everyone who contributed to the completion of this thesis. This journey has been challenging, but the support and guidance I received along the way were invaluable.

Firstly, I would like to acknowledge Dr. Aida Rajic. Her initial belief in me and her academic and personal support during the early stages of this project were instrumental in setting the foundation for this work. I am also deeply grateful to Professor Nic Bury. His unwavering support throughout the project, his guidance during both the good times and the challenging ones, and his belief in my abilities have been invaluable. His role extended beyond that of a supervisor, providing mentorship and advice that was crucial in bringing this project to fruition. I would also like to thank Alistar Mathie, who stepped in to provide supervision during the completion stages of the project. His academic guidance was essential in bringing this project to a successful conclusion.

For their professional contributions and advice, I would like to thank Dr. Richard Wingate and his lab for providing the mouse models to make this project possible and the valuable and insightful discussions which aided in this project's direction. I would like to extend thanks to Dr. Svetlana Gretton and David Ling for the invaluable and limitless technical support provided throughout the years. Their ability to provide the affirmation I needed and help me focus when I was overthinking my decisions in the lab was truly appreciated. Lastly, I want to acknowledge the crucial role my parents have played in my academic journey. Their unwavering faith in me and their consistent support have been indispensable. I am constantly reminded of the fact that there are many individuals who are more talented but did not have the same opportunities due to the lack of the kind of support my family provided me. For this, I am profoundly grateful.

Covid statement

The Covid-19 pandemic has undeniably disrupted our research trajectory, particularly in our pursuit to comprehend the implications of transient maternal hypothyroidism. The following points encapsulate the key areas of our research that were affected:

1. **RNA-scope ISH Study**: The pandemic led to the loss of an RNA-scope ISH study on LHX-9 in embryonic mouse brain samples. This study was crucial for understanding the impact window of hypothyroidism during cerebellum development and investigating the role of the dentate nucleus.
2. **Chapter 4 Constraints and Lost Research Time**: The pandemic imposed severe time constraints, limiting the scope of Chapter 4 and resulting in a loss of six crucial months of research time. This significantly affected the ability to optimize and adjust the juvenile samples, restricting the understanding of sexual dimorphism in the sample group.
3. **Unavailability of Planned Experiments and Absence of Follow-up Experiments**:
   Several planned experiments and improvements, such as enhanced CT scans, became unfeasible due to the pandemic. Time restrictions also prevented the conduction of follow-up experiments based on initial findings and other research that emerged during the period, leading to assumptions rather than empirical conclusions.
4. **IHC Follow-up**: A follow-up experiment involving TBR2 was intended to allow investigation into potential changes in the interposed nucleus. This was expected to provide insights into whether the observed effects were confined to the output from the dentate nuclei or if juvenile social behaviour was a result of combined effects from multiple nuclei. There was also an interest in having another look at Reelin in an earlier model or, given the information gained from Purkinje data, in a more specific section focusing more on its role in granule cells and Purkinje migration. However, it remained completely unaffected in unpublished cortical data, so it seemed undisputed unless local to the cerebellum.

Chapter 1: Introduction and Literature Review

1.1 THYROID HORMONE SECRETION AND METABOLISM

TH is a steroid that is important for normal brain development, such as neuron development and the formation of neurotransmitters, with the maternal thyroid playing an important role (de Escobar, Obregón et al. 2004, Patel, Landers et al. 2011). Thyroid receptors are present in the foetal brain beginning in the first trimester of pregnancy, with the expression of the isoforms TRβ1 and TRα1 starting as early as the 8th week of gestation in humans. Despite this, the foetal thyroid gland does not reach maturity until late in the first trimester, with the active section of TH only commencing after 18 weeks in humans and beginning in mice around E16.5 (Iskaros, Pickard et al. 2000, Fernández, López-Márquez et al. 2015).The TH plays a key role in overall development, including helping normal brain development. Disruption of normal TH function has been shown to lead to many neurodevelopmental disorders, such as impaired cognition, behavioural issues, and abnormal cortical morphology(Román, Ghassabian et al. 2013, Päkkilä, Männistö et al. 2014, Lischinsky, Skocic et al. 2016).

The production of TH is regulated by the hypothalamic–pituitary–thyroid (HPT) axis. The purpose of the HPT axis is to control the levels of TH in circulation. TH production starts at the hypothalamus, which secretes the tripeptide Thyrotropin-releasing hormone (TRH) (Zoeller, Tan et al. 2007). TRH is then transported to the anterior pituitary, where it binds to a G-coupled protein receptor in a thyroid-stimulating hormone (TSH)-producing cell called a thyrotroph. G-coupled protein receptor binding in thyrotrophs allows for the activation of phospholipase C, the hydrolysis of Phosphatidylinositolphosphatidylinositol 4,5-bisphosphatef (PIP2) to Inositol triphosphate (IP3), the generation of Diglycerol (DAG) and the release of Ca++. This release of Ca++ then stimulates the release of TSH from thyrotroph cells(Shahid,

Ashraf et al. 2018). TSH is a heterodimer formed of an alpha subunit, which is common to other hormones, such as follicle-stimulating hormone, and the beta subunit, which is unique to TSH (Koibuchi and Yen 2016). TSH binds to G-coupled protein receptors called TSH receptors located primarily on the thyroid. This ligand binding increases the gene transcription of thyroglobulin and the sodium iodide symporter (NIS). Thyroglobulin is a TH precursor that forms Triodothyronine (T3) and Thyroxine (T4) when combined with iodine. The mechanism of action of anti-thyroid drugs such as MMI or Propylthiouracilpropylthiouracil (PTU) acts to prevent the iodination of thyroglobulin, preventing TH synthesis. The HPT axis is highly regulated, with internal feedback loops within the axis. As shown in Fig. 1.1, high serum levels of TH create negative feedback control over the release of TRH from the hypothalamus and TSH from the pituitary, allowing for optimal levels of TH at all times and overall homeostasis (Feldt-Rasmussen, Klose et al. 2018).

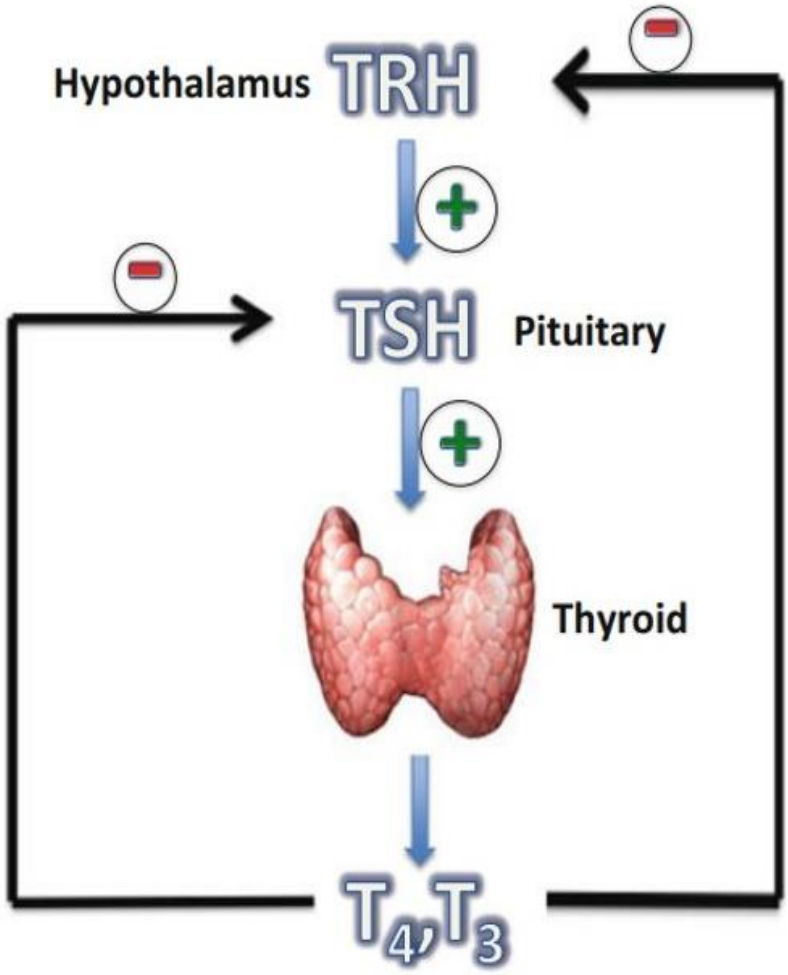

Figure 1-1 Regulation of the HPT axis:

High serum levels of T4 and T3 exert negative feedback effects on the release of TRH from the hypothalamus and TSH from the pituitary. This is mediated through the negative transcriptional regulation of genes for TSH and TRH by ligand-bound thyroid receptors (Koibuchi and Yen 2016).

TH is released from the thyroid gland in its inactive form, the prohormone T4, or its active form, T3. Approximately 95% of the TH released is T4, which allows for further regulation of TH activity downstream. TH is formed from two phenolic tyrosyl rings, which are then bound by iodine. The removal or addition of these iodine atoms determines the form of TH. Therefore, TH activity and binding are regulated by T3 levels and T3 creation through the deiodination of T4 by 3 iodothyronine deiodinases (Dio1, Dio2, Dio3). Deiodinases act through the removal of an iodine atom through outer ring deiodination (ORD) or from the inner tyrosyl ring by Dio1 and Dio3, causing inactivation through inner ring deiodination (IRD). ORD facilitates the conversion of T4 to T3, whereas IRD inactivates T4 to rT3 and T3 to T2 (Figure 1.2) (Bianco and Larsen 2005).

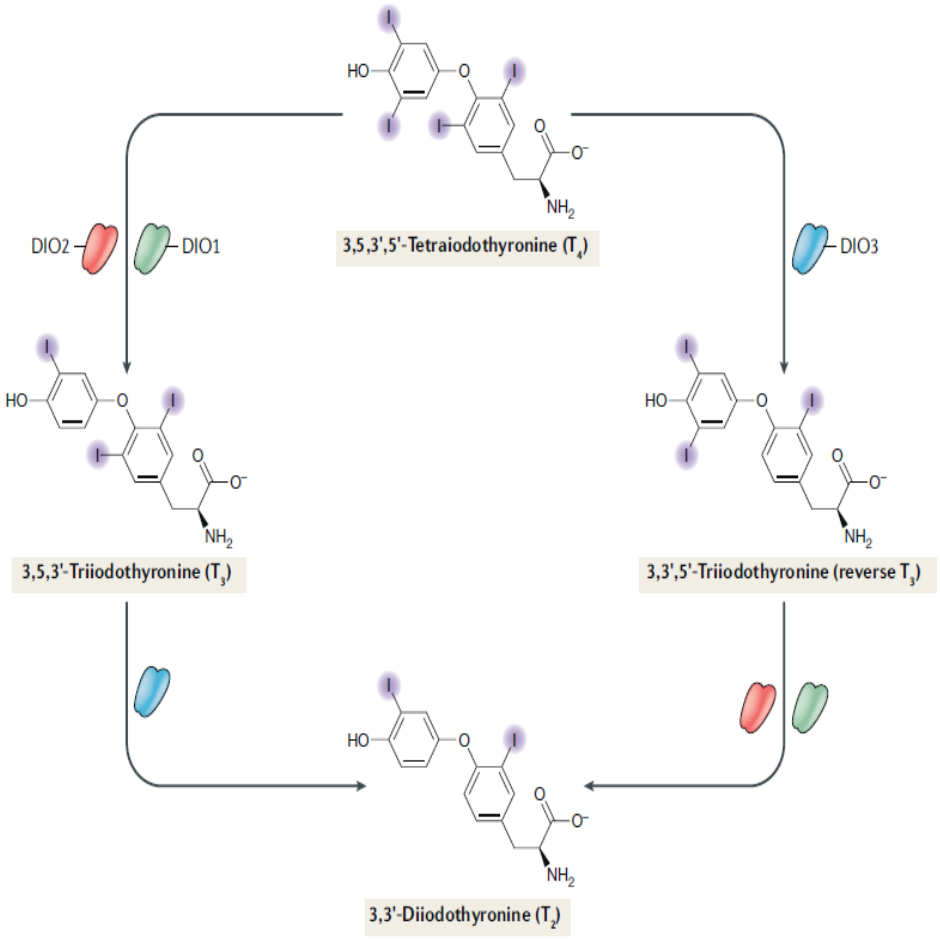

Figure 1-2 Effects of deiodinases on thyroid hormones:

T4 is modulated by either DIO1 or DIO2 to form T3 through the removal of an iodine atom from, the outer tyrosol ring. DIO 2 modulates T4 through the removal of an iodine atom from the inner tyrosol ring to form reverse T3. The removal of a second iodine atom from either T3 or reverse T3 converts it into the inactive T2 form of TH (Luongo, Dentice et al. 2019).

The conversion of T4 to T3 is facilitated by both DIO2 and DIO1; however, their affinities for T4 differ. At physiological concentrations, T4 acts as a better substrate for DIO2 than DIO1, with DIO1 requiring a much higher concentration of T4 (Luongo, Dentice et al. 2019). In the cerebellum, deiodinase activity primarily involves DIO2 and DIO3. Specifically, DIO2 (Type 2 deiodinase) activity is low during the late fetal stage and at birth but increases significantly during the first postnatal week. Moreover, type 1 deiodinase (DIO1) activity remains notably prominent in the cerebellum (Gereben, Zavacki et al. 2008, Barez-Lopez, Bosch-García et al. 2014). Together, both the HPT axis and regulation by deiodinases allow for control of the serum levels of T3 and T4, which can then be transported across the Blood–brain barrier (BBB) to the site of activation.

The transport of TH is an important regulator of TH circulation within the CNS as well as a regulator of foetal levels of TH during development. This includes the transport of TH across epithelial barriers such as the BBB or the placenta. Both the BBB and the placenta act as semipermeable barriers to separate either the brain in the case of the BBB or the foetus from the surrounding blood flow. Therefore, during pregnancy, TH transporters are essential for the movement of THs from the mother to the foetus and from foetal systemic circulation to the CNS.

The majority of TH is not free in circulation. Instead, a large amount is bound to carrier proteins such as mammalian-specific T4-binding globulin (TBG), albumin, and transthyretin (prealbumin, TTR) (McLean, Rank et al. 2017). TH that is bound to these carrier proteins is not available for uptake into cells, as only TH in free circulation is available for transport via membrane transporters. These membrane transporters include monocarboxylate transporters 8 and 10 (MCT8/10), organic anion-transporting polypeptide 1C1 (OATP1C1), and L-type amino acid transporters 1 and 2 (LAT1/2) (Heuer and Visser 2009).

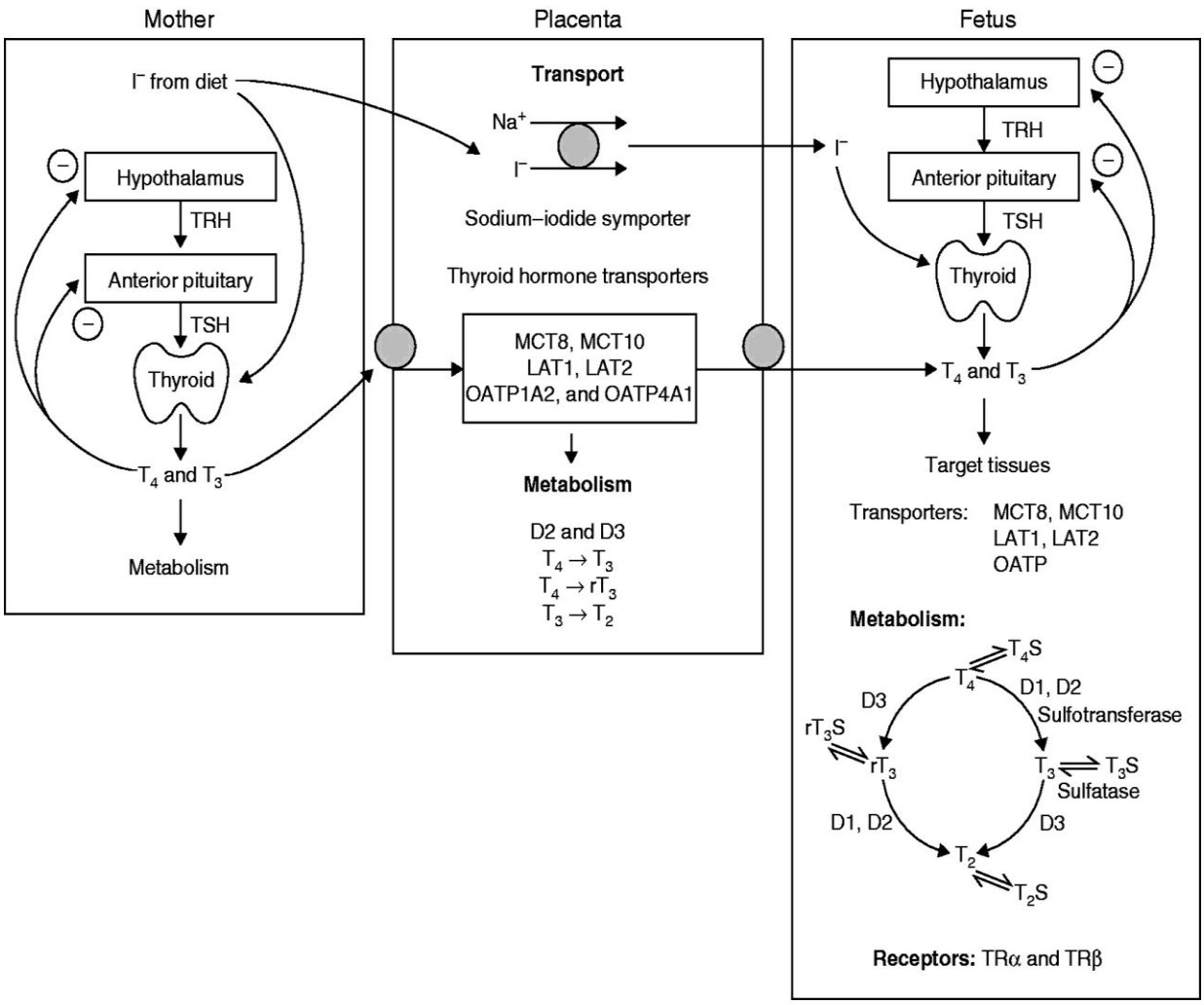

Figure 1-3 Factors affecting the bioavailability of thyroid hormones in the foetus, placenta, and mother. Maternal Synthesis: synthesis of T4 and T3 hormones in the mother, influenced by dietary intake and metabolic pathways. Transport Mechanisms: transport of these hormones via transporters, specifically MCT8 and OATP. Foetal Metabolism: Conversion of T4 into T3 in the foetus, mediated by deiodinases. (Forhead and Fowden 2014).

Cellular responses to TH vary and are mediated by its binding to a variety of receptors. Thyroid receptors belong to the nuclear hormone receptor superfamily type II in mammals, a family that contains TH receptors (TRα and β (RARα, β, and γ)) and Vitamin D receptor (VDR). TRs form heterodimers with RXR and, as such, bind to target DNA at sites called T3-response elements (TREs). Two genes are responsible for the coding of these receptors, *Thrα/THRA and Thrβ/THRB,* in mice and humans, respectively (Flamant, Baxter et al. 2006).

TR expression changes in a spatial–temporal fashion, with many tissues expressing multiple isoforms. During early brain development, the primary receptor expressed is TRα1, which is expressed in the cerebellum at E13.5 and the neocortex at E15.5. In later stages of development, such as the perinatal and postnatal periods, TRβ1 is expressed in specific neuronal populations, such as Purkinje cells and the hypothalamus (Bradley, Towle et al. 1992, Flamant, Gauthier et al. 2017).

TRs are ligand-regulated transcription factors that bind to TREs on target genes in the presence or absence of TH. In the absence of TH, TRs recruit corepressors and histone deacetylases, allowing them to cause transcriptional repression of the target gene. TH binding to the TR results in structural changes in the ligand-binding domain, making the binding of repressors less favourable and allowing for the recruitment of coactivators, therefore increasing transcriptional activation (Fig 2.5.3) (Koibuchi and Yen 2016).

Thyroid hormone receptors (TRs) play pivotal roles in regulating gene expression. They function by forming either homodimers or heterodimers with the Retinoid X receptor (RXR), and these dimers bind to specific Thyroid response elements (TREs) located in the promoter regions of target genes (Lazar 2003) (Barra, Velasco et al. 2004). The regulation of these genes by Thyroid hormones (THs) can be either positive or negative.

In positive regulation, the binding of THs to TRs acts as a switch, toggling between the repression and activation of gene transcription. In the absence of THs, unbound receptors recruit corepressors and histone deacetylases, which maintain chromatin in a compact state, leading to a decrease in gene transcription. However, when THs bind to TRs, they trigger a conformational change that displaces the corepressor complex and instead recruits transcriptional coactivators. These coactivators interact with various transcription factors and cofactors that possess histone acetyltransferase activity, altering the chromatin conformation to make the gene more accessible to the basal transcriptional machinery, thereby stimulating gene expression(Grøntved, Waterfall et al. 2015).

In contrast to the well-understood mechanism of positive regulation by THs, the mechanism of negative regulation remains elusive, with several models proposed. One such model suggests a switch from coactivator recruitment to corepressor recruitment on a ‘negative’ TRE upon the binding of THs(Ramadoss, Abraham et al. 2013). This intricate interplay between positive and negative regulation by TRs underscores their crucial role in maintaining metabolic balance in the body. Misregulation of these processes can lead to various thyroid disorders, highlighting the importance of understanding TR function(Bernal 2007).

However, not all the cellular activity of TH occurs through its binding to TRs. Cellular T3 is thought to activate secondary messengers such as calcium ions (Ca++) and cAMP (Cheng, Leonard et al. 2010). Indirect genomic actions can be mediated by the prohormone T4, which binds to the plasma membrane receptor integrin αvβ3 and can lead to changes in gene expression, resulting in cell proliferation and angiogenesis (Davis, Goglia et al. 2016). These effects are similar to those of traditional TR binding, suggesting a crossover between the direct and indirect genomic action of TH.

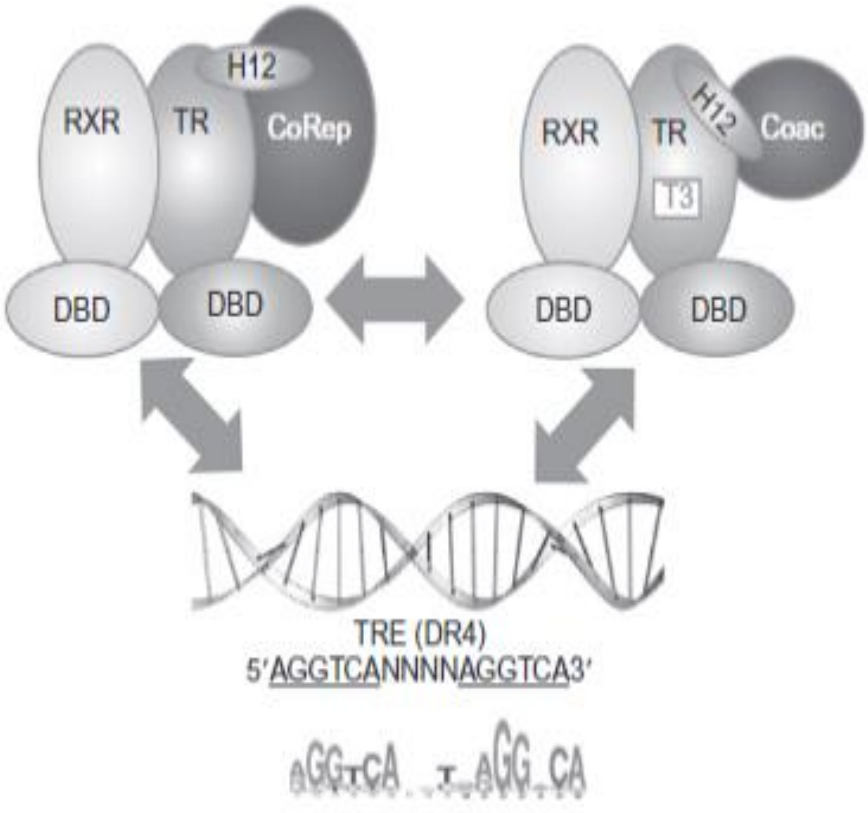

Figure 1-4 Model of TR-mediated transcriptional regulation: Left: In the absence of TH binding, TRs recruit corepressors, allowing them to cause transcriptional repression of TREs. Right: TH binding results in a structural change to TRs, allowing for the recruitment of coactivators to increase transcription at TREs (Flamant, Gauthier et al. 2017).

Thyroid Hormone disruption in neurodevelopment

Abnormal thyroid signalling has been found to have adverse effects on neurodevelopment. This is due to the large number of important roles that THs play during brain development. For example, THs stimulate vital processes such as the growth of axons, synapse formation, and the myelination of neurons (Williams 2008). Maternal hypothyroidism in rats has been shown to impact cortical progenitor cells during foetal development, with a reduction in both neuronal progenitor proliferation and neuronal differentiation. This was thought to be due to the initial downregulation of Pax6, which was detected via RT–PCR (Mohan, Sinha et al. 2012).

Thyroid receptors are present in the developing brain from the first trimester, but the foetal thyroid gland matures around the end of the first trimester and only begins to secrete TH around week 16 or E16 in mice (Fernández, López-Márquez et al. 2015). TH is essential for healthy brain development and regulates processes such as neuronal migration, neurite outgrowth, and synaptogenesis (Mohan, Sinha et al. 2012).

TR target genes, such as RELN, are thought to be responsible for their role in neuronal migration and have been linked to ASD due to dysfunctions (Su, Yang et al. 2022). Maternal hypothyroidism was induced in MMI-treated rats at gestational day 6, and a reduction in the expression of RELN was detected via both immunostaining and PCR. The hypothyroid group also exhibited aberrant neuronal migration. Furthermore, the defects observed could be rescued with TH replacement in the embryo between E12 and E15 (Pathak, Sinha et al. 2011). As RELN has strong ties to cognitive disorders such as ASD, understanding its disruption in hypothyroidism may help form a causal relationship between hypothyroidism and an increased risk of ASD.

In humans, mutations of the MCT8 gene lead to neurodevelopmental cognitive disorders, including the X-linked cognitive disorder Hendon Dudley, which is characterized by severe intellectual disability and muscle hypoplasia (Kersseboom, Kremers et al. 2013). Interestingly, knockout of the MCT8 gene in mice does not lead to the adverse neurological effects observed in humans. However, double knockout of MCT8 and another TH transporter, OATP1C1, led to a state of severe hypothyroidism, suggesting redundancy between the two transporters. Unlike single *MCT8* knockout mice, which exhibit changes in neurodevelopment, both *MCT8* and OATP1C1 double knockout mice presented delayed cerebellar development and myelination and compromised differentiation of GABAergic neurons within the cerebellar cortex. This led to a similar phenotype to Hendon Dudley disorder in humans (Mayerl, Müller et al. 2014).

Rat models have shown that treatment with a low dose of the antithyroid drug PTU in drinking water during second-trimester pregnancy has adverse effects on fetal brain development. Induced transient maternal hypothyroidism between gestational day 19 and perinatal day 2 resulted in cortical heterotopia and clusters of ectopic neurons in the brain (Figure 1.5). These effects were shown to be related to a reduction in the expression of Sonic hedgehog (SHH), an important developmental morphogen previously linked to thyroid activity (O'Shaughnessy, Thomas et al. 2019). Short-term administration of T3 has been shown to increase not only Shh mRNA expression but also coreceptor Patched (Ptc) and Smoothened (SMO) expression, suggesting that TH plays a key role in regulating this pathway (Desouza, Sathanoori et al. 2011).

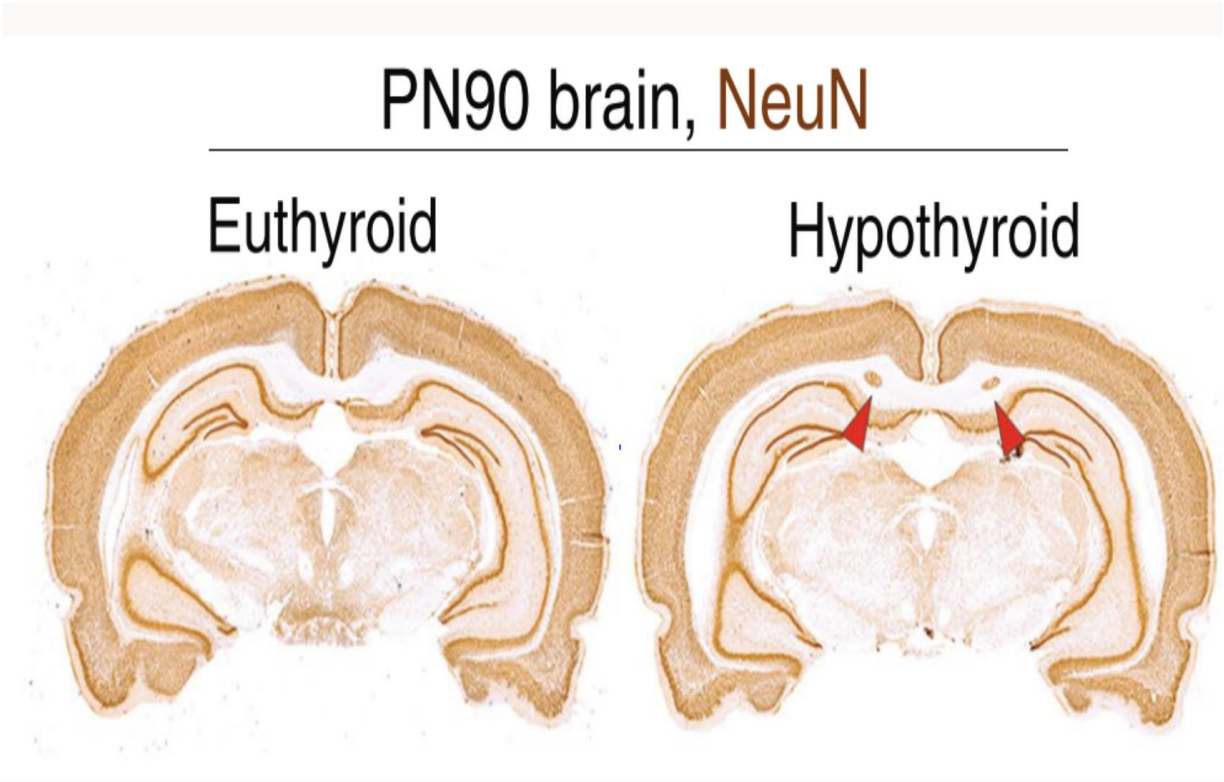

Figure 1-5 Perinatal exposure to the antithyroid agent PTU results in cortical heterotopia formation: Neuronal nuclei (NeuN)-stained coronal sections from the brains of adult rats born to control (left) or hypothyroid (right) mothers. Red arrows indicate heterotopia (O'Shaughnessy, Thomas et al. 2019).

1.2 DISEASE AND DIAGNOSIS OF AUTISM

ASD has been recognized since its earliest description as a condition characterized by deficits in social interaction and unusual sensory–motor behaviours (Kanner 1943). Kanner's seminal work linked ASD to intellectual disability and social interaction deficits, noting that affected children often related better to inanimate objects than to people. However, Kanner's perspective did not view ASD as a neurodevelopmental disorder but rather as an emotional issue, with early theories suggesting a lack of parental emotional warmth as a potential cause.

Today, ASD is understood to be a highly heritable neurodevelopmental disorder (Lai, Lombardo et al. 2014). This shift in perspective, from viewing ASD as an emotional disorder to recognizing it as a developmental disorder, has been largely influenced by neuroanatomical research. Histological studies revealed abnormalities in certain brain areas in individuals with ASD compared with controls (Bauman and Kemper 1985). These areas presented decreased cell size but increased cell density, primarily in the limbic system, a brain region closely associated with cognitive function (Kemper and Bauman 1993).

Our understanding of ASD as a neurodevelopmental disorder has expanded, and numerous potential biomarkers have been identified (Frye, Vassall et al. 2019, Shen, Liu et al. 2020). However, many of these biomarkers are still in development and require validation against clinically relevant comparison groups, and to date, no disease-modifying therapies targeting the core symptom domains (social communication impairment and restrictive/repetitive behaviour) are currently available. The heterogeneity of ASD complicates biomarker development, as

research has yet to find a one-size-fits-all approach to biomarker discovery. This lack of reliable biomarkers means that ASD diagnosis currently relies on behavioural analysis, and at present, there are no therapies designed to modify the core symptom domains of ASD, specifically addressing social communication impairment and restrictive or repetitive behaviour (Anagnostou 2018).

The current clinical diagnosis of ASD is based on criteria established by the American Psychiatric Association in the 5th edition of the Diagnostic and Statistical Manual of Mental Disorders (DSM-5 2013). This characterization outlines the disorder on the basis of two primary areas: social–communicative impairments and restricted–repetitive or stereotyped behaviours. Significant changes were introduced in the DSM-5, including the requirement for the disorder to be noticeable from a young age, even if the traits had not fully manifested. Additionally, disorders previously diagnosed separately, such as Asperger's syndrome or Rett syndrome, were unified under the umbrella term of ASD (Achkova and Manolova 2014).

Behavioural diagnosis is also used to determine the presence of ASD-like traits in animal models of the disorder. Behavioural assays, such as the three-chamber social approach task, serve as indicators of social avoidance, with a preference for interaction with another animal suggesting normal behaviour (Crawley 2007). Restricted/repetitive behaviours can be assessed through tasks such as marble burying tests, which involve observing the frequency of spontaneous burying behaviours displayed by the animal.

However, phenotyping via behavioural diagnostic assays has limitations. ASD is a highly heterogeneous disorder characterized by variations in genotype and phenotype between individuals (Lombardo, Lai et al. 2019). This complexity is often overlooked

in current behavioural diagnoses (Anderson 2015), leading to increased research aimed at improving the diagnosis and treatment of ASD. Considering these challenges, leveraging modern work to further understand the physiological processes underlying ASD may be beneficial. This approach could have significant utility for both the diagnosis and monitoring of treatment progress. By focusing on the physiological aspects of ASD, we may gain a more nuanced understanding of the disorder and develop more effective strategies for diagnosis and treatment. Therefore, understanding the genetic and environmental causes of this disorder and the pathophysiology of its underlying mechanisms is essential.

1.3 AUTISM AND GENETICS

Epidemiological studies have indicated a clear genetic component of ASD, with upwards of 80% of the causal variance for the disorder linked to inheritance (Sandin, Lichtenstein et al. 2017). The heritability of ASD is demonstrated through relative Recurrence risk (RR) scores, which indicate a greater risk for individuals with affected siblings or close relatives (Sandin, Lichtenstein et al. 2014). Notably, monozygotic and dizygotic twins presented higher RR scores than more distant relatives did, underscoring the strong heritability of ASD. Recent studies involving monozygotic and dizygotic twins, which are diagnosed on the basis of behavioural traits such as motor coordination, social behaviour, and attention deficit, highlight the heritability of ASD. Despite high heritability scores, features expressed within monozygotic twins were uncorrelated, suggesting that ASD comprises independent developmental liabilities (Pohl, Jones et al. 2019).

The genetic complexity of ASD is evident in the lack of common loci for ASD. Genome-wide association studies (GWASs) have opened avenues for further genetic

insights, but unlike disorders such as schizophrenia, which has well-defined risk loci, ASD heterogeneity presents challenges (Grove, Ripke et al. 2019). To address this, gene-wide prediction studies have focused on the functional characterization of ASD-related genes. Leveraging databases such as the SFARI Gene database, researchers have utilized gene interaction network models to understand functional interconnections. This analysis clustered genes on the basis of their functional pathways, revealing disrupted molecular pathways linked to synaptic transmission, neuronal function, and histone modification (Krishnan, Zhang et al. 2016). For example, the *Shank2* gene, which is involved in synaptic transmission, was found to be disrupted in ASD (Zaslavsky, Zhang et al. 2019). Similarly, the *RELN* gene, which plays a key role in neuronal migration, was also affected (Bonora, Beyer et al. 2003). Additionally, the *TET3tet* (methylcytosine dioxygenase 3) gene , which is associated with histone modification, has been shown to be altered in ASD (Beck, Petracovici et al. 2020). These examples highlight the diverse molecular pathways affected by ASD and underscore the complexity of this disorder.

ASD exhibits phenotypic pleiotropy, leading to a high comorbidity rate. For example, *RELN* is also epigenetically implicated in schizophrenia (Guidotti, Grayson et al. 2016). Genetic overlap studies between ASD and other neuronal phenotypes revealed strong correlations with schizophrenia, major depression, and epilepsy (Grove, Ripke et al. 2019).

Recent studies emphasize that the clinical variability and heterogeneous genetic architecture of ASD make it difficult to elucidate its exact mechanisms (Di Giovanni, Enea et al. 2023). While some ASD-related diseases have monogenic syndromes, such as TSC1, which links genetic mutations of the mTOR pathway to epilepsy and ASD, most ASD cases are idiopathic and involve disruption of various neurodevelopmental pathways.

The complexity of the genetic foundations of ASD requires further elucidation. Despite progress, more than 1000 different genetic causes of ASD have been identified. The intricate interplay between genetic and environmental factors (see section 2.4) leaves the etiology of 70% of ASD cases unknown (Chiurazzi, Kiani et al. 2020).

Advances in sequencing technology have identified potential ASD risk genes, particularly those related to synaptic activity (Ebert and Greenberg 2013).
Molecular studies continue to explore the genetic landscape and mechanisms of ASD. Whole-exome sequencing (WES), Whole-genome sequencing (WGS), microRNA, long noncoding RNA, and CRISPR/Cas9 models are employed to uncover the aetiology of ASD and develop personalized treatments (Gill, Clothier et al. 2021). Genetic contributions to ASD involve various types of common and rare variants, with more than 100 risk genes being implicated in rare, potentially damaging mutations (Havdahl, Niarchou et al. 2021). In summary, the complexity of ASDs arises from their heterogeneous nature and intricate genetic architecture. Advances in genomic analysis, while revealing potential risk genes, highlight the need for further exploration to understand their underlying mechanisms to create more effective strategies for diagnosis and treatment.

1.4 ENVIRONMENTAL FACTORS IN AUTISM AETIOLOGY

Prevalence

While ASD is a highly heritable disorder, genetics does not account for its entire aetiology. While the exact aetiology is unknown, large population studies have provided insight into the nongenetic factors that play a possible role in the risk architecture of ASD. A good example can be seen in the proposed connection between increased maternal age and ASD. A meta-analysis of 27 previous population studies was performed. (Wu, Wu et al. 2017). Overall, advanced maternal and paternal age was associated with an increase in ASD risk, with an 18% increase in risk with an increase in age of 10 years.

Prenatal risk factors of ASD Risk:

Maternal nutrition during pregnancy, a prominent area of investigation for understanding the environmental risk factors associated with ASD, has been shown to be significantly correlated with ASD risk. Deficiencies in essential nutrients such as vitamin D and folic acid have been of particular interest. An epidemiological study conducted using comprehensive data from a Swedish whole population register spanning nearly three decades (1972--2001) revealed potential links between maternal vitamin D deficiency and increased ASD risk. The study by Magnusson and colleagues (2016) revealed a noteworthy correlation between lifetime vitamin D deficiency in expectant mothers and an increased risk of ASD in their offspring, a correlation that did not extend to intellectual disability, underscoring the specificity of the association(Magnusson, Kosidou et al. 2016).

In addition to maternal nutrition, various elements of maternal lifestyle and exposure have been investigated as prenatal factors that might play a role in the development of ASD, which typically appears early in a child's life (Bölte, Girdler et al. 2019). These elements include changes in sex hormones, obesity, diabetes, and maternal inflammation (Abdallah, Larsen et al. 2013, Baron-Cohen, Auyeung et al. 2015, Li, Fallin et al. 2016). The potential impact of the maternal immune system on the foetal Central Nervous System (CNS) is also a topic of interest, given that pregnancy complications are associated with neurodevelopmental disorders (Bilbo, Block et al. 2018). Certain congenital viral infections, such as rubella and cytomegalovirus, which are linked to brain calcification, microcephaly, and ASD, can disrupt brain development (Shuid, Jayusman et al. 2021). Zika virus (ZIKV), known for causing microcephaly, structural brain abnormalities, and neurological changes, is being studied for its potential role as an ASD risk factor, given its impact on brain development (Cranston, Tiene et al. 2020).

Drugs and pollutant exposure:

The relationships among drugs, toxic exposure, and the risk of ASD constitute a multifaceted domain. One prominent avenue of research delves into the potential for these factors to disrupt hormonal systems, thereby impacting foetal development. This disruption is a focal point for understanding how certain substances may contribute to ASD risk. Valproate, a pharmaceutical drug, is a prime example of a known substance linked to an elevated risk of ASD in offspring (Christensen, Grønborg et al. 2013). Studies have revealed its potential to interfere with neural development, thus raising concerns about its use during pregnancy.

Environmental toxins such as polyhalogenated aromatic hydrocarbons (PHAHs), including polychlorinated biphenyls (PCBs) and PDBEs, and polyfluoroalkyl substances (PFASs) are linked to altered neurodevelopment in humans. Prenatal exposure to environmental contaminants that act as endocrine-disrupting chemicals (EDCs) may be linked to an increased likelihood of ASD and the appearance of behavioural defects (Panesar, Kennedy et al. 2020, Oh, Bennett et al. 2021, Sethi, Keil Stietz et al. 2021). Findings from animal models have indicated that neurodevelopment is sensitive to hormone action in a time- and dose-dependent manner (Auyeung, Lombardo et al. 2013). A common mechanism observed from prenatal exposure to these chemicals results in alterations in both T4 and TSH (Leijs, Tusscher et al. 2012, Coperchini, Croce et al. 2021). While there is evidence that these EDCs may affect T4 carrier proteins, their exact mechanism of action is still unknown (Cesh, Elliott et al. 2010, Coperchini, Croce et al. 2021). This interference could contribute to the risk of ASD (Diamanti-Kandarakis, Bourguignon et al. 2009, Kalkbrenner, Schmidt et al. 2014). This could be a reason for the sporadic nature of ASD.

Research is ongoing to elucidate the extent of their impact and the mechanisms through which they might contribute to the risk architecture of ASD. In summary, the exploration of maternal nutrition and drug/toxic exposure during the prenatal period may identify possible reasons for the sporadic nature of ASD compared with genetic effects alone.

1.5 GENE–ENVIRONMENT INTERACTIONS

While ASD is strongly influenced by genetics, genetic factors alone cannot fully account for its aetiology. As previously discussed, ASD is a highly heritable disorder with identified causative genes, but no single gene or chromosomal defect can comprehensively explain ASD, as it contributes to only a minority of ASD cases. Research has increasingly underscored the importance of environmental factors in ASD development. ASD occurs sporadically, suggesting that a combination of genetic and environmental factors may offer a more comprehensive explanation. Although the precise cause remains elusive, extensive population studies have illuminated nongenetic factors that are likely to play a role in shaping the risk profile of ASD (Saxena, Babadi et al. 2020). Moreover, hundreds of genes have been identified as either causative or risk factors for ASD, and exposure to environmental chemicals, including endocrine disruptors, has been linked to adverse effects on human health, including neurodevelopmental disorders (Cheroni, Caporale et al. 2020).

An increasing body of evidence suggests that epigenetic processes play a significant role in the development of ASD, with a growing number of studies highlighting the role of epigenetic factors. Recently, the causal role of epigenetic dysregulation in ASD has been underscored by the discovery of a specific mutation in genes related to epigenetic regulation in patients with ASD (LaSalle 2023). Two primary molecular epigenetic mechanisms are implicated in gene expression: DNA methylation and histone modification. Additionally, noncoding RNAs are key components in the regulation of chromatin structure and gene expression.

These mechanisms are highly sensitive to environmental factors and influence gene function without altering the DNA sequence. Specifically, aberrant DNA methylation, a key epigenetic process, has been implicated in shaping the developmental trajectory of ASD (Keil-Stietz and Lein 2023, Stoccoro, Conti et al. 2023). A highly

studied epigenetic factor with strong links to ASD is Methyl-CpG binding protein 2 (MeCP2), which is both an activator and repressor of transcription. Specific methylation of the MeCP2 promotor has been linked to ASD aetiology (Lu, Liu et al. 2020, Lax, Do Carmo et al. 2023). It has also been linked with the epigenetic regulation of other causative genes, such as *RELN* and *GAD1*, within the cerebellum (Zhubi, Chen et al. 2014). The influence of environmental factors on the aetiology of ASD is believed to stem from intricate interactions between genes with low-risk associations and various environmental influences (Chaste and Leboyer 2012). These mechanisms are responsive to environmental cues and can modulate gene function without altering the underlying DNA sequence through epigenetic regulation (Stoccoro, Conti et al. 2023). This crossover between the environment and genetics observed in epigenetic studies may provide insight into the spontaneous nature of the disorder. Recent research has focused on the role of prenatal maternal environmental factors in the development of ASD. One area of particular interest is the impact of maternal folic acid deficiency. Studies have shown that this deficiency is associated with alterations in the methylation levels of key ASD-related genes, including *MECP2*, *OXTR*, and *RELN* (Gallo, Stoccoro et al. 2022).

Furthermore, these investigations shed light on the phenomenon of sexual dimorphism in ASD. The methylation patterns of certain genes appear to differ between males and females, adding another layer of complexity to our understanding of this disorder (Stoccoro, Gallo et al. 2022). This evidence underscores the intricate interplay between genetics and the environment in ASD and may pave the way for future research into its spontaneous nature.

Studies employing models of environmental exposure in both humans and rodents have revealed intergenerational epigenetic impacts that encompass neurological traits and social behaviours, such as those observed in individuals with ASD (Escher, Yan et al. 2022). These findings suggest that environmental exposure may have generational effects.

1.6 THE CEREBELLUM

The structure of the cerebellar cortex is cytoarchitecturally diverse, with its connectivity built from 4 different kinds of neuron granule cells, Purkinje cells, 2 inhibitory interneuron Golgi cells, and basket/stellate cells (D'Angelo 2018). These are spread across 3 layers in the cerebellar cortex. The molecular layer comprises basket cells along with dendrites from Purkinje and granule cells, the Purkinje layer, which contains the cell body of Purkinje cells, the granule cell layer, which contains Golgi interneurons, the cell body of granule cells, and the DCN (Fig. 1.6) (Voogd and Glickstein 1998). The connectivity of the cerebellar cortex is regulated mostly through Purkinje cells. Signals from other areas of the brain are relayed to the cerebellum from the pontine nucleus to granule cells via mossy fibres. This allows glutamatergic granule cells to send excitatory signals to Purkinje cells through parallel fibres. In the cerebellar cortex, all inputs to the cerebellum come to Purkinje cells. The Purkinje cell's singular output is to the DCN, which acts as the only output cell of the cerebellar cortex. The DCNS forms at the rhombic lip and is indicated by the transcription factors Pax6, Lhx9, TBR1, and TBR2 (see section 1.7 for gene function) and members of the NeuroD family (Fink, Englund et al. 2006, Green and Wingate 2014, Pieper, Rudolph et al. 2019). The number of DCNS varies between species, with all mammals having 3--5 DCNS and birds having 2 DCNS but lacking the dentate nucleus, which projects to the dorsal thalamus and thought to be key for the cerebellum’s cognitive functions (Kelly and Strick 2003). The volumes of the 2 DCNS, the fastigial nucleus and the

interposed nucleus are significantly decreased in mouse models of Fragile-Xs syndrome, suggesting a key role in the cerebellum's cognitive function (Ellegood, Pacey et al. 2010).

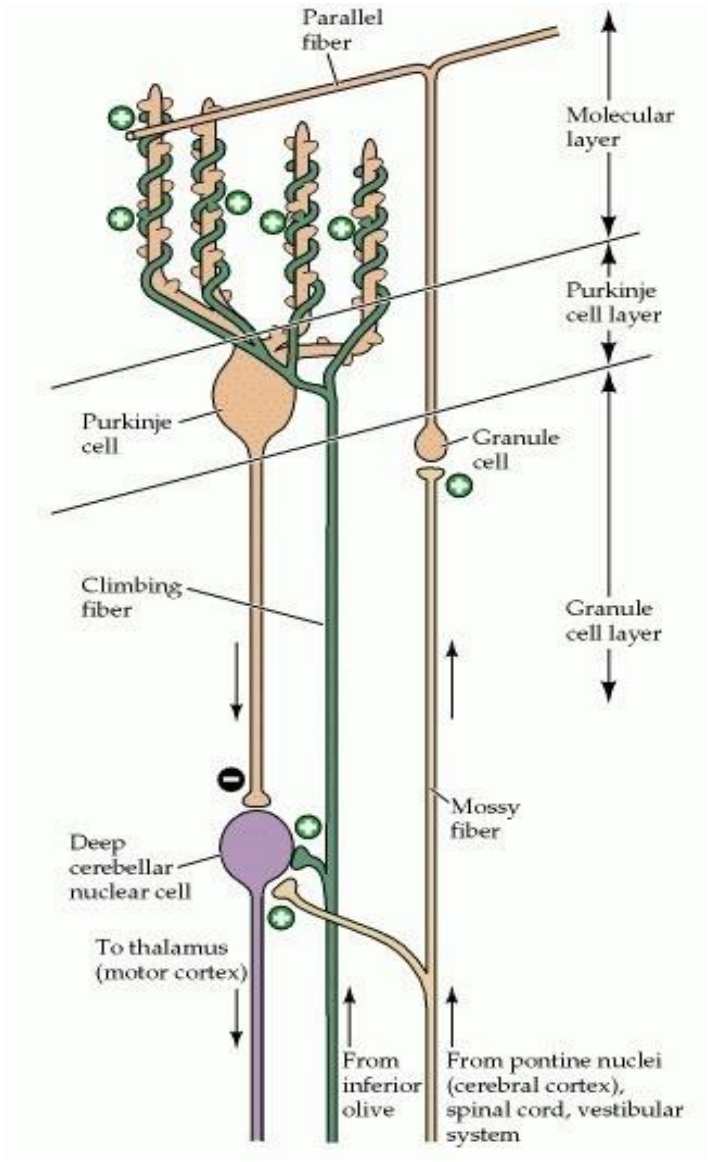

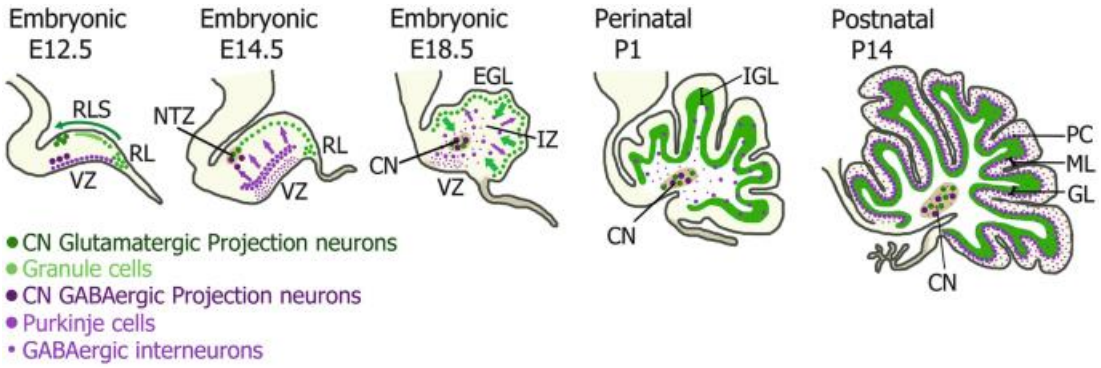

Previous page: Figure 1-6 Connectivity of the cerebellar cortex: Organisation of the cerebellar cortex inputs from parallel fibres converge onto Purkinje cells. The Purkinje cells then regulate cerebellar output through modulation of the DCN (Purves, Augustine et al. 2001).

Below the process by which different types of neurons develop within the cerebellum. Initially, glutamatergic and GABAergic neurons emerge from distinct regions—the Rhombic lip (RL) and Ventricular zone (VZ), respectively. They subsequently migrate through intermediary zones, eventually finding their places within the cerebellar architecture by postnatal day 14(Prekop, Delogu et al. 2023).

Cerebellar development and neurogenesis

The entire neurogenesis of the key cells of the cerebellum unfolds temporally from two distinct progenitor zones situated on the dorsal side of the anterior hindbrain: the rhombic lip and the ventricular zone (van Essen, Nayler et al. 2020). These zones, which are specific to the cerebellum, are responsible for generating glutamatergic and GABAergic cells, respectively. Initially, cerebellar neurogenesis is established along the anterior–posterior axis of the developing brain, preceding the establishment of these two distinct progenitor zones through dorsal–ventral patterning. These progenitor zones subsequently initiate a temporal sequence of cell production, characterized by cell migration and morphological rearrangements, to ultimately integrate the glutamatergic and GABAergic cell types and form the functional circuits of the adult cerebellar cortex and cerebellar nuclei (Hawkes and Consalez 2023).

In mice, neuron development timing varies significantly. The development of the cerebellum involves a complex interplay of multiple cell types over an extended timeline. Initial neurogenesis of the cerebellum in mice begins around Embryonic day 9-10 (E9-E10) with the formation of early cerebellar structures(Dalvand, da Silva Rosa et al. 2022). During the initial stages of cerebellar development, the first cell types to emerge are the cerebellar nuclei neurons and Purkinje cells, which develop between embryonic days 10.5 and 13.5, with their birth dates influencing their eventual

positioning in mediolateral clusters. GABAergic Interneurons (INs) in the cerebellar nuclei are produced between E10.5 and E11.5. Later-born granule cells, produced from E13.5 onwards, provide cues for Purkinje cell maturation(Hashimoto and Mikoshiba 2003). The production of Golgi cells spans from E13.5 to postnatal stages, peaking around E14–E16. Late-born GABAergic interneurons, such as stellate and basket cells, arise from secondary precursors in the Prospective white matter (PWM) from E13 to P5, peaking around birth. (Leto, Arancillo et al. 2016). This diversity underscores the role of spatial and temporal identities in producing specific neuronal subtypes. RL-derived glutamatergic neurons suggest a temporal shift in progenitor identity, transitioning from CN neurons to GCs and UBCs(Leto, Arancillo et al. 2016). Late-stage RL progenitors express markers for either GCs (PAX6) or UBCs (TBR2). Cerebellar compartmentation begins around E10 in the VZ of the fourth ventricle. PC subtype specification occurs during terminal mitosis between E10 and E13 in the Ptf1a-expressing progenitor domain. Birth dating studies reveal two PC populations: an early-born group (E10–E11.5) that becomes Zebrin II (ZII)+ and a later-born group (E11.5–E13) that becomes ZII−. Zebrin II is a molecular marker distinguishing different PC subtypes(Leto, Arancillo et al. 2016). The correlation between PC birthdates and adult stripe locations indicates that subtype specification and positional information are intrinsic to the cerebellum, independent of external activity or inputs.

Significant cerebellar growth occurs during the third trimester and early infancy in humans, and the first two weeks postnatally in mice, driven by granule cell precursors (GCPs). This growth increases the cerebellum's surface area, forming lobules. Foliation, the process of forming lobules, begins at embryonic day 16.5 (E16.5) in mice with the sequential development of fissure bases, termed anchoring centres. These centres, characterized by distinct properties of GCPs, PCs, and Bergmann glia (BG), serve as origins for lobule extension The development of cerebellar foliation is orchestrated by anchoring centres, which initiate at the base of each fissure. These

centres are characterized by increased proliferation and inward thickening of granule cell precursors (GCPs), indentation of the Purkinje cell layer, and radial projection of Bergmann glial fibres (Sudarov and Joyner 2007). A tri-layer model suggests that surface wrinkling may explain anchoring centre initiation and positioning (Lejeune, Javili et al. 2016). The timing of granule cell production differs among cerebellar zones, with delayed onset in the central zone contributing to distinct lobule morphologies (Legué, Gottshall et al. 2016). Clonal analysis reveals that granule cell precursors divide symmetrically and undergo oriented cell divisions, leading to anteroposterior polarized growth. Fissure bases act as boundaries for GCP dispersion, allowing each folium to develop as a unit. This modular development enables differential regulation of cell division planes and numbers, ensuring appropriate cell partitioning into each folium (Legué, Riedel et al. 2015). The timing and positioning of these centres are critical, in determining the morphology of intervening lobules and the allocation of cells for distinct long-range neural circuits. This complex process transforms the cerebellum's smooth surface into a highly folded structure, enhancing its functional capacity.

Spatial patterning of rhombic lip production and ventricular zone production

The formation of the rhombic lib as well as the cells originating from it is dependent on the expression of the basic helix-loop-helix transcription factor Atonal1 (Atoh1) (Machold and Fishell 2005, Wang, Rose et al. 2005). The early cerebellum produces glutamatergic cells in the cerebellum in a spatial-temporal manner, including early cerebellar development of granule cells and cerebellar nuclei as well as perinatal formation of glutamatergic unipolar brush cells. Upon initial formation, progenitors of the cerebellar nuclei migrate from the rhombic lip to form a transient pool of cells at the lateral edge of the cerebellar anlage called the Nuclear transition zone (NTZ)

(Fink, Englund et al. 2006). These progenitors then migrate into the white matter to form distinct cerebellar nuclei within the white matter.

Unlike the glutamatergic cells produced from the rhombic lip, the GABAergic cells produced at the cerebellar ventricular zone—Purkinje cells, small neurons of the cerebellar nuclei, basket, stellate, and Golgi interneurons—migrate directly from the ventricular zone radially into the cerebellum. Like the rhombic lip's dependence on the expression of Atoh1, the ventricular zone is dependent on the expression of the basic helix-loop-helix transcription factor Ptf1a (Hoshino, Nakamura et al. 2005).

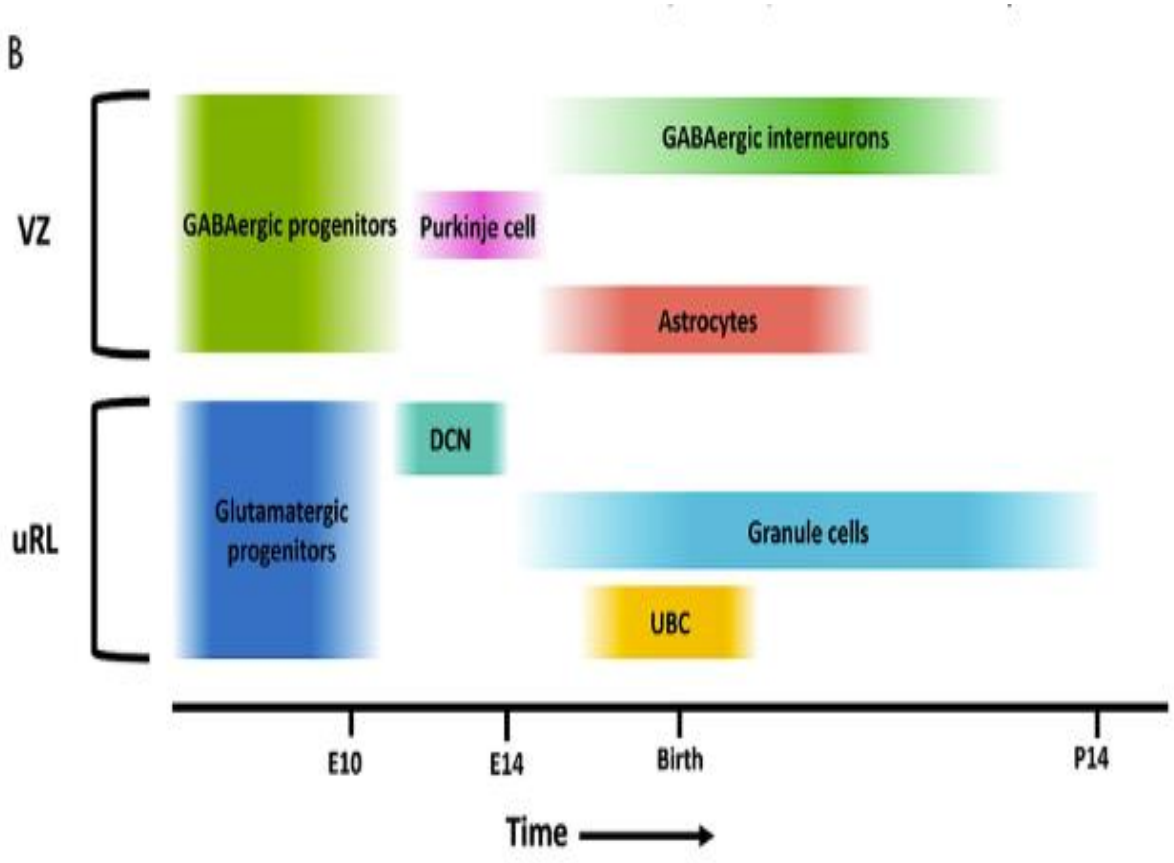

Figure 1-7 Adapted from (van Essen, Nayler et al. 2020): Timeline of cell production from progenitors in two germinal zones, the VZ and the uRL.

Despite their important role in function, our understanding of Cerebellar nuclei (CN) development remains incomplete. In the last decade, there has been a notable increase in our understanding of (CN) development owing to gene expression and genetic fate mapping studies at the turn of the century. Between embryonic days 10 and 12.5, a group of cells expressing Atoh1 in the Rhombic lip (RL) gives rise to glutamatergic CN projection neurons. CN cells, which later develop into various types of neurons, including granule cell precursors for the external granule layer (EGL) and the DCN, begin travelling after E12.5. From E12.5 to E14.5, these cells migrate from the rhombic lip (RL) across the dorsal surface of rhombomere 1 via a pathway known as the subpial rhombic lip migratory stream (RLS). They accumulate at the NTZ, a temporary region located at the edge of the cerebellar structure where nuclear neurons mature with distinct, time-specific transcription factor profiles.

In mammals, the lateral dentate nucleus, like extracerebellar neurons, expresses the LIM-homeodomain gene Lhx9. Both of these populations project to the thalamus, suggesting a role for Lhx9 in specifying axonal projections(Green and Wingate 2014). Following this, projection neurons in the interposed and medial nuclei, which originate from the RL, are characterized by their expression of Tbr2 and TBR1, respectively (Englund, Fink et al. 2005, Fink, Englund et al. 2006). These neurons extend axons to various targets in the hindbrain, midbrain, and ventral diencephalon.

Between embryonic days 14.5 and 16.5, CN cells within the NTZ moved into the white matter. The exact mechanism of this movement is unclear; it could be due to active migration towards the Ventricular zone (VZ) or displacement caused by significant changes in cerebellar shape as granule cell precursors in the EGL rapidly proliferate. These precursors eventually become the most numerous types of neurons in the brain.

Gliogenesis in the cerebellum.

The cerebellum is a complex neural structure that houses not only an intricate network of neurons but also a diverse population of glial cells, including astrocytes and oligodendrocytes, which play pivotal roles. For instance, Bergmann glia, with their radial extensions, guide granule cell migration, while velate astrocytes remain less explored. Oligodendrocytes, responsible for myelin sheath formation, exhibit intriguing external distributions, with hints of internal subpopulations.

Astrocytes, a crucial type of glial cell, are integral to brain function. During embryonic development, Radial glia (RG) serve as neural progenitors. Initially involved in neurogenesis, RG cells also possess gliogenic potential. Traditionally, it was believed that gliogenesis began around embryonic day 14 (E14) in mice, following the delamination of RG cells from the ventricular zone (VZ). However, recent studies have shown that individual embryonic RG cells exhibit gliogenic properties as early as E12, challenging previous assumptions and highlighting the complex spatiotemporal pattern of astrocyte formation. RG cells originating at E12 mainly contribute to astrocytes in the hemispheres, while those originating at E14 primarily populate the vermis. Notably, gliogenesis during this phase occurs exclusively in non-neuronal elements. The early origins of radial glial cells can be traced back to primitive bipolar

cells in ventricular germinal zones (Buffo and Rossi 2013, Cerrato, Parmigiani et al. 2018, Cerrato and Buffo 2021).

The development of oligodendrocytes—the myelin-producing cells of the central nervous system—remains a fascinating area of study. Early hypotheses suggested that these cells arise from subependymal layers of the fourth ventricle, migrating into the cerebellum via specific routes. Recent insights from avian studies indicate that cerebellar oligodendrocytes emerge from the ventral midbrain, a region rich in neural progenitors. During cerebellar embryogenesis, the transcription factor Ascl1 (also known as Mash1) orchestrates their fate. Initially expressed in the Ventricular neuroepithelium (VN), Ascl1 guides early oligodendrocyte specification, but as development progresses, Ascl1 expression shifts to the PWM (Mecklenburg, Garcia‐López et al. 2011). Around E14 in mice, oligodendrocyte precursors appear within the cerebellar parenchyma, although they do not originate from local germinal sites. Chick brains exhibit a similar timeline, with oligodendrocytes emerging around E5 and subsequently invading cerebellar territory between E9 and E12. Despite these observations, the precise extracerebellar source of mammalian oligodendroglia remains an unknown. Recent fate-mapping studies propose the Olig2-expressing neuroepithelial domain in the ventral rhombomere 1A as the primary source of cerebellar oligodendrocytes. However, a second wave of precursors generated locally by the cerebellar VZ plays a minor role(Hashimoto, Hori et al. 2016)..

Cerebellar Morphology in ASD

The cerebellum was initially thought to be associated with only motor deficits in individuals with ASD. As time has passed, the importance of the cerebellum in the aetiology of ASD is slowly beginning to be understood, with research beginning to state its importance after the turn of the decade; however, there are still many differing opinions on its exact role in the disorder (Fatemi, Aldinger et al. 2012). Recent work, however, has changed the understanding of the role of the cerebellum in individuals with cognitive disorders such as ASD. Early evidence for the cerebellum's cognitive role was observed in behaviour studies of human patients, with a cerebellar pathology with strong changes in behaviour observed in patients who had suffered damage to the posterior lobe of the cerebellum and vermis. These behavioural changes related to cerebellar alterations were initially described as “cerebellar cognitive affective syndrome”. The behavioural changes observed, such as a change in social behaviour that fell under this banner, are similar to those observed in individuals with ASD (Schmahmann and Sherman 1998).

During the critical developmental window of the first trimester, key output neurons in the cerebellum, including Purkinje cells and Deep cerebellar nuclei (DCNs), begin to form. These neurons play a central role in the cerebello-thalamocortical pathway, which regulates the cerebellum’s cognitive functions.

A notable change observed in the cerebellum of ASD patients is a reduction in the number of Purkinje cells. Many ASD patients show this reduction in postmortem observations of their cerebellar cortex (Skefos, Cummings et al. 2014). Purkinje cells play important roles in the communication of the cerebellum with cortical areas of the brain, such as the posterior parietal cortex and the prefrontal cortex. They take in

synaptic signals from parallel fibres and regulate outgoing signals from the DCN through inhibitory GABAergic signalling.

Animal models of ASD have associated cerebellar regions with the disorder, specifically highlighting the impact of Purkinje cell-specific knockouts of the ASD-related gene Tuberous sclerosis complex 1 (*TSC1*) in mice. This results in social communication and repetitive behaviour traits commonly observed in ASD patients (Tsai, Hull et al. 2012). Tuberous sclerosis complex, a disorder with a high rate of comorbidity with ASD, can be observed in relation to Purkinje cell loss and ASD in animal models. Localized knockout (KO) of *TSC1* in Purkinje cells results in a reduction in Purkinje cell number and retention of behavioural traits such as abnormal social interaction, repetitive behaviour, and observed in full KO of the *TSC1* gene (Tsai, Hull et al. 2012).

Purkinje cell loss is also prominent in other animal models of ASD (Kelly and Strick 2003). For example, in mice that have been given the epilepsy drug valproate during the early stages of pregnancy, when exposed to valproate during this stage of development, animal models show impaired social behaviours and restricted, repetitive behaviours akin to ASD, making them a valuable tool for research (Kim, Kim et al. 2011).

Histological analysis of these models revealed a significant decrease in Purkinje cells (Fig. 1.8) (Spisák, Román et al. 2019). The valproate model also provided further insight into the role of Purkinje cells in the cerebrocerebellar circuitry via Blood-oxygen-level-dependent functional magnetic resonance imaging (BOLD-FMRI). BOLD-FMRI allows for the observation of brain activity by detecting the increase in oxygen levels when a neuron is firing. Mice with fewer Purkinje cells exhibit lower

neuron firing in the somatosensory complex in response to a sensory stimulus, and the Purkinje number is inversely proportional to the BOLD response. This could be interpreted as follows: 1. Purkinje cells are responsible for inhibitory or regulatory projections to these areas or 2. Both Purkinje cell numbers and cerebral circuits are typically changed by a common factor during neurodevelopment.

These studies highlight the nature of ASD as a connectivity disorder which is further supported by the genetic mutations in knockout in synaptic-related proteins such as the SHANK family of proteins. As such cell types such as the Bergmann glia—the radial glia of the cerebellum, which form intimate functional connections with cerebellar Purkinje neurons are possible candidates for ASD pathology.

Further insight into the interaction between Purkinje cells and Bergmann glia within the cerebellum that may be relevant to ASD pathology can be seen in a recent study. The study's findings that Purkinje cells release dopamine, which then activates D1 receptors on Bergmann glia, underscore the importance of these glial cells in modulating cerebellar function. This dopaminergic signalling pathway influences Purkinje cell output and, consequently, cerebellar-dependent behaviours such as motor and social activities (Li, Saliba et al. 2023). Additionally, elevated levels of GFAP mRNA have been detected in the cerebellum of autistic individuals, suggesting glial activation in this condition (Edmonson, Ziats et al. 2014).

Given that individuals with autism exhibit alterations in Bergmann glia morphology and elevated GFAP mRNA levels, the disruption of this dopaminergic signalling could contribute to the cerebellar abnormalities observed in ASD. Thus, understanding these cellular interactions offers a promising avenue for exploring the underlying mechanisms of ASD and developing potential therapeutic strategies.

Furthermore, research indicates that individuals with autism show several changes in BG morphology, including the loss of vertical processes and disrupted cell body arrangement in the Molecular layer. These changes are associated with significant disorganization of granule cells, as BG play a crucial role in granule cell migration(Wegiel, Kuchna et al. 2013).

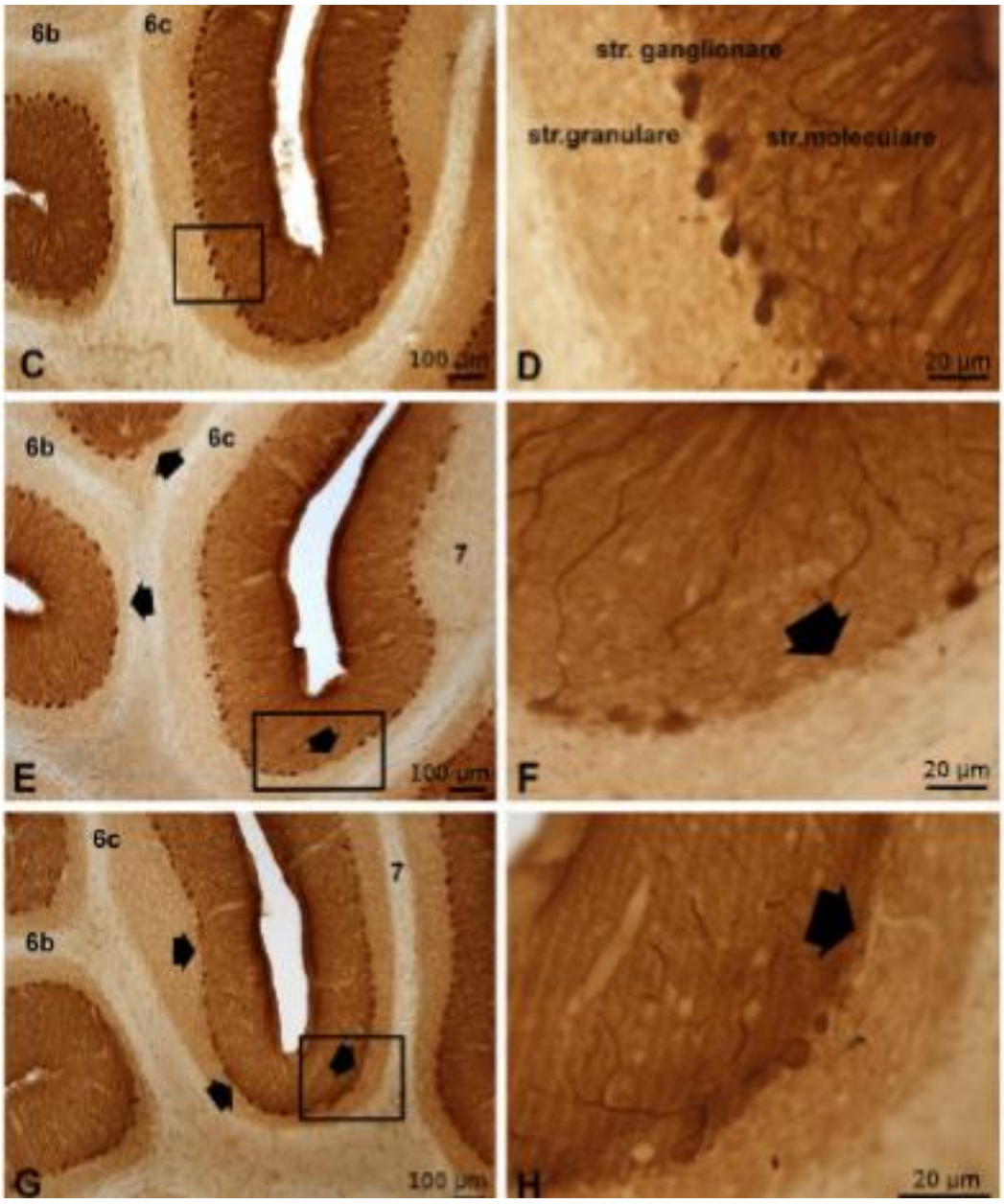

Figure 1-8 Purkinje cell loss in response to valproate exposure: Calbindin D28k (CB) immunostained sagittal section of the rat cerebellar vermis. Purkinje layers are observed in untreated (C, D) and valproate-treated (E-H) exposed mouse brains, with arrows indicating large areas lacking Purkinje cells (Spisák, Román et al. 2019).

Purkinje cells play an important role in the communication of the cerebellum with other areas of the brain, such as the prefrontal and somatosensory cortex, in synaptic signals from parallel fibres and the regulation of outgoing signals from the DCN through inhibitory GABAergic signalling, with the ability to regulate cognition thought to be regulated by the dentate nucleus (Figure 1.9) (Basson and Wingate 2013).

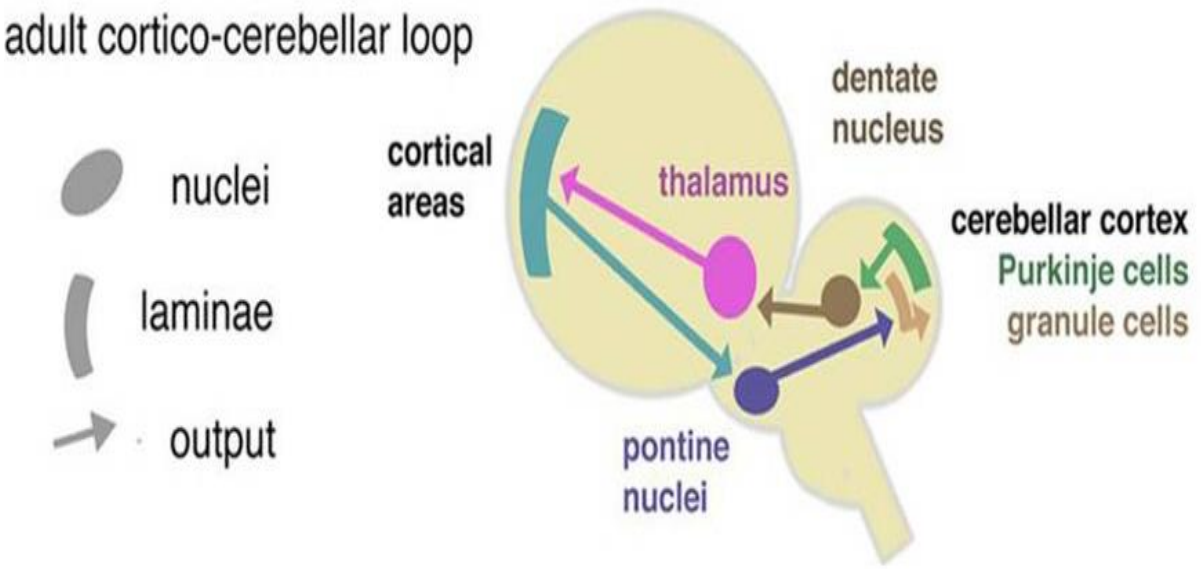

Figure 1-9 Cortico-cerebellar closed loops for the modulation of cortical activity: Cortical activity is predicted to feed into the cerebellum via the pontine nucleus. The cerebellum from the dentate nucleus sends information back to the cortical areas from the thalamus.

Cerebellar circuitry changes in ASD

One of the first studies assessing this functional cortico-cerebellar connectivity in ASD was by (Khan, Nair et al. 2015), who used Resting-state fMRI (rs-fMRI) and examined the difference in cortico-cerebellar connectivity between children with ASD and those with typical development. This study revealed that children with ASD presented increased functional connectivity of the cerebellum to motor areas but reduced connectivity to areas of the brain related to cognitive function, providing an argument for the role of adverse cortico-cerebellar connectivity in ASD pathology. To explore further whether disruption of cortico–cerebellar connectivity manifests within ASD, large-scale fMRI studies investigating differences in cortico–cerebellar connectivity between individuals with ASD and control individuals have been performed (Ramos, Balardin et al. 2019). In a sample of 708 subjects, there was consistent atypical cortical–cerebellar connectivity in ASD patients.

Thyroid and the Cerebellum

TH has been shown to play an important role in cerebellar development via a reduction in Purkinje cell dendrite branching (Heuer and Mason 2003)In cerebellar cell culture T3 acts on Purkinje cells directly through localized TRα1 receptors. This was also observed in chick studies in which the TH transporter *MCT8* was knocked down in Purkinje cell precursors. As in the cerebellar cell culture studies, this resulted in a reduction in dendritic branching and poor differentiation of the Purkinje cell progenitors. THs are vital for cerebellar development, particularly in the formation and maturation of BG and the migration of granule cells. Research indicates that THs accelerate BG formation and morphological development in hyperthyroid rats, while hypothyroidism results in delayed BG maturation and an increase in cell numbers (Seress 1978, Clos, Legrand et al. 1980). The TRα1 receptor, found in Purkinje cells and BG, is crucial for normal cerebellar development and indirectly influences granule

cell migration (Fauquier et al., 2014). THs stimulate astrocytes to secrete Epidermal growth factor (EGF), which enhances granule cell migration and BG elongation via the mitogen-activated protein kinase pathway (Martinez, Eller et al. 2011). This TH-EGF signalling pathway is essential for proper cerebellar development, and its disruption may lead to neuroendocrine disorders associated with migration deficits. These findings underscore the intricate relationship between THs, BG, and granule cells in cerebellar ontogenesis. Similarly, it results in nonautonomous effects, such as a reduction in granule cell precursor proliferation. Notably, this mutation resulted in the loss of Pax6, a DCN marker (Delbaere, Vancamp et al. 2017). Similar results may be obtained through knockouts in other structures of the cerebellum. Like Purkinje cells, cerebellar nuclei show a high presence of *Mct8* mRNA during the first 2 weeks of embryonic development. Colocalization studies of MCT8 with the DCN markers TBR1, LHX9, and Pax6 revealed a possible role for T3 in the development of these cells (Delbaere, Van Herck et al. 2016).

1.7 INTRODUCTION TO THE MODEL

In our study, we utilized a maternal hypothyroid mouse model kindly provided by Richard Wingate from King's College London to investigate the link between maternal hypothyroidism and ASD. This model involves administering 0.1% MMI, an antithyroid drug, to pregnant mice in their drinking water (supplemented with 0.475% sucralose) from E0 to E13.5. The control mice received 0.457% sucralose. The induction of hypothyroidism was confirmed through ELISA analysis, which revealed a significant decrease in T3 and T4 levels at 14 days gestation in the MMI-treated group (Figure 1.10) compared with those in the control group. This treatment was applied to a total of 16 litters.

Behavioural analyses of these hypothyroid mice revealed both similarities and differences compared with their untreated counterparts. Notably, these differences manifest in social responses and anxiety levels, as depicted in Figure 1.10. These behavioural traits are key to our investigation, as they provide insights into the potential effects of maternal hypothyroidism on offspring.

The brains of offspring from these mice are subsequently carefully harvested and subjected to further morphological and molecular analyses, which form the core of this thesis study. For detailed information on the harvested brain data, please refer to the table presented in Supplementary Table 1.

In summary, our research model is based on maternal hypothyroidism induced by early gestational antithyroid treatment in mice, resulting in the behavioural deficits observed in juvenile offspring. This model will serve as a critical tool in our quest to elucidate the complex relationship between maternal thyroid function and the development of ASD.

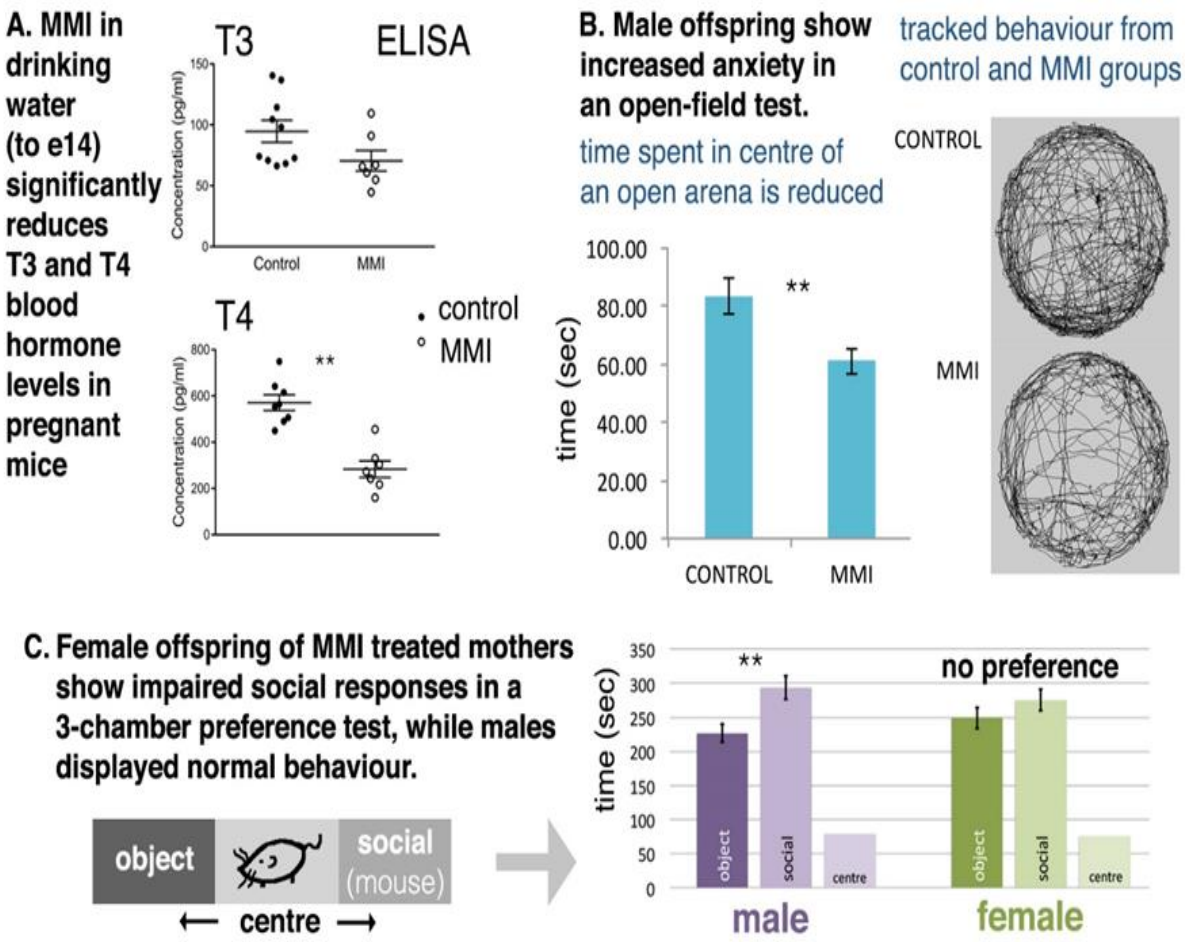

Figure 1-10 Impact of transient gestational hypothyroidism on offspring anxiety and social behaviour: A. Transient gestational hypothyroidism was measured via ELISA at T3 and T4 (leading to B) increased anxiety in male offspring and C) impaired social responses in female offspring in a three-chamber preference test. Adapted from (Pitsiani, Wilson et al. 2018).

Table 1 T4 concentration comparison between breeder groups

	MMI T4 pg/ml	Control T4 pg/ml
1	158	447.7
2	215	487
3	239	504
4	271	549
5	302	562
6	329	613
7	449	636
8		746

1.8 AIMS AND OBJECTIVES

ASD represents a complex and diverse range of neurodevelopmental conditions that have puzzled researchers and clinicians alike. Understanding the factors contributing to the onset of ASD is crucial for both research and clinical practice. This aims to investigate and analyse the neuroanatomical and molecular distinctions between the brains of a control group of mice and a transient maternal hypothyroid mouse model of ASD. To achieve this goal, we employed μCT technology to examine changes in neuromorphology and molecular alterations were assessed through immunohistochemistry.

Chapter II. Neuroanatomical Assessment: Large White Matter Structures and Cerebellar Components

We aimed to assess potential variations in CNS structures implicated in ASD pathology. Specifically, we examined large white matter structures such as the corpus callosum, fornix, external capsule, anterior commissure, and arbour vitae. We hypothesise that the transient maternal hypothyroid mouse model will exhibit significant neuroanatomical differences in these structures compared with those of control mice, potentially indicating a link between maternal hypothyroidism and ASD-related neuroanatomical changes.

III. Molecular studies in prenatal transient hypothyroid mouse brains

Chapter III delves into the molecular landscape of prenatal transient hypothyroid mouse brains. This part of our investigation aims to uncover the underlying molecular mechanisms and changes occurring in response to maternal hypothyroidism during critical developmental periods. We hypothesize that there will be altered expression of molecular markers associated with both hypothyroidism and ASD in prenatal transient hypothyroid mouse brains. These findings may reveal the molecular pathways through which maternal hypothyroidism affects neurodevelopment and contributes to ASD. Our study is unique in its focus on the indirect effects of transient maternal hypothyroidism, which is pharmacologically induced during the first trimester of pregnancy. This is a departure from previous studies that investigated primarily congenital or perinatal hypothyroidism.

IV. Molecular studies of postnatal day 30 (P30) transient hypothyroid mouse brains

Chapter IV extends our molecular investigations, shifting the focus to postnatal day 30 (P30) transient hypothyroid mouse brains. In this study, we explored molecular alterations to better understand the long-term consequences of transient maternal hypothyroidism. We hypothesize that P30 transient hypothyroid mouse brains exhibit enduring molecular changes, potentially indicating persistent effects of maternal hypothyroidism on neurodevelopment.

Common Experimental Aspects in Chapters 3 and 4

Within both Chapters 4 and 5, we undertake a common experimental aspect. This involves conducting a comparative analysis of key molecular markers across different developmental stages, aiming to identify patterns and changes that might provide insights into the link between maternal hypothyroidism and neurodevelopmental disorders such as ASD. The following genes were selected for analysis*: RoRα, TBR1,* and *Pax6.*

T-boxbrain1 (TBR1), a transcription factor from the T-box family, plays a major role in the development of various neurons, especially those in the cerebral cortex, and is a high-confidence risk factor for ASD (De Rubeis, He et al. 2014). Notably, TBR1 is highly expressed in the deep layers of the cerebral cortex, where it aids in differentiating projection neurons. Specifically, TBR1 expression begins at the onset of corticogenesis on embryonic day 10.5 (E10.5). Embryos show prominent TBR1 expression in the mantle zone and cortical plate of the telencephalic vesicle, as well as in the olfactory bulb and cerebellum. After birth, TBR1 expression levels gradually decline. Additionally, TBR1 is specifically expressed in the cells of the cerebellum's fastigial nucleus. The DCNs, which are generated between embryonic days 10.5 and 12.5, also express TBR1. TBR1 is linked to ASD, and patients with ASD often have mutations in one allele of TBR1 (Huang and Hsueh 2015). TBR1 is highly expressed in the cortex's deep layers, where it aids in differentiating projection neurons (Barnard, Jahncke et al. 2022). It is also known to regulate the expression of several ASD-related genes that are vital for cortical development (Chuang, Huang et al. 2015).In the cerebellum, TBR1 is specifically expressed in the cells of the cerebellum's fastigial nucleus (Green and Wingate 2014). Additionally, TBR1 is stimulated in pyramidal neurons treated with T3, a form of TH, suggesting its role in neuronal differentiation and proliferation (Teng, Liu et al. 2018).

Pax6, a paired homeodomain transcription factor, plays a pivotal role in various developmental processes within the CNS. Its expression patterns change dynamically during embryonic development, influencing neuronal fate specification and maintenance.

During early embryogenesis, Pax6 is expressed primarily in proliferative neuroepithelia. It persists in specific cell groups within the forebrain and hindbrain (Duan, Fu et al. 2013). Notably, at E11, Pax6 exhibits robust expression in the proliferative neuroepithelia of the ventricular zone in the forebrain and hindbrain. Additionally, it is present in the floor and the Mesencephalic reticular formation (mRt) in the midbrain. By E12, Pax6 expression emerges in the nucleus of the lateral lemniscus in the rhombencephalon but disappears from the midbrain floor.

Beyond its spatial expression, Pax6 has multifaceted roles in CNS development. It is essential for the development of all rhombic lip lineages, including granule cells cerebellar nuclear neurons and unipolar brush cells (Engelkamp, Rashbass et al. 1999, Englund, Fink et al. 2005). This is highlighted through studies on the *Pax6* mutant mouse (*Pax6*sey/sey) which underscore its role as a key regulator of cell survival in cerebellar nuclear neurons (Yeung, Ha et al. 2016). Pax6 along with other rhombic lip markers TBR1 and TBR2 is first detected in the rhombic lip and NTZ from E11.5 to E12.5 but expression is lowered as development progresses.

Genome-wide microarray analysis has identified downstream genes regulated by Pax6 in the developing cerebellum. Furthermore, Pax6 activates the expression of Tlx3, a homeobox gene, in cerebellar granule neuron progenitors starting at E15 (Divya, Lalitha et al. 2016)

Pax6. regulates processes such as proliferation, specification, differentiation, cell death, migration, and cell adhesion (Manuel, Mi et al. 2015, Ypsilanti and Rubenstein 2016, Kikkawa, Casingal et al. 2019). Additionally Pax6 is considered an ASD risk gene, influencing genes associated with ASD, including those involved in cell–cell

adhesion, ion transport, and transcriptional regulation (Kikkawa, Casingal et al. 2019) (Umeda, Takashima et al. 2010). It has been suggested that PAX6 for the mechanism of action of ASD environmental factors such as the anti-epileptic drug valproate (Kim, Lee et al. 2014). Genome-wide microarray comparisons between wildtype and Pax6-null cerebellar tissue have identified numerous differentially regulated transcripts, including those involved in the rhombic lip lineage (Ha, Swanson et al. 2012).

RAR-related orphan receptor alpha (RORα), a transcription factor, is expressed in many populations in the developing central nervous system (Ino 2004, Vitalis and Mariani 2018). It has a wide variety of functions in neural and nonneural tissues, including the regulation of many genes, which results in RORα controlling many physiological processes (Jetten 2009). In the developing cerebellum, RORα is expressed in Purkinje cells (Wilson and Wingate 2006). RORα serves as a specific marker for these cells. In mice, Purkinje cell precursors exit the mitotic cycle and the ventricular zone during E11–E13, and they begin to express RORα by E12.5 (Gold, Baek et al. 2003).

Studies have shown that RORα can bind to the promoter regions of more than 2,500 genes, 438 of which are included in autism gene databases (Hu, Sarachana et al. 2015). The consistent presence of Purkinje cell loss, abnormal neurotransmission, underdeveloped deep nuclei, and chronic neuroinflammation has been documented in patients with ASD (Fatemi, Aldinger et al. 2012, Stoodley, D'Mello et al. 2017). These characteristics are also found in mice deficient in RORα, and the function of RORα is known to be diminished in the brains of individuals with ASD (Sarachana, Xu et al. 2011, Guissart, Latypova et al. 2018). Therefore, examining RORα staining could increase our understanding of the role of the cerebellum in ASD and other

disorders related to neurodevelopment. The TH on the early dendritic differentiation process of Purkinje cells is known to depend on the nuclear transcription factor RORα (Vitalis and Mariani 2018).

In this thesis, we embark on a multifaceted exploration of neuroanatomical and molecular aspects, aiming to shed light on the intricate relationship between maternal thyroid function and neurodevelopment, with implications for disorders such as ASD. The subsequent chapters delve into specific objectives and methodologies to address these aims. The effects of transient depletion of TH on the early development of the avian cerebellum were previously examined. Early hypothyroidism in chicks disrupts the formation of the nuclei that comprise the output of the cerebellum well before TH-dependent events in cortical and cerebellar development (Delbaere, Van Herck et al. 2016).

Therefore, we hypothesized that thyroid-dependent cerebellar disconnection may underlie cognitive deficits in late life. Hence, transient early gestational hypothyroidism might result in discrete cerebellar functional and anatomical consequences that are distinct from the cortical phenotypes associated with late embryonic and early postnatal hypothyroidism.

Chapter 2: Assessment of the large white matter structures within a maternal hypothyroid mouse brain using a modified staining technique and X-ray absorption computed tomography (µCT).

2.1 ABSTRACT

X-ray absorption computed tomography (μCT) has faced challenges in neuropathology because of the low inherent contrast in soft tissues. In this study, we employed the established iohexol protocol, which is known for enhancing soft tissue contrast, to investigate neuroanatomical alterations in a maternal hypothyroid mouse model of ASD in comparison with those in untreated mice.

Our primary research objective focused on the Corpus callosum (CC), fornix, and deep cerebellar nuclei (DCNs) as potential structural biomarkers of ASD. Utilising high-resolution μCT imaging, we aimed to identify and delineate subtle neuroanatomical changes associated with ASD. Furthermore, we explored potential associations between these structural alterations and maternal hypothyroidism.

The iohexol staining protocol, with as little as 3 days of immersion, allowed us to achieve clear visualisation of white matter structures, which was further enhanced by reducing the interpixel distance of the μCT scanner to 9 microns. This technique enables precise imaging of brain structures, providing clear differentiation between gray and white matter.

This research highlights the utility of μCT imaging for investigating neuroanatomical changes associated with ASD, offering valuable perspectives on the potential effects of maternal hypothyroidism on the developing brain. While our findings were inconclusive, this research underscores the complexity of the relationship between maternal thyroid function and ASD, emphasizing the need for further exploration.

2.2 INTRODUCTION

ASD encompasses a group of neurodevelopmental disorders characterised by core symptoms such as impaired social communication and repetitive behaviours (DSM-5 2013). Despite its high prevalence, ASD remains a behaviourally defined disorder with no reliable biological markers, and its underlying pathogenesis remains poorly understood owing to the involvement of a wide variety of possible risk factors. One of these risk factors is the thyroid status of the mother during pregnancy, which has been linked to an increased risk of developmental problems (Ahmed 2018, Andersen, Andersen et al. 2018, Rotem, Chodick et al. 2020).

The most severe maternal hypothyroidism is associated with cretinism, a neurodevelopmental disorder characterized by cortical and cerebellar atrophy (de Escobar, Obregón et al. 2004). Additionally, evidence suggests that transient gestational hypothyroidism, although not leading to overt brain structure changes such as cretinism, is still associated with an increased risk of ASD (Perri, De Mori et al. 2021, Björnholm, Orell et al. 2023).Thus, transient gestational hypothyroidism represents an intriguing ASD risk factor to investigate, as it bridges the gap between possible environmental and genetic influences on ASD development.

To study the mechanisms linking transient maternal hypothyroidism to ASD, we employed a mouse model in which pregnant dams received either 0.1% MMI (in 0.475% sucralose) or the control (0.457% sucralose) in their drinking water between E0 and E13.5. This model targets a critical developmental window, as the foetus relies entirely on the mother for thyroid hormone during the first trimester of pregnancy in humans and E16.5 in mice (Moog, Entringer et al. 2017). While this model demonstrates behavioural pathology resembling ASD, the specific mechanisms

responsible for these effects are not fully understood. Therefore, it is essential to identify appropriate diagnostic studies to establish a link between the MMI group and ASD.

Over the last decade, several MRI studies have been conducted to detect neuroanatomical abnormalities in models of neurodevelopmental disorders, which have utilized comparative imaging studies in diagnostic research (Steadman, Ellegood et al. 2014, Stoodley, D'Mello et al. 2017). Although neuroimaging studies on ASD have shown some inconsistencies, there is overall evidence supporting alterations in white matter connectivity within the brain. However, these findings can be contradictory, with both atypical reductions and increases in CC size observed, depending on the age and the ASD clinical subgroup, mirroring the heterogeneity observed in other aspects of ASD pathology (Pina-Camacho, Villero et al. 2013, Pua, Bowden et al. 2017). Changes in white matter connectivity are likely contributing factors to key behaviours in individuals with ASD, including impaired social communication (Ameis and Catani 2015). In parallel, rodent studies have shown that early TH deficiency can lead to malformations in white matter tracts, with the CC being particularly vulnerable (Gravel, Sasseville et al. 1990, Ferreira, Pereira et al. 2007). Multiple genetic and environmental factors have resulted in changes in cerebellar morphology. Postmortem studies and responses to causal factors, such as ASD in animal models, reveal losses of key structures such as Purkinje cells. Furthermore, many disorders associated with malformations of the cerebellum, such as Joubert syndrome, present issues in social and cognitive function, such as ASD (Holroyd, Reiss et al. 1991).

Owing to the nature of the disorder, neuroimaging of ASD patients has struggled to account for the heterogeneity of genetic and environmental factors across individuals with the disorder. To mitigate these issues, neuroimaging studies have been performed on animal models with known ASD-linked genetic changes to reduce the number of confounding factors. To categorize ASD-related genes by their action on neuroanatomy, 26 genetic and behavioural models were examined (Ellegood, Anagnostou et al. 2015). Effect sizes were then calculated against the relevant control and compared across all models to attempt to create clusters. While changes were heterogeneous across the models, there were consistent changes in the parietal–temporal lobe, cerebellar cortex, frontal lobe, hypothalamus, and striatum (Figure 2.2.1) (Ellegood, Anagnostou et al. 2015).

A study examining three such models focused on morphological differences between their genetic mouse models and WT cerebellar structures. The selected SNPs were those in the Neuroligin-3 (*NL3 KI*) gene, an ASD-associated SNP that codes for a synaptic adhesion molecule; *MECP2*, which is associated with Rett syndrome; and Integrin β3 (*ITGB3*), a gene associated with serotonin transport and increased ASD susceptibility (Steadman, Ellegood et al. 2014). While anatomical changes were observed in all 3 models, all the changes were heterogeneous, suggesting differing mechanisms of action between the genes to reach similar cognitive phenotypes. Interestingly, changes were observed in ITGB3, where the DCN was bilaterally smaller, suggesting a change to the cerebellothalamic pathway.

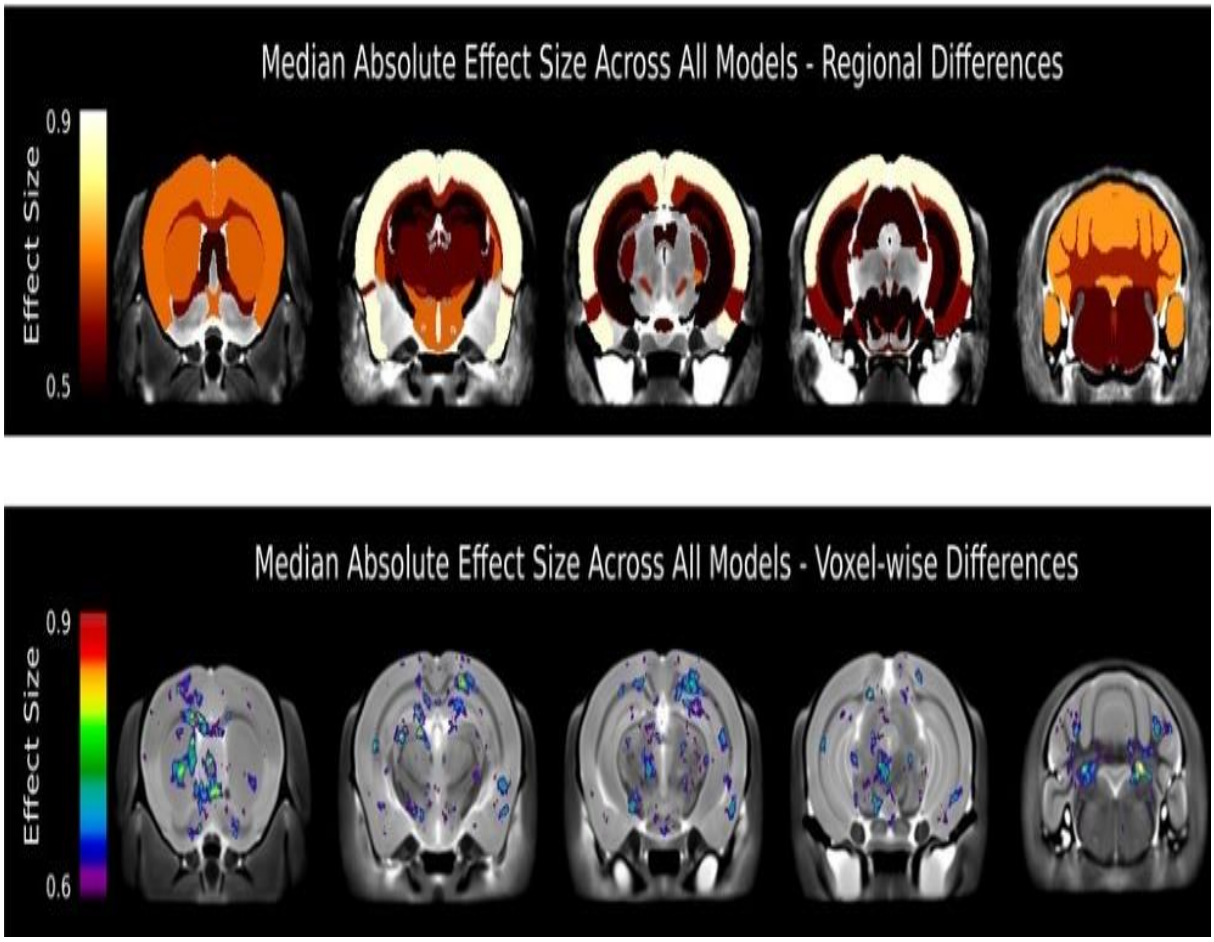

Figure 2-1 Median absolute effect size across 26 models: MRI scans of coronal brain slices showing the effect size of changes (based on Cohen's d) across 26 models of ASD. A) Regional differences in areas with an effect score greater than 0.5 in areas such as the cerebellar cortex (far right). B. Voxel differences with an effect score greater than 0.6 in areas such as the hippocampus itself (Ellegood, Anagnostou et al. 2015).

Furthermore, neuroimaging and histopathology studies related to ASD have consistently suggested atypical cerebellar development (Kelly and Strick 2003, Fatemi, Aldinger et al. 2012, Kelly, Meng et al. 2020). Similarly, in a chick model, early transient hypothyroidism disrupts the formation of cerebellar nuclei before TH-dependent events in cortical and cerebellar development (Delbaere, Van Herck et al. 2016). Therefore, neuroimaging studies can provide invaluable insights into the cause of ASD-like behaviour within our model.

For diagnostic and developmental studies, high-quality three-dimensional imaging of soft tissues at the micrometre scale has become essential. While MRI scanners have been the gold standard for neuroimaging because of their ability to provide excellent spatial resolution and soft tissue contrast between the grey and white matter of the brain, they are not without drawbacks. MRI machines are expensive to purchase and maintain and require up to 12 hours for image acquisition (Kircher and Willmann 2012). In contrast, Microcomputed tomography (μCT) has been widely applied in the diagnosis of mineralized tissues such as bones or teeth. However, its applications for soft tissues have been limited compared with those of MRI because of low X-ray attenuation in low-density materials. Moreover, even the most advanced MRI scans cannot achieve resolutions below 35 microns and may suffer from geometric distortions, leading to inaccuracies in measuring anatomical structures (Fransson, Merboldt et al. 2002). Researchers have used radio-opaque contrast agents to overcome these limitations and enhance contrast (Chen, Arad et al. 2018).

µCT can present a cost-effective alternative to MRI, which allows for rapid data acquisition. µCT scans work on the principle of attenuation of X-rays as they pass through an object (Boerckel, Mason et al. 2014). The attenuation of a sample depends on its density, making it useful for imaging high-density materials such as bone but poor at differentiating two objects of low attenuation. Therefore, µCT scans have struggled to acquire contrast between soft tissues such as white and gray matter in the brain due to the similar attenuation values of X-rays in low-density materials.

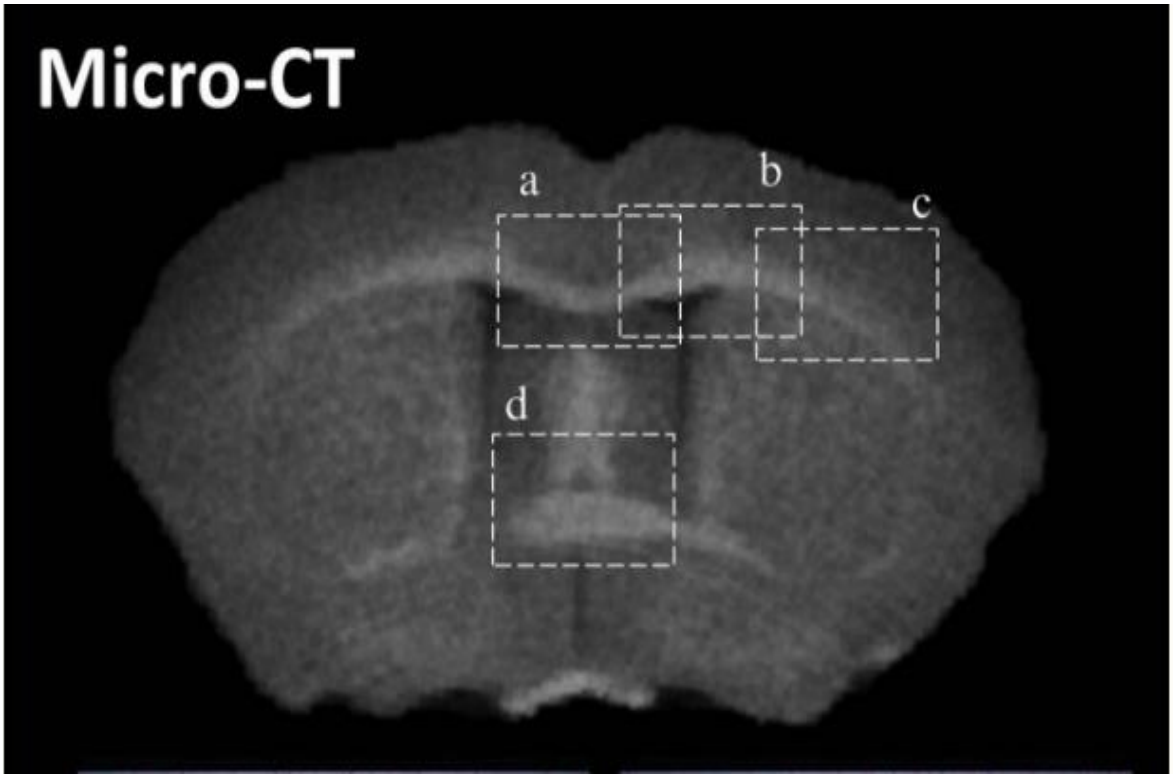

Figure 2-2 Contrast between white and grey brain matter after nonionic iodinated contrast agent staining: Coronal µCT image after 7 days in 150 mg/ml nonionic iodinated contrast agent. The white matter structures of the a) corpus callosum, (b) cingulum, (c) external capsule, and (d) anterior commissure are visible (Saito and Murase 2012).

To compensate for the lack of difference in this attenuation between tissue types, tissues have been perfused with radio-opaque dyes such as Phosphotungstic acid (PTA) or potassium iodide (Anderson and Maga 2015). Radio opaque dyes are water soluble and therefore result in better attenuation of vascular structures. While ionic iodine-based stains have proven successful for other tissues, they currently have not been proven to be an effective alternative for MRI clinical neuroimaging. A better contrast can be achieved via the use of nonionic, water-soluble contrast agents. As these stains are nonionic, they have a lower chance of unwanted interactions with biological structures such as peptides or cell membranes. Nonionic contrast stains such as iohexol can provide soft tissue contrast to identify white matter changes within the brain (Figure 2-2.) (Saito and Murase 2012, Miki, Sakuma et al. 2022). As staining techniques improve, µ-CT could be a reliable neuroimaging alternative to micro-MRI, making neuroanatomical studies less expensive faster and more widely available.

In this study, the nonionic contrast stain iohexol was used to achieve superior differential attenuation between grey and white matter. By employing this optimised contrasting protocol, we aimed to identify detectable anatomical and white matter structural changes in the MMI 14 mouse model compared with the control mice via contrast-enhanced µCT coupled with image analysis software.

2.3 METHODOLOGY

2.3.1 Contrast agents

The water-soluble nonionic iodinated contrast agent Iohexol (Omnipaque, GE Healthcare AS) has been used successfully by (Saito and Murase 2012) for soft tissue visualisation. The concentration of the dye supplied by the manufacturers was 300mg of Iohexol per mL. Iohexol was then diluted with 4% paraformaldehyde to the required concentration of 150–200 mg/mL. After rehydration, the brains were immersed in the diluted iohexol solutions and left for periods of between 3 days and several weeks before being scanned.

2.3.2 µCT scanning.

Forty-five mouse brains were scanned via a SkyScan 1027 scanner at 124 µA and 80 kV via a 1 mm aluminium filter. The brains were all scanned at 15× magnification, corresponding to an isotropic interpixel distance of 19.14 µm. Tomographic images were obtained via the 3D imaging software Tomomask. The brains were also scanned at isotropic interpixel distances of 9.0 µm (N=3) and 4 µm (N=4) on a SkyScan 1272 scanner, and the results were compared with those obtained using an isotropic interpixel distance of 19.3 µm.

2.3.3 Image processing

Skyscan NRecon software version 1.5.1.4 was used to reconstruct the projection data (Tarplee and Corps 2008). Having obtained the projection data in the form of an image stack of 2-D TIFF (tagged image file format) files, the data were viewed as a 3-D model via DISECT software (www.disectsystems.com; (Greco, Bell et al. 2014). The TIFF image stacks were loaded into the masking and segmenting software 'Tomomask' at full resolution (www. tomomask.com). The acrylic tube surrounding the brain was 'removed' from the images. These image stacks were then individually reloaded into Tomomask.

2.3.4 Quantitative image analysis and measurements

Corpus Callosum and Fornix

Volumetric measurements of the CC and fornix were taken from 20 (5 control females, 5 control males, 5 treated males, and 5 treated females) P30 juvenile brains, which were scanned at an isotropic interpixel distance of 19.14 µm. The CC and Fornix borders were manually traced and filled via the Tomomask paint mask feature. The sections were masked at the beginning of the first visible lateral ventricle, with every fifth section masked until the corresponding section in the contralateral hemisphere. The CC and fornix volume were obtained via Tomomask software by multiplying these areas by the section thickness and the intersection distance and summing the results of all the sections masked.

Total Cerebellum Volume and Dentate Nucleus

The total volume of the cerebellum was calculated from a cohort of 46 brains (12 control females, 11 control males, 13 treated males, and 10 treated females) at 19 µm through the whole masking of the cerebellum via the Tomomask paint feature. The criteria for masking the dentate nuclei were determined through comparison with a stereotaxic mouse atlas (Paxinos and Franklin 2019). Brains of suitable quality and contrast (n = 18; 7 controls and 11 MMI) were selected. The dentate nuclei on the right and left sides were measured separately for each mouse. Dentate nuclei were then masked via the paint mask feature of the Tomomask before the software was used to calculate the volume.

2.3.5 Statistical analysis

To determine the effect of maternal thyroid disruption on neuroanatomy in our experimental group. Differences in structure between treatment and sex were computed via two-way ANOVA. Further analysis of single-variable comparisons was performed via Student's t test. Statistical analysis was conducted in the R statistical environment. (https://www.r-project.org/).

Table 2.1 Criteria for exclusion of scanned brains.

Criteria	Description
Image Integrity	- Check for significant distortions or squishing in brain images. -Ensure intact brains. -Check for significant artefacts which may cover the area of interest.
White Matter and Grey Matter	- Evaluate distinguishability of white matter (axons) and grey matter (neurons). - Ensure that the staining has thoroughly penetrated the entire sample, allowing for complete Visibility
Image Distortions	- Assess distortions in brain images. - Verify alignment accuracy post-scanning.

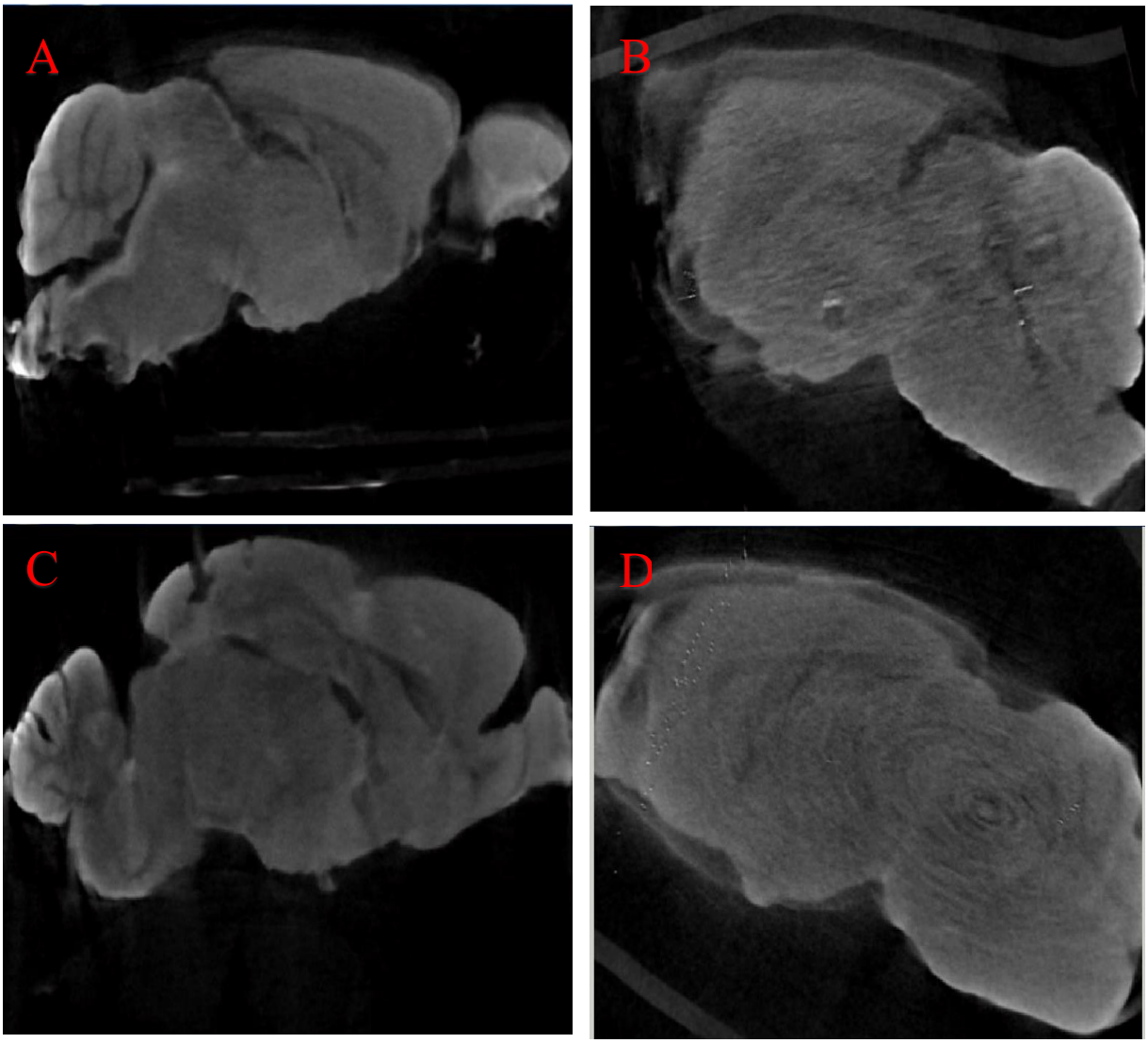

Figure 2.3: Artifacts Observed in Sections Post Micro-CT Analysis: Common artifacts identified in sections, leading to their exclusion from further analysis. **A** shows an example of tissue splitting along areas of interest. **B** illustrates compression artifacts, where tissue appears squished. **C** demonstrates image warping, which affects the cerebellum. **D** depicts heavy spiral artifacts.

2.4 RESULTS

2.4.1 Iohexol staining provides suitable white matter contrast.

Iohexol staining resulted in a clear visualisation of large white matter structures such as the CC; structural demarcations of the cingulum, amygdala, fornix, and arborvitae of the cerebellum (Figure 2.3 A, B, C). Furthermore, the scans followed these initial scans at an interpixel distance of 9 µm. While gross anatomical detail of large white structures could be seen in both scans, the reduction of the interpixel distance to 9 µm provided more detailed neuroanatomy and shaper outlines than those seen in the scanned images at an interpixel distance of 19 µm. This improved structural detail in the 9 µm scans allowed for the visualization of smaller neuroanatomical structures, such as the Mammillothalamic tract (mt) and the Fasciculus retroflex (fr) (Figure 2.3 D, E, F).

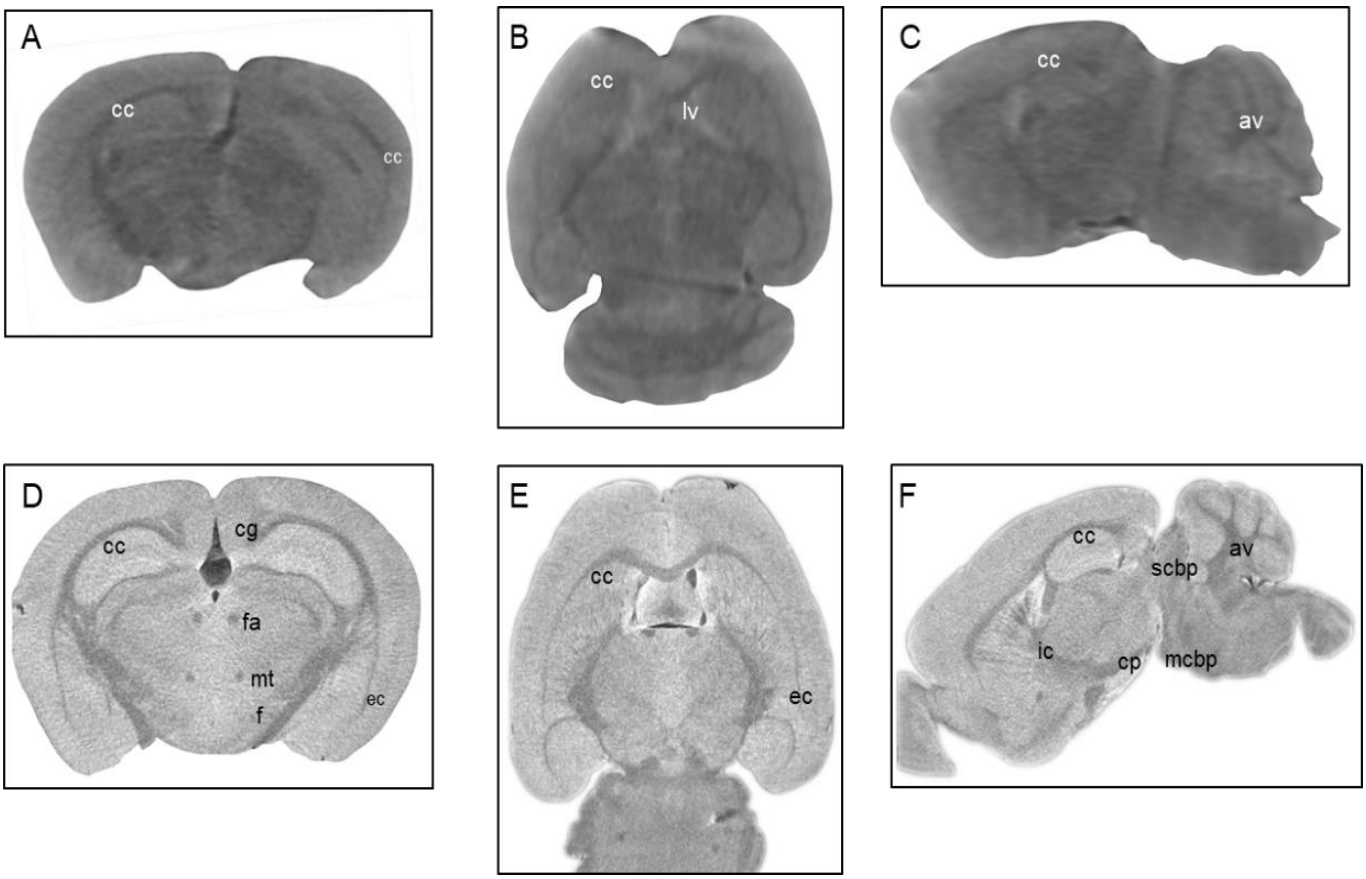

Figure 2-4: µCT scans of mouse brains after treatment with 150–200 mg/ml iohexol for 7–14 days. Panels A, B, and C were scanned at a resolution of 19.3 µm; panels D, C, and E were scanned at a resolution of 9 µm. Panels A, D: Coronal view; panels B and E: horizontal view; panels C and F: sagittal view. Many distinct white brain matter structures are visible in all panels of the corpus callosum (cc), cingulum (cg), external capsule (ec), anterior commissure (ac), fornix (f), mammillothalamic tract (mt), fasciculus retroflexus (fr), Arborvitae of the cerebellum (av), medial cerebellar peduncle (mcbp), superior cerebellar peduncle (scbp) and cerebral peduncle (cp) .

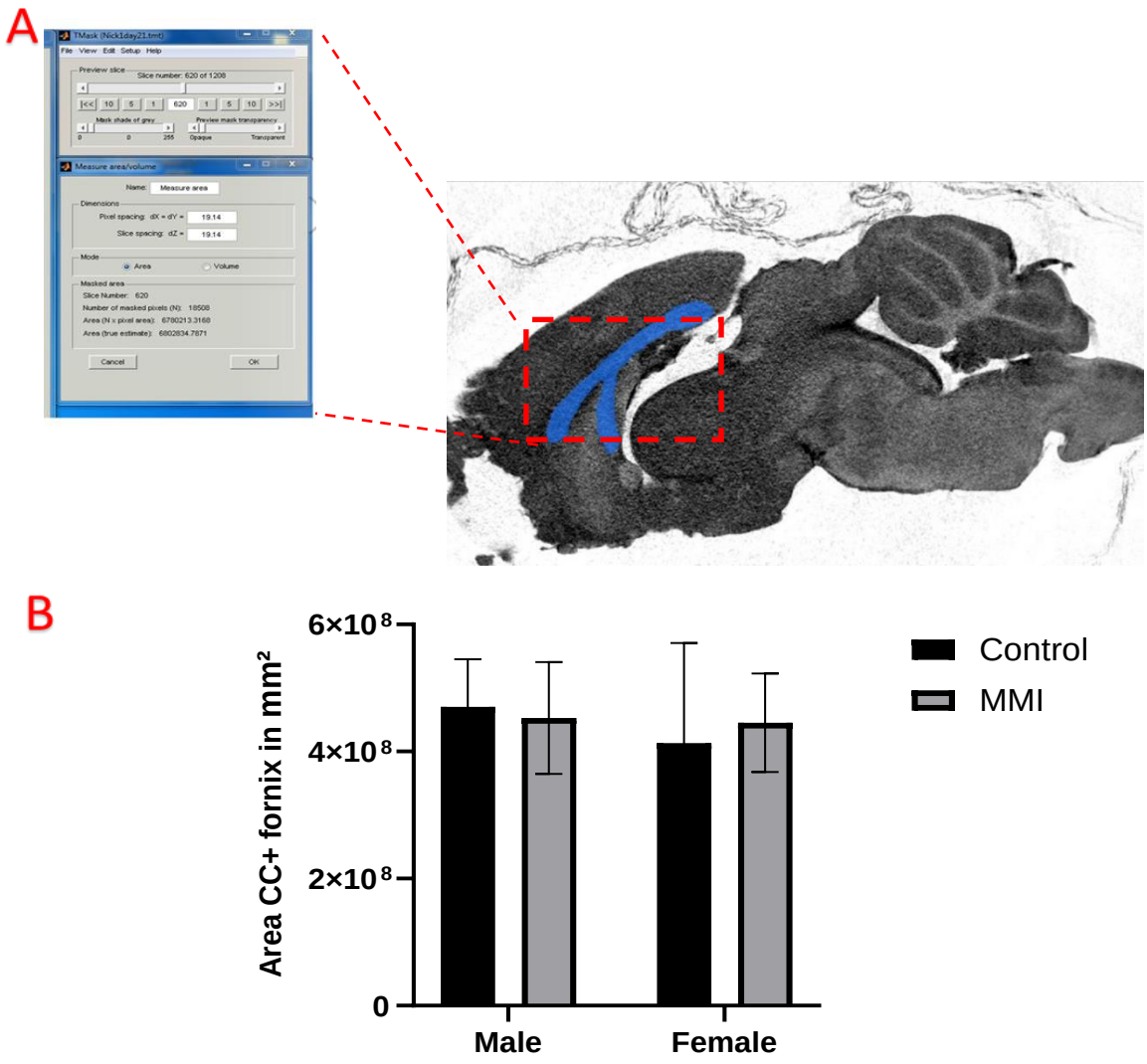

Figure 2-5 Comparative measurements of the total area of CC and Fornix using the Tomomask software:

A: Masking of Corpus Callosum (CC) and Fornix (masked in blue) within the Tomomask software on a 4 µm brain at three months old. The software measured masked pixels before converting the measurements into microns. B: Histogram: representing the area of the Corpus callosum (CC) and Fornix at the midbrain of 19 µm brain scans between Controls n= 21 (10 Male,11 Female) and the progeny of mothers given the antithyroid drug MMI during the early stages of pregnancy N= 22 (13 Male, 9 Female). Error bars represent the 95% confidence interval. .No significant difference was seen between the groups when grouped by treatment F=0.081 P= 0.777 or Sex F=0.982 P=0.328

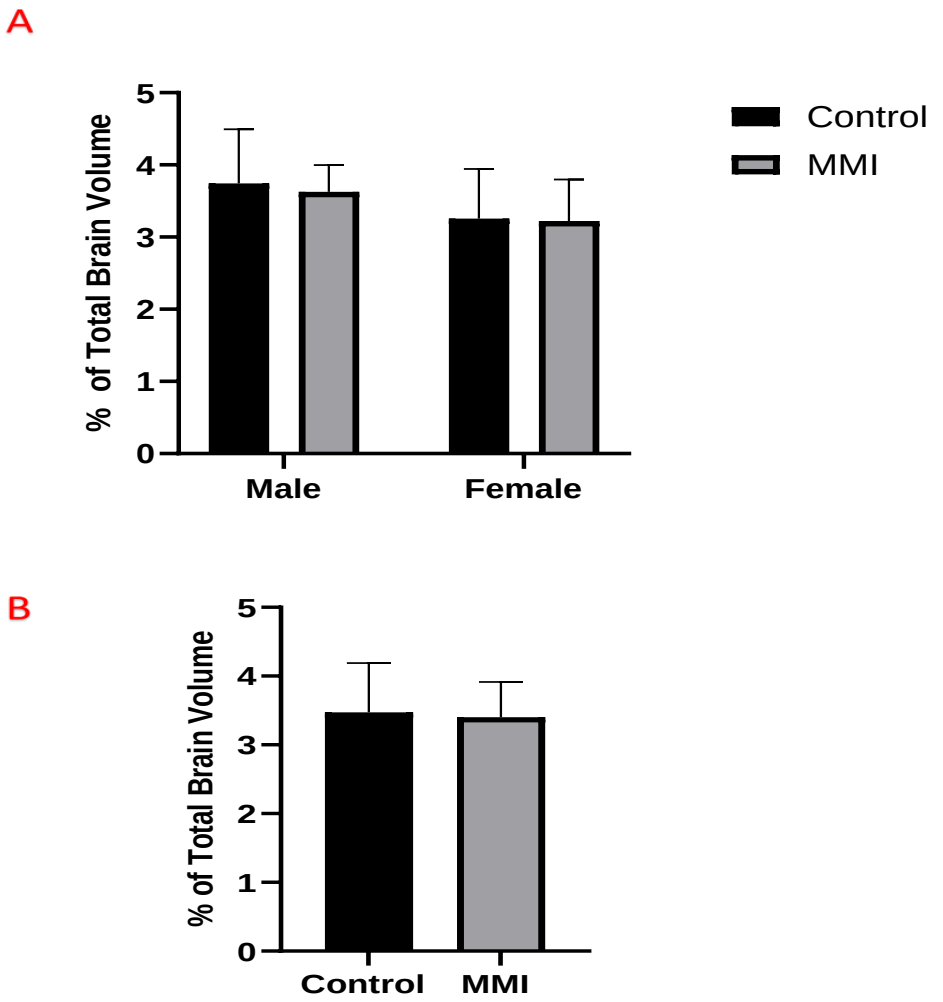

Figure 2-6 Comparative measurements of the size of the CC and Fornix as a percentantage of total brain volume using the Tomomask software: A): Histogram representing the % total of the brain volume of the Corpus callosum (CC) and Fornix 19 µm brain scans between Controls, n= 9 (4 males, 5 females), and the progeny of mothers given the antithyroid drug MMI during the early stages of pregnancy, n= 9 (4 males, 5 females). The error bars represent the 95% confidence intervals. The volumes of the corpus callosum and fornix were not significantly different, with p values of 0.8017 and 0.1490 for treatment and sex, respectively. B): Histogram representing the % total brain volume of the CC and Fornix between all control brains (N=10) and all MMI brains (n=10). The error bars represent the standard errors. The volumes of the corpus callosum and fornix were not significantly different (p=0.3647 F=1.949)

2.4.2 Comparative measurements of large white matter structures

Our initial analysis compared the total area of the CC and fornix between MMI and control brains at three months of age via 19.14-micron CT. We next proceeded to analyse the total volumetric difference in the CC and Fornix between MM1-14 and control brains at three months, adjusting for total brain volume. For the total area of the CC and Fornix, there was no significant effect for Treatment ($F=0.081$, $p = 0.777$) or Sex ($F=0.982$, $p=0.328$). (Figure 2.4).

Analysis of ex vivo structural CT data at 19.14 µm revealed no significant effect of treatment on the volume between MMI and control brains at three months ($F=0.06$ $P=0.8017$ and no significant effect was detected between the sexes ($F=2.333$, $p=-0.1490$))(Figure 2.5). To create a more statistically robust model, we performed a Student's t-test to compare the % volume of CC and fornix of all the MMI groups to that of all the controls, and the results remained insignificant ($p=0.3647$ $F=1.949$) Therefore our findings failed to confirm our initial hypothesis.

A

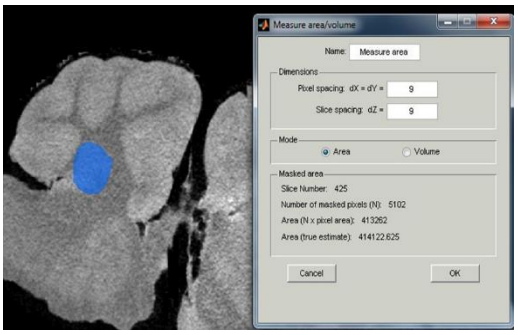
Measure area/volume
Name: Measure area
Dimensions
Pixel spacing: dX = dY = 9
Slice spacing: dZ = 9
Mode
Area
Volume
Masked area
Slice Number: 425
Number of masked pixels (N): 5102
Area (N x pixel area): 413262
Area (true estimate): 414122.625
Cancel
OK

B

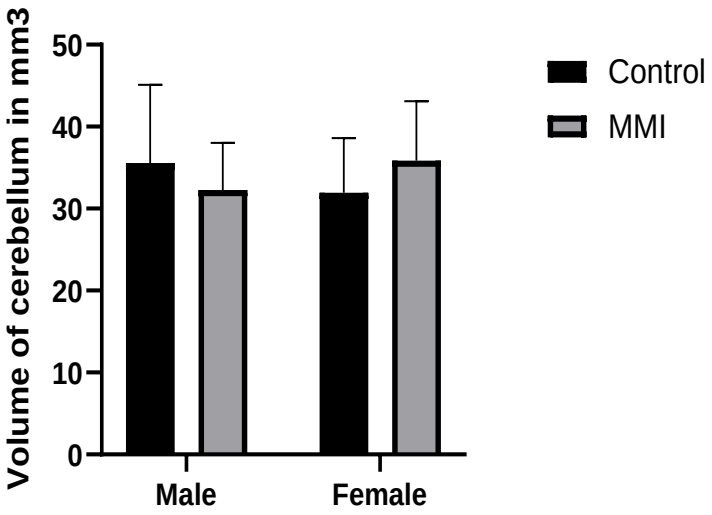
Volume of cerebellum in mm3
50
40
30
20
10
0
Male
Female
Control
MMI

C

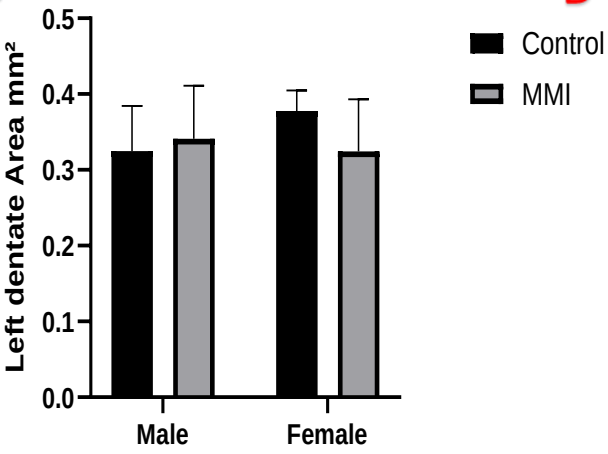
Left dentate Area mm²
0.5
0.4
0.3
0.2
0.1
0.0
Male
Female
Control
MMI

D

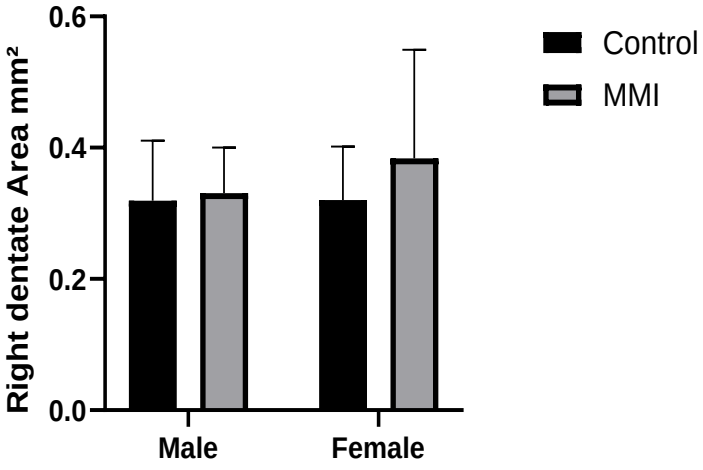
Right dentate Area mm²
0.6
0.4
0.2
0.0
Male
Female
Control
MMI

E

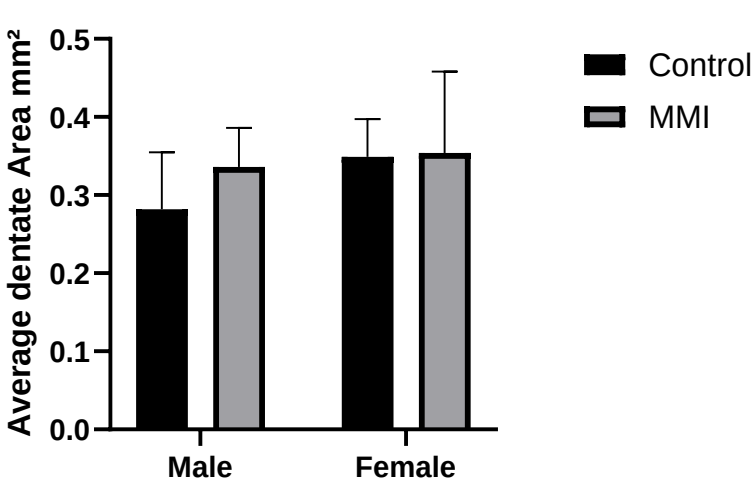
Average dentate Area mm²
0.5
0.4
0.3
0.2
0.1
0.0
Male
Female
Control
MMI

Previous page: Figure 2-7 Anatomical measurements of the cerebellum between MMI and control brains: (a) Measurement of the dentate nucleus through masking in the Tomomask software at 9 µm. (b) Bar plots representing the total volume of the cerebellum between controls, n = 21 (10 males, 11 females), and the progeny of mothers given the antithyroid drug MMI during the early stages of pregnancy, n = 22 (13 males, 9 females). No significant difference was observed between the groups when grouped by treatment (F=0.081, p=0.777) or sex (F=.0.982, p=0.3287) (c, d, e). Bar plots represent the area of the dentate nucleus at the left and right hemispheres and a combined average. The error bars represent the 95% confidence intervals. No significant difference was detected between any of the groups.

Left. Dentate: Treatment F=.208 P=.655 or sex F=0.113. P=0.742,

Right Dentate: Treatment F=0.402, P=0.536; sex F=0.427. P=0.524,

Average Dentate: Treatment F=0.180 P=0.678, Sex F=0.579. P=0.459

2.4.3 Comparative measurements of cerebellar structures.

A comparison of the total volume of the cerebella between control and MMI brains at 3 months of age via 19 µm scans revealed no significant difference between the groups ($F = 0.081$, $P = 0.777$; sex $F = 0.982$, $P = 0.328$; Figure 2.7). In addition, no significant differences were detected between the left dentate nucleus (treatment $F = 0.208$, $P = 0.655$ and sex $F = 0.113$, $P = 0.742$), right dentate nucleus (treatment $F = 0.402$, $P = 0.536$ and sex $F = 0.427$, $P = 0.524$) and average dentate size (treatment $F = 0.180$, $P = 0.678$ and sex $F = 0.579$, $P = 0.459$).

2.5 DISCUSSION

MMI treatment significantly decreased the T3 and T4 levels of mothers at 14 days gestation (Figure 1.10 Table 1.1). Further behavioural studies on the progeny of these mice revealed significant differences in behaviour in an open-field test of anxiety and a three-chamber test for sociability (Figure 1.10). These behavioural phenotypes are sex-specific, with male offspring showing heightened anxiety and female offspring showing reduced social interaction. These results are consistent with those of mouse models of ASD, suggesting that this is a reliable, simple mouse model of human ASD and that the first 13 days of pregnancy is a sensitive period for hypothyroidism. Second, we were able to obtain relevant neuroanatomical information via the nonionic contrast stain Iohexol (Figure 2.4). This allowed for the visualization of larger white matter structures such as the CC and fornix in low-resolution scans (Figure 2.5) and the measurement of smaller systems such as the dentate nucleus in high-resolution scans (Figure 2.7). This method's quick sample processing and size can provide an efficient methodology for visualizing brain structures. These benefits may prove helpful in reducing the cost and time needed for large-scale comparative studies in neurological disorders where there are proposed abnormalities in the white matter of the brain, such as ASD. However, this technique has not been without its critiques, as it was argued that despite the ability of non-ionic contrast agents to fully penetrate larger samples, such as adult brains, it did not provide as good contrast as other contrasting agents, such as osmium stain or iodine, at 3.5–4 μm (Pinto, Matula et al. 2022). However, the utilisation of iodine and osmium as staining agents in the examination of brain tissue samples poses significant obstacles. The application of iodine has been observed to reduce the size of these samples, thereby compromising their suitability for subsequent experimental investigations. On the other hand,

osmium, while effective, presents its own set of challenges due to its high toxicity and cost, which limits its practicality in the clinical environment.

We did not find any anatomical differences in the measurements of the CC and Fornix areas at the midline level (as shown in Figure 2.5). This contradicts some findings in ASD studies, where variations are often observed in the CC on the midsagittal plane compared with controls (Piven, Bailey et al. 1997, Hardan, Minshew et al. 2000). However, studies focusing solely on area measurements are currently less common.

Our study investigated the sexual dimorphism in the volume of the CC and fornix between male and female brains and between MMI brains and control brains. We conducted two-way ANOVA to compare the volume of the CC and fornix as a percentage of the total brain volume (Figure 2.6). Our results revealed no significant difference for either treatment or sex treatment ($F=0.081$, $p = 0.777$ and sex $F=0.982$, $p=0.328$). This finding suggests that there is no sexual dimorphism in the brain regions that we examined. This lack of change in white matter development in a sex-specific manner is inconsistent with previous data from early maternal hypothyroid mothers, which revealed differing white matter changes between males and females (Björnholm, Orell et al. 2023). Other studies that investigated maternal hypothyroidism and structures such as the corpus callosum revealed differences that lacked a sexual dimorphism component (Samadi, Skocic et al. 2015). Therefore, to investigate whether there was any change in the volume of the CC or fornix after MMI treatment, compared with the % volume independent of sex, we grouped males and females to create a more statistically powerful model. These results showed no significant effect, as indicated by the F score and p-value ($F=1.949$, $p = 0.3647$). This lack of significance suggested that a larger sample size or higher quality imaging, such as 9 µm or 4 µm scans, might have been necessary to achieve significant results using

this protocol. This is especially relevant considering that other studies have observed very small percentage changes with higher quality scans.; however, the priority should be to first investigate other brain regions at this quality to determine if there are any differences in sexual dimorphism. Overall, our study provides evidence that there is no sexual dimorphism in the volume of the CC or fornix between male and female brains and between MMI and control brains.

Our analysis does not account for the specific regional differences in CC size previously reported in ASD comparative studies. Previous results have shown that the anterior CC tends to be larger in ASD models, whereas the posterior CC shows signs of shrinkage (Samadi, Skocic et al. 2015). Therefore, further regionalization of our current measurements in the future would be of interest. We also need to account for our narrow window of maternal hypothyroidism, which is likely to have the greatest impact because, owing to the dependency of foetal thyroid hormone during this period, changes in CC are greater in mothers with multiple trimesters of hypothyroidism (Samadi, Skocic et al. 2015). In our study of white matter, the scope may have been too broad. While we observed trends, the results were not statistically significant. However, recent studies focusing on the microstructures of white matter within areas such as the corpus callosum, cerebellum, and bilateral thalami have revealed a strong correlation with hypothyroidism (Cooper, Kaden et al. 2019, Cao, Chen et al. 2023). These studies have taken a more targeted approach, examining specific subsections rather than the entire structure and showing results with microscopic diffusivity. This suggests that if we refine our approach and narrow our focus in future studies, we may uncover significant findings; however, to match the results seen from something such as microscopic diffusivity, it is likely that the experiment would need high-quality scans to remove artefacts. It would be beneficial

to reference these studies in future work to provide a foundation for this more targeted approach to data analysis.

We also failed to detect any significant differences in cerebellar volume between the control and MMI groups or between male and female mouse brains. A fundamental DCN in the dentate nucleus (Figure 2.7). The changes expected in these regions were subtle, and it is of little surprise that no change was observed when a small sample size was used.

This lack of significant difference in the anatomy of these brains suggests that the behavioural phenotype results from relatively subtle cell number changes, physiology, or connectivity. To further understand the link between maternal hypothyroidism and ASD, it will be necessary to survey these brain structures at the molecular level. Overall, we hope that future studies using this model will provide insight into the role that maternal hypothyroidism may play in the development of ASD and provide data that may be clinically useful in the future.

Chapter 3: Molecular studies in a prenatal transient maternal hypothyroid mouse model of autism spectrum disorder

3.1 ABSTRACT

This chapter delves into the intricate relationship between thyroid hormone (TH) disruption and autism spectrum disorder (ASD) in the context of early gestational antithyroid treatment in mice. Immunohistochemical (IHC) techniques were used to scrutinize the expression and localization of proteins related to ASD and TH disruption in the developing mouse cerebellum.

This research focuses on protein expression patterns, particularly those of markers such as TBR1, a distinguishing factor for fastigial nuclei (FNs), and RORα, which is essential for the early dendritic differentiation of Purkinje cells (PCs). Pax6, a marker specific to the granule cell layer, was also investigated.

This study involves IHC analysis of murine embryos, including those exposed to MMI, a TH-disrupting agent, and control embryos for comparison. The accuracy of IHC localization and quantification allows for a detailed examination of these markers, providing insights into their roles in cerebellar development and potential interactions with THs related to ASD.

This work serves as a link between THs, ASD-associated gene expression, and the complex processes that govern early cerebellar development. These findings illuminate the multifaceted factors contributing to neurodevelopmental disorders and the associations between early gestational TH disruption and ASD-related behavioural deficits.

By thoroughly examining the molecular landscape of embryonic mouse brains via IHC, this chapter enhances our understanding of the network of genes potentially involved in ASD and TH disruption. These findings emphasize the complexity of early cerebellar development and underscore the pivotal role of our IHC method in revealing the intricate molecular relationships involved in this process.

3.2 INTRODUCTION

In the exploration of ASD aetiology, the traditional focus has been on the prefrontal cortex and limbic system, but there is now a growing acknowledgement of the pivotal role of the cerebellum (Schmahmann, Guell et al. 2019), where outwards connections such as the cerebello-thalamocortical pathway orchestrate brain-wide inputs and outputs (Ramos, Balardin et al. 2019, Kelly, Meng et al. 2020, Su, Xu et al. 2021). While the primary output of the cerebellum's cognitive function has traditionally been thought to be the dentate nucleus, recent studies have provided further support for the roles that the interposed and fastigial nuclei play in moderating cognitive effects in the brain and mediating behaviours (Behnke, Stevenson et al. 2018, Carta, Chen et al. 2019, Judd, Lewis et al. 2021). Intriguingly, studies in chick models have revealed the consequences of direct thyroid interference in cerebellar nuclei and Purkinje cell dendritic outgrowth (Delbaere, Vancamp et al. 2017). Epidemiological studies have underscored the correlation between maternal thyroid status and ASD (Andersen, Andersen et al. 2018), highlighting the importance of comprehending the biological pathways at play. The presence of thyroid receptors in the foetal brain and the role of THs in critical developmental processes such as neuronal migration and synaptogenesis offer a compelling framework (Mohan, Sinha et al. 2012). The cerebellum, a shared nexus in ASD and hypothyroidism, merits special attention, given its role in the cerebello-thalamo-cortical pathway. Markers such as TBR1 and PAX6, which are intimately linked to ASD pathology, prompted us to delve deeper into their mechanistic involvement (Jeon, Kim et al. 2014, Den Hoed, Sollis et al. 2018).

In this chapter, we aim to assess whether the cerebellar disruptions observed due to direct thyroid interference in a chick model can be extrapolated to our transient maternal hypothyroid mouse model (Delbaere, Van Herck et al. 2016). This investigation holds the key to unravelling how hypothyroidism may underlie ASD-like behavioural phenotypes during early brain development and sheds light on whether it is divergent in early developmental pathways between chick and mouse models. Our molecular analysis focused on examining markers associated with glutamatergic neurons within the cerebellar nuclei and granule cells, including TBR1 and Pax6. Additionally, we will investigate markers indicative of changes in cerebellar morphology, such as those linked to Purkinje cells, such as RoRα (see section 1.8 for marker descriptions). Expanding our analysis into the thalamus, we will employ PAX6 as a marker to investigate the projection targets originating from the cerebellum within the cerebello–thalamo–cortical pathway. We anticipate that alterations in the expression patterns of these markers will provide critical insights into how hypothyroidism impacts cerebellar neurogenesis and its broader implications.

3.3 METHODOLOGY

3.3.1 Sections

Tissue collection and preparation:

Fixed paraffin-embedded C57BL/6 MMI-treated mouse brain tissue at E16.5 was provided by our collaborator, Dr. Richard Wingate, from King's College London. Additionally, a set of control brains from C57BL/6 mice at E16.5 was also provided by Dr. Richard Wingate.

Additional Control Group:

In addition to the brains provided by Dr Richard Wingate, we obtained another set of six formalin-fixed untreated E16 C57BL/6 mouse control brains from Charles River.

Paraffin Embedding Preparation

Fresh paraffin was prepared on the day of embedding by melting paraffin wax at 80°C. The melted paraffin was poured into clean plastic moulds of appropriate sizes and left undisturbed to cool and solidify. The paraffin-embedded blocks were stored in an oven at 80°C to maintain them in a molten state until further use.

3.3.2 Dehydration and clearing

The process of dehydration was carried out to remove water and prepare the samples for embedding. This was achieved via the addition of a series of ethanol solutions on a nutator with gentle rocking. The samples were first placed in 70% ethanol and left overnight. This was followed by a one-hour immersion in 95% ethanol. The samples were then subjected to another 30-minute immersion in 95% ethanol. The samples were subsequently immersed in 100% ethanol for one hour and then for an additional 30 minutes. This sequential process ensured the effective dehydration of the samples.

Following the dehydration process, the samples underwent a clearing process to achieve tissue transparency. This involved placing the samples in Histoclear (National Diagnostics NAT1330) in an incubator with gentle rocking for one hour. The clarity of the tissues was assessed post clearing. If optimal transparency was not achieved, the samples were returned to Histoclear for an additional 30 minutes. This clearing process was repeated until satisfactory transparency was obtained.

After clearing, the tissues were ready for infiltration and embedding. The cleared tissues were infiltrated with molten paraffin at 80°C. This infiltration process involved two sequential one-hour immersions in paraffin. This ensured that the tissues were thoroughly infiltrated and ready for the embedding process.

3.3.3 Tissue Orientation

Cooling and orientation: To orient the tissues properly within the paraffin blocks, the moulds were allowed to cool until a thin white bottom layer of wax formed. Flame-polished pipette tips were used to carefully orient the samples to the desired position before the paraffin solidified completely.

Tissue sections for immunohistology analysis were obtained via a microtome (Leica Microsystems). Coronal sections, 16 µm thick, containing the cerebellar nuclei and thalamus were sequentially cut from paraffin-embedded blocks. The sections were collected on positively charged Superfrost glass slides (Thermo Scientific).

Deparaffinization

Sixteen-micron-thick paraffin sections were immersed in successive washes of Histoclear (2x).

5 min), 100% ethanol (3 min), 90% ethanol (3 min), 70% ethanol (3

minutes), 50% ethanol (3 min), 30% ethanol (3 min), and PBS (2x 5

Minutes).

Heat-based antigen retrieval.

Antigen retrieval was conducted via a protocol adapted from (Zaqout, Becker et al. 2020) using 0.1 M citrate buffer (pH 6). The container holding the slides was microwaved at 800 W in an antigen retrieval solution for exactly 8 minutes. Immediately after the solution started to boil, the container was left in the microwave for an additional 3 minutes. The container and its contents were then transferred to an ice box for cooling. For 10–15 minutes, the solution was allowed to cool to 50°C. The temperature of the solution was monitored via a thermometer.

The container with the slides was then reheated in a microwave for another 3 minutes. The container was then transferred to an ice box where the solution cooled to room temperature for 30--45 minutes.

Immunofluorescence

Following antigen retrieval, the sections were delineated via a liquid-blocking Super-PAP pen and subsequently blocked in 5% BSA for one hour at room temperature. Primary antibodies, including TBR1 (ABCAM ab31940), BIIIT anti-mouse (Sigma T8660), -RELN (Developmental Studies Hybridoma Bank, catalogue #R4B), -RORα (Developmental Studies Hybridoma Bank), -NeuroD2 (Developmental Studies Hybridoma Bank), and monoclonal Pax6 (Developmental Studies Hybridoma Bank, catalogue No. PAX6), were prepared. These antibodies were diluted in 1% BSA in a permeabilization solution to a final dilution, as specified in Table 2.1. The diluted antibodies were added to the corresponding slide, which was covered with parafilm to prevent evaporation, and incubated overnight at 4°C.

After incubation, the slides were washed twice in PBS for 10 min and once for 10 min in a permeabilization solution of 0.25% PBS/gelatin/Triton. The slides were subsequently incubated overnight at 4°C in 1% BSA with secondary antibodies and permeabilized with 0.25% PBS/gelatin/Triton solution containing 1/1000 DAPI (Sigma). The secondary antibody Alexa 488-conjugated anti-rabbit was used for TBR1, and Alexa 568-conjugated anti-mouse was used for the remaining antibodies.

Following secondary antibody incubation, the slides were washed three times in PBS for 10 minutes and once in a 10 mM CuSO4/50 mM NH4Cl solution for 10 minutes. The slides were then mounted with a coverslip for long-term storage via Flouromount (Fisher 00--4958--02). The sections were observed, and images were captured systematically at different magnifications ranging from 5X to 20X via an inverted fluorescence microscope (Zeiss, Axio Observer Z1).

Table 3.1 List of Antibodies used for IHC experiments.

Primary Antibody	Stored concentration	5ug/ml in 200µl	As a dilution	Secondary antibody
Pax6 61µg/ml (DSHB)	30.5µg/ml	32.78ul (40µl)	1 / 6	Alexa Fluor Anti Mouse 548 Igg 1/400
NeuroD2 68ug/ml (DSHB)	34ug/ml	29.4ul (40µl)	1/6.8	Alexa Fluor Anti Mouse 548 Igg 1/400
RoRα 42ug/ml (DSHB)	21ug/ml	47.6ul (50µl)	1/5.6	Alexa Fluor Anti Mouse 548 Igg 1/400
TBR1 ABCAM ab31940	N/A	N/A	1/200	Alexa Fluor Anti Rabbit 488 1/400

3.3.4 Semiquantitative analysis

For each strain, we established cell detection parameters. We selected standard-sized areas based on the normal staining patterns of our region of interest from the Allen Brain Atlas http://atlas.brain-map.org/. Within these areas, we counted cells that tested positive via the positive cell detection command in QuPath software (Bankhead, Loughrey et al. 2017). This process provided the total number of positive cells within the annotated area.

To ensure no variance in measurement across all control samples of a stain, we determined the standard parameters of the staining threshold, cell size, and Gaussian sigma. This helped us remove potential artefacts and background.

We further classified tissue staining according to staining intensity. This was accomplished by applying manually created thresholds using a minimum of three slides per primary antibody of interest. To eliminate potential measurements of nonspecific binding and staining artefacts that could influence the density percentage, we utilized standard region sizes and regional areas. Specifically, we ensured that any unwanted background staining or other artefacts, which might have inadvertently been stained but were not our cells of interest, were excluded from our measured data. The percentage represents the proportion of positive cells in relation to the total cell count within the analysed area.

3.3.5 Statistical analysis

Statistical analyses were conducted via GraphPad Prism version 10.0.0 for Windows, GraphPad Software, Boston, Massachusetts, USA, www.graphpad.com, as indicated in the text and figure legends. We performed a 2-tailed Student's t test to compare the MMI-treated group with the control group. Differences were considered significant when $p \leq 0.05$. The error bars in all the figures represent the ± SEM.

3.4 RESULTS

3.4.1 Induced transient maternal hypothyroidism affects TBR1 expression in the prepontine hindbrain of a 16.5-month-old mouse.

Our initial investigation focused on the effects of transient maternal hypothyroidism induced by MMI treatment on TBR1 expression in the cerebellar precursors of E16.5 mouse brains. This phenomenon was examined through immunohistochemical analysis of the E16.5 prepontine region, as illustrated in Figure 3.1.

The control group displayed extensive staining, primarily within the fastigial nucleus. This finding contrasted with that of the MMI-treated brains, which exhibited a significant reduction in TBR1 staining. A semiquantitative analysis of the TBR1-positive cells yielded noteworthy results. The data revealed a statistically significant difference in cell density percentage ($F=12.8$, $p = 0.0334$). This finding was further supported by the results of the cell count analysis, which also revealed a significant difference ($p = 0.0255$, $F=296.5$).

3.4.2 Immunohistochemical analysis of RoRα staining in early 16.5 embryonic mouse brains.

We observed a specific pattern in the immunohistochemical staining of RoRα in early 16.5 embryonic mouse brains, with RoRα staining localising within the presumed Purkinje layer and EGL (Figure 3.2). A semiquantitative analysis was conducted to assess the density of RoRα positive cells in both the MMI-treated and control brains. The analysis revealed a decrease in Purkinje cell density in the MMI-treated brains, with a statistically significant p value ($p = 0.0135$), although the F value was not significant ($F=1.098$). These findings suggest potential effects of MMI on Purkinje cell development.

3.4.3 Pax6 remains unchanged within the granule-cell layer of transient maternal hypothyroidism brains.

Immunohistochemical examination of the Pax6 marker in the E16.5 prepontine region revealed no significant alterations within the granule cell layer of transient maternal hypothyroidism brains. Consistent Pax6 staining was observed in both the control and MMI-treated brains, indicating stable Pax6 expression.

Further validation was sought through a semiquantitative analysis. The results did not reveal any statistically significant difference in the density of Pax6-positive cells ($p = 0.5497$, $F=3.263$) or in the level of Pax6 expression ($p = 0.6924$, $F=4.396$) between the two groups. These findings suggest that transient maternal hypothyroidism does not significantly affect Pax6 expression or the density of Pax6-positive cells.

3.4.4 Pax6 levels remain unchanged in the embryonic prethalamus after MMI treatment.

The examination of Pax6 staining in the prethalamus did not reveal any significant difference between the brains of the MMI-treated and control groups (Figure 3.4). This finding was further confirmed by semiquantitative analysis, which revealed no significant difference in Pax6 expression ($p = 0.6640$, $F=23.77$) between the two groups. These findings suggest that transient maternal hypothyroidism does not significantly affect Pax6 expression within the prethalamus.

16.5 Prepontine Hindbrain

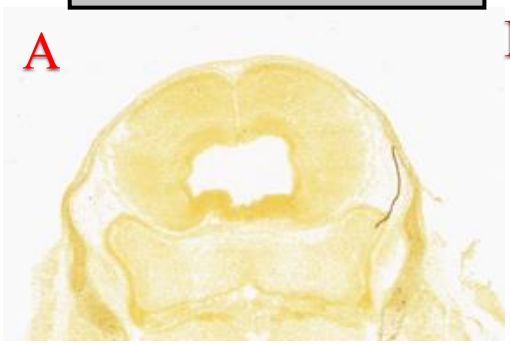

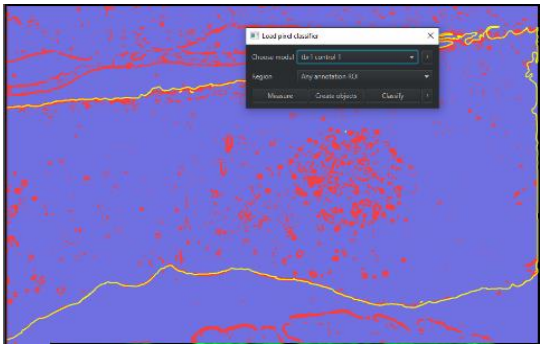

TBR1 10x

DAPI/ TBR1 10x

Control

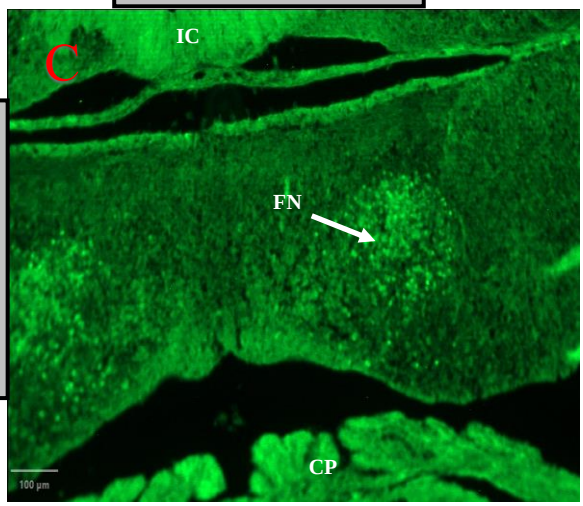

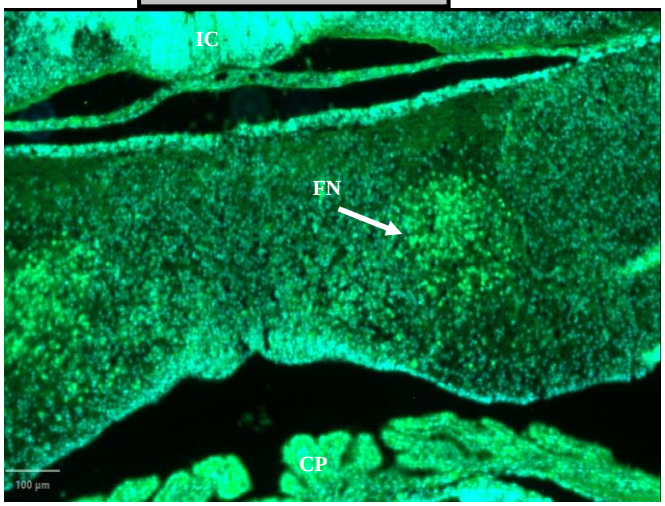

MMI

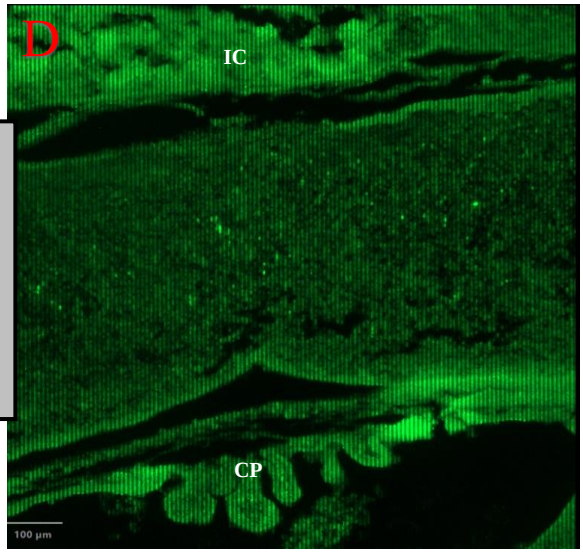

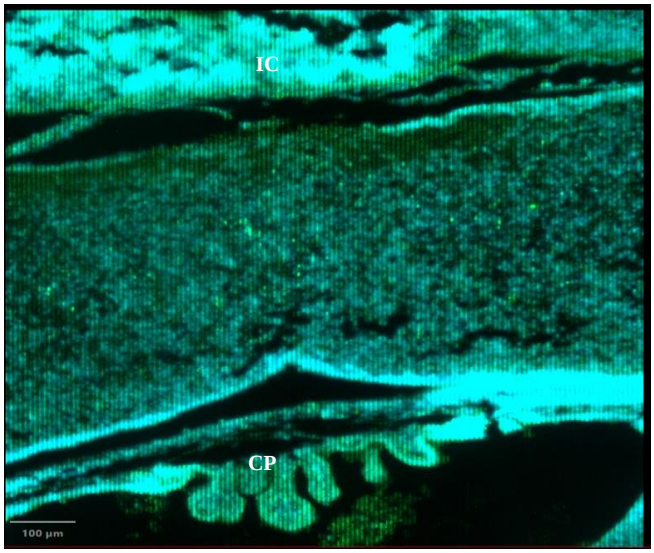

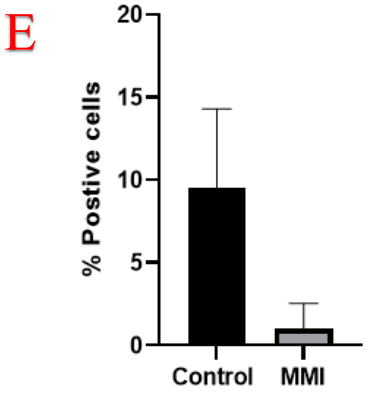

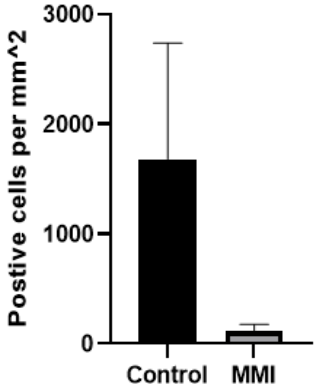

Previous page Figure 3.1 TBR1 staining in E16.5 cerebellum. (a): Section position represented in allen brain atlas E16.5 Coronal section http://developingmouse.brain-map.org/experiment/siv?id=100075063. (b) Quantification of positive cells within the cerebellar vermis using QuPath thresholding in the region of interest (ROI) (c) Representative images depicting TBR1 staining in the Fastigial Nucleus (FN) for the Control and MMI groups), respectively N=3 mice per group, with n=5 sections per mouse Scale bars: 100 µm. (c) Quantification of TBR1 staining using image analysis with the Qupath program, measuring the density of TBR1 expression in each group p=0.04 and the F=12.8. d) Quantitative analysis of the number of TBR1 positive cells in the cerebella. The percentage represents the proportion of positive cells in relation to the total cell count within the analyzed area . The p=0.0255 and the F=295.1. Data are presented as mean ± SD. The asterisk (*) indicates a p-value ≤ 0.05. Abbreviations: FN: Fastigial Nucelus, IC: Inferior colliculus CP: Choroid Plexus.

A

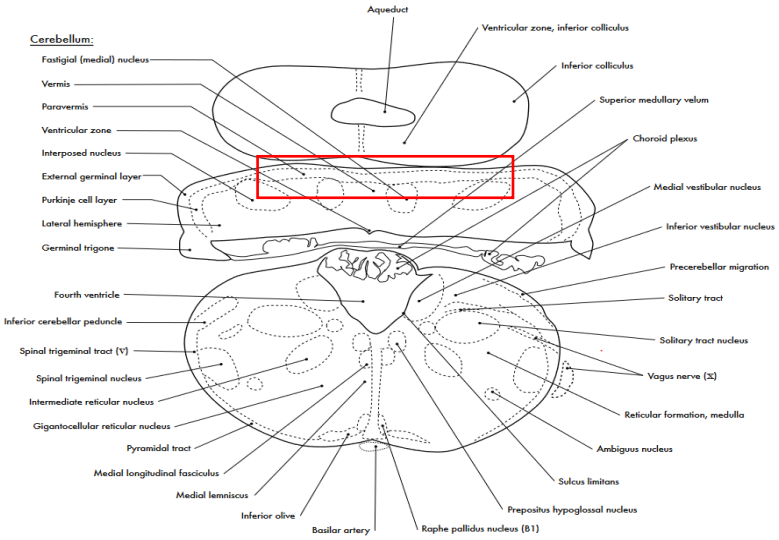
Aqueduct
Ventricular zone, inferior colliculus
Cerebellum:
Fastigial (medial) nucleus
Inferior colliculus
Vermis
Superior medullary velum
Paravermis
Choroid plexus
Ventricular zone
Interposed nucleus
Medial vestibular nucleus
External germinal layer
Inferior vestibular nucleus
Purkinje cell layer
Lateral hemisphere
Precerebellar migration
Germinal trigone
Fourth ventricle
Solitary tract
Inferior cerebellar peduncle
Solitary tract nucleus
Spinal trigeminal tract (V)
Vagus nerve (X)
Spinal trigeminal nucleus
Reticular formation, medulla
Intermediate reticular nucleus
Gigantocellular reticular nucleus
Ambiguus nucleus
Pyramidal tract
Sulcus limitans
Medial longitudinal fasciculus
Medial lemniscus
Prepositus hypoglossal nucleus
Inferior olive
Basilar artery
Raphe pallidus nucleus (B1)

B

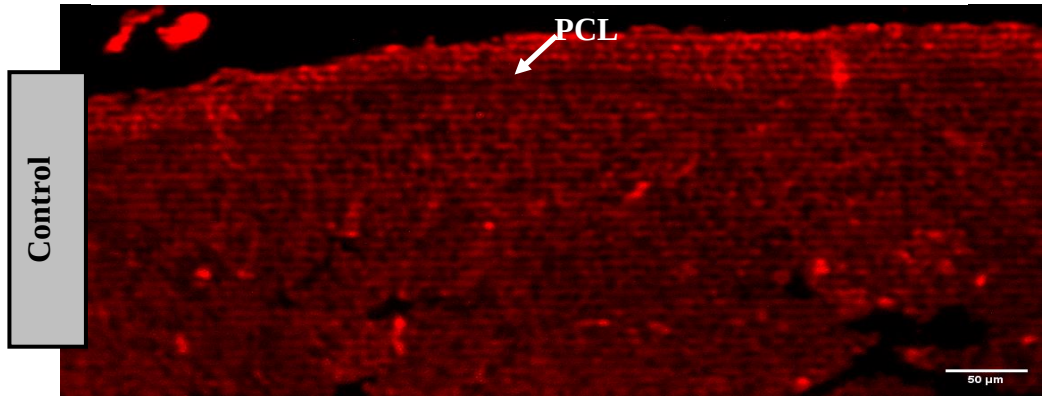
Control
PCL
50 µm

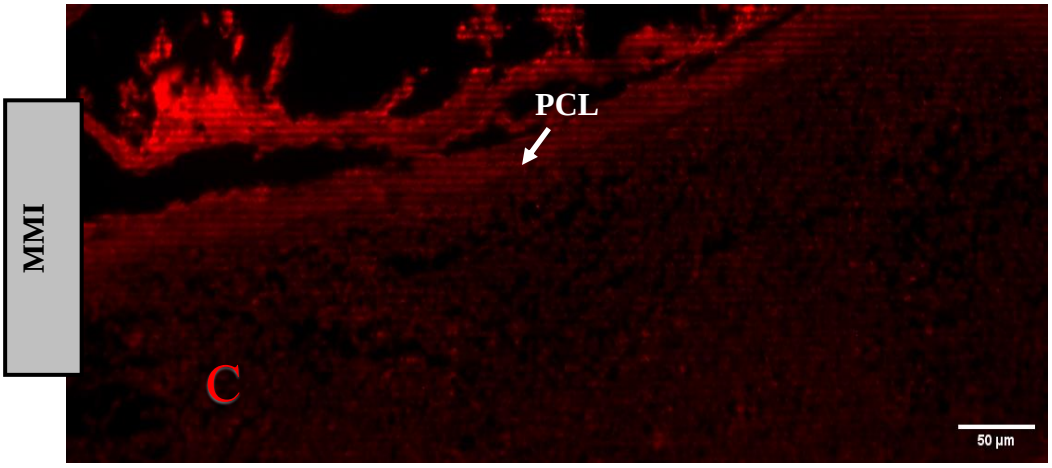
MMI
PCL
C
50 µm

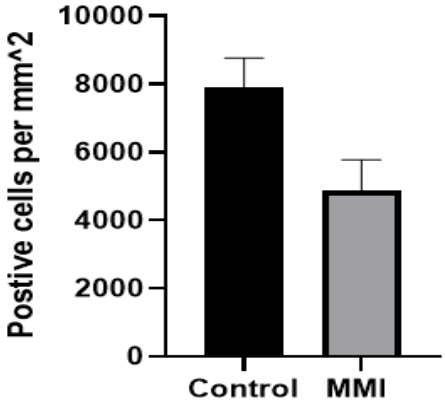
Postive cells per mm^2
10000
8000
6000
4000
2000
0
Control
MMI

Previous page Figure 3.2 RoRα staining of Purkinje cells in 16.5 cerebellum.

a) E16 brain atlas of coronal section of the cerebellum highlighting ROI (Schambra 2008) (b) Representative images of RoRα staining in the granule cell layer and Purkinje cell layer in the Control and MMI groups, respectively N=3 mice per group, with n=5 sections per mouse Scale bars are 50 μm. (b) Quantification of RoRα staining image analysis with the Qupath programme, measuring the density of RoRα expression in each group, Quantitative analysis of the number of RoRα -positive cells in the cerebella Data are expressed as mean ± SD *p value p value ≤ 0. P=.0.0135 F=1.098. Abbreviations: EGL: external granule layer, PCL: Purkinje Cell Layer

A

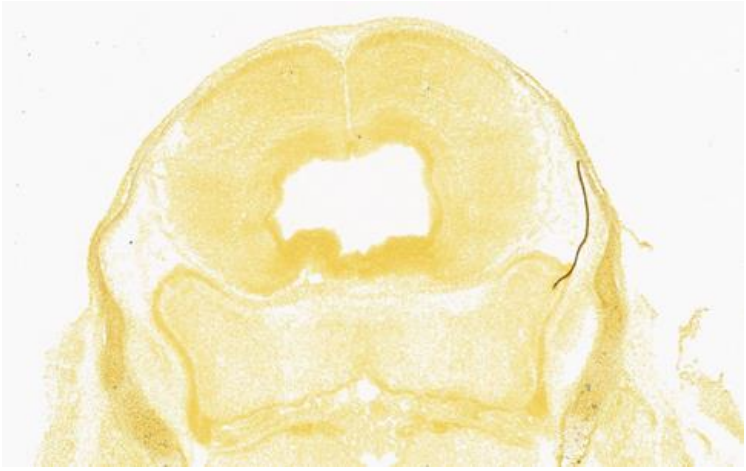

B

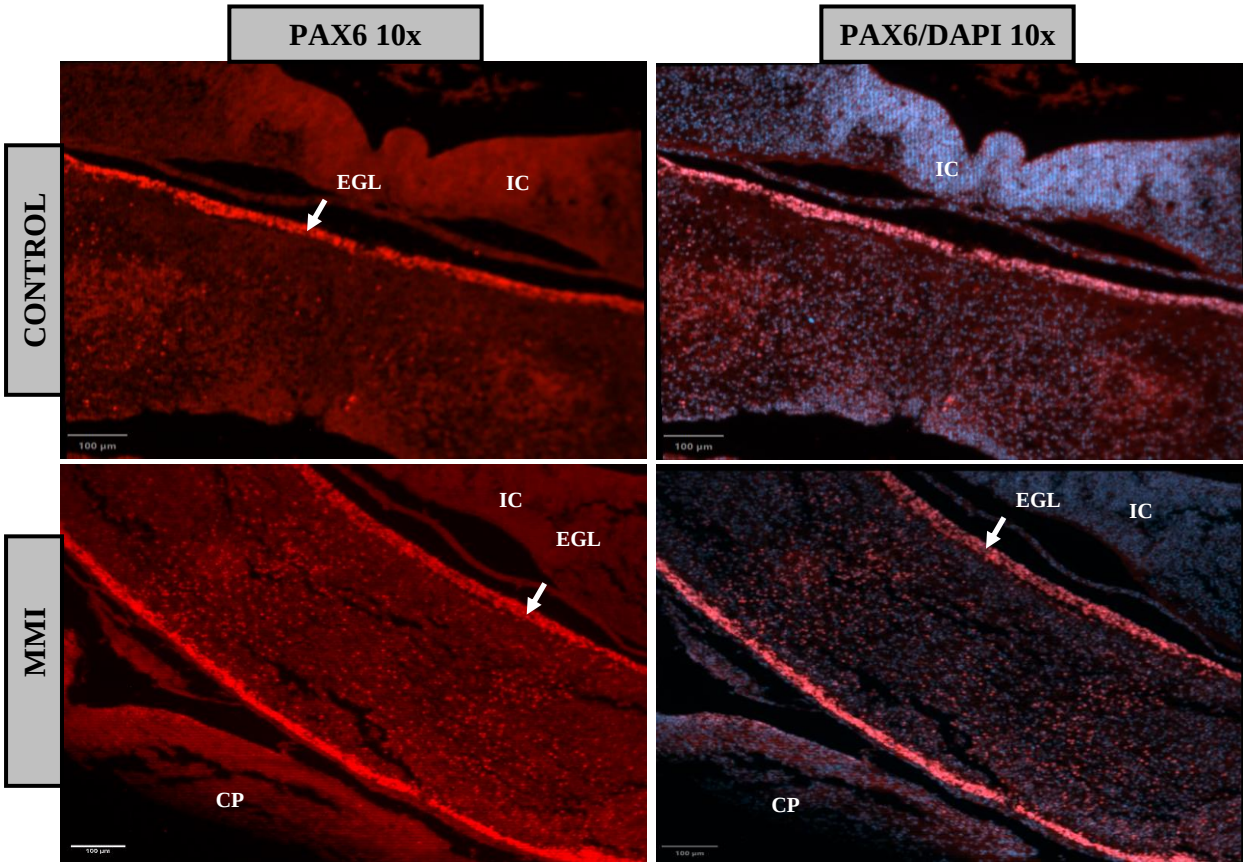
PAX6 10x
PAX6/DAPI 10x
CONTROL
MMI
EGL
IC
IC
IC
EGL
EGL
IC
CP
CP

C

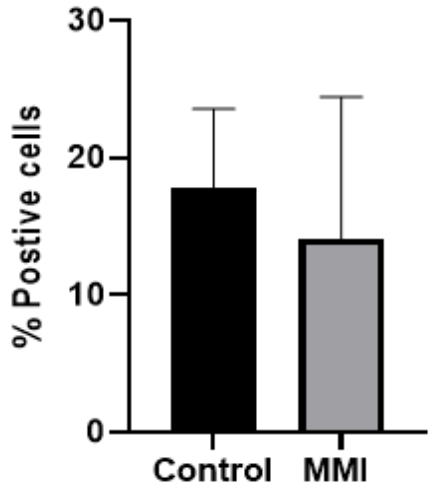
% Postive cells
30
20
10
0
Control
MMI

D

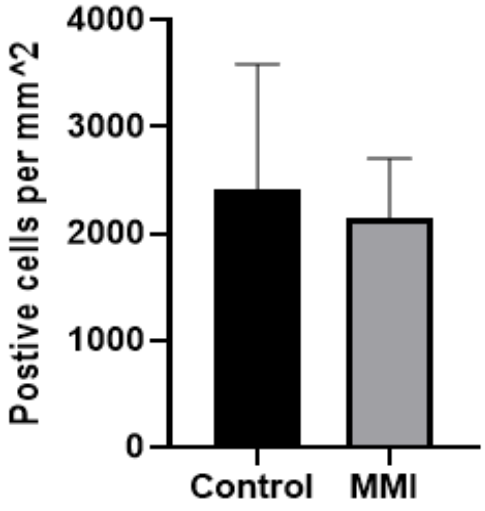
Postive cells per mm^2
4000
3000
2000
1000
0
Control
MMI

Previous page Figure 3.3 Pax6 staining in E16.5 cerebellum. Above: Section position in E16.5 mouse brain represented in Allen brain atlas http://developingmouse.brain-map.org/experiment/siv?id=100075063. (a) Representative images of Pax6 staining in the granule cell layer in the Control and MMI groups respectively N=3 mice per group, with n=5 sections per mouse Scale bars, 100 µm. (b) Quantification of Pax6 staining image analysis with the Qupath program measuring density of Pax6 expression in each group p=0.5497 F=3.263 c) Quantitative analysis of the number of Pax6 positive cells in the cerebella p=0.6924 F=4.396. Data are expressed as: mean ± SD *p value ≥0.05; Abbreviations: EGL: External Granule Layer, IC: Inferior colliculus CP: Choroid Plexus.

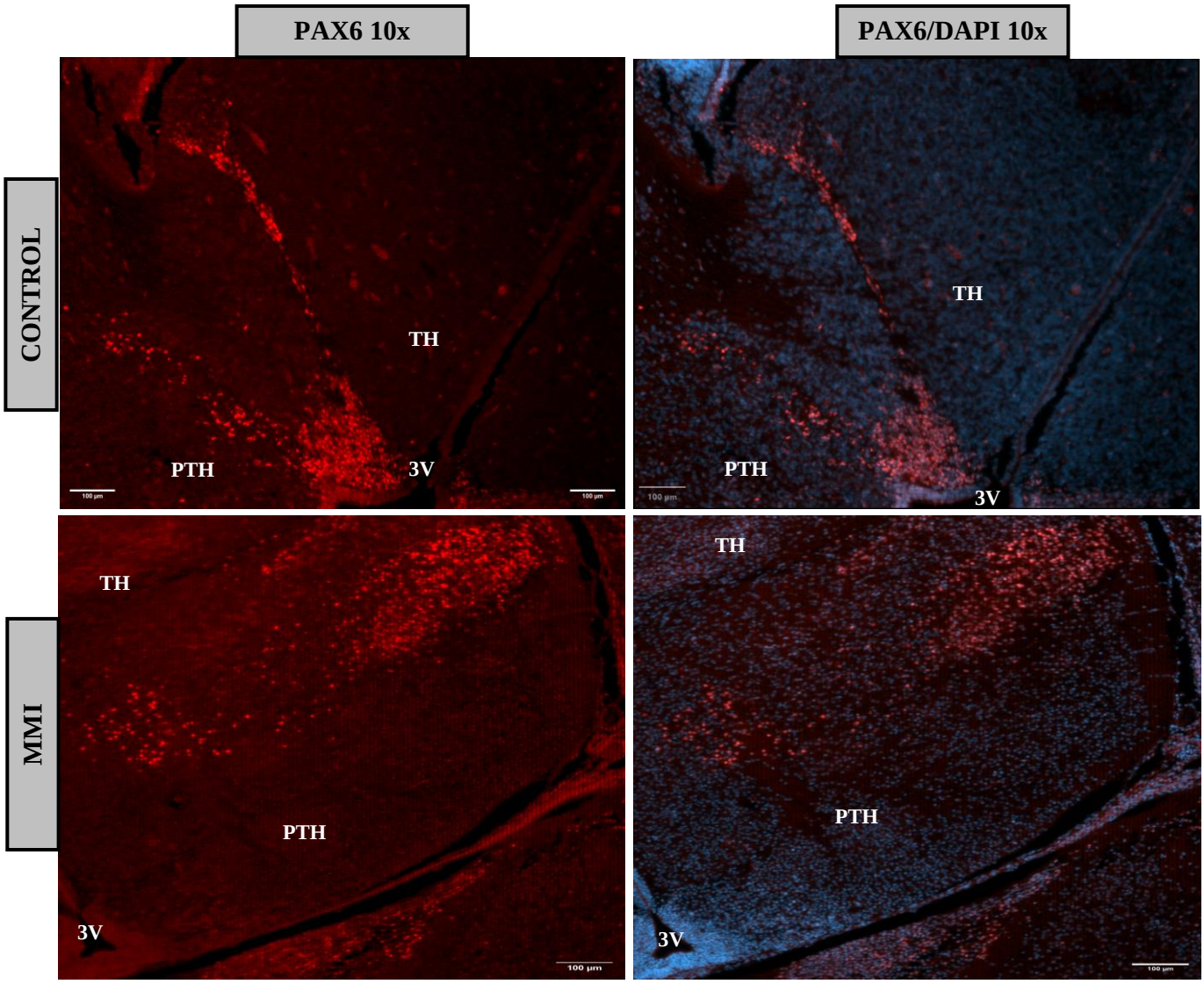
PAX6 10x
PAX6/DAPI 10x
CONTROL
MMI
TH
PTH
3V
100 µm

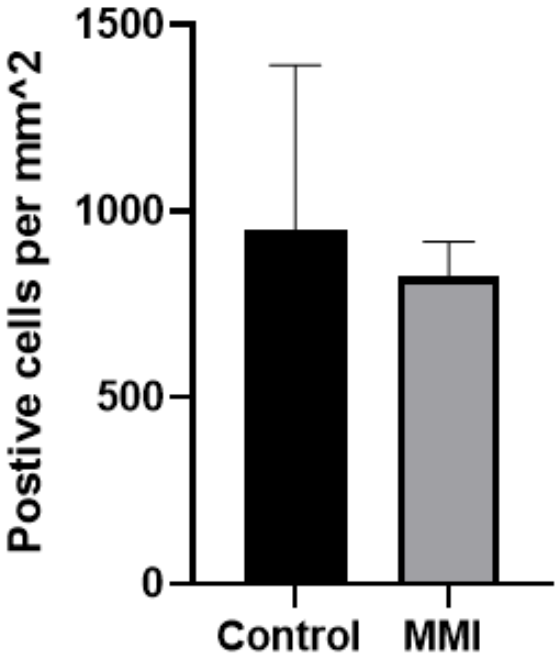
Postive cells per mm^2
1500
1000
500
0
Control
MMI

Previous page Figure 3.4 Pax6 staining in E16.5 Prethalamus. (a) Representative images of Pax6 staining in the E16.5 Prethalamus in the Control and MMI groups respectively N=3 mice per group, with n=5 sections per mouse . Scale bars are 100 μm. (b) Quantification of Pax6 staining image analysis with the Qupath programme, measuring the density of Pax6 expression in each group Quantitative analysis of the number of Pax6-positive cells in the cerebella p=6640 F=23.77. Data are expressed as mean ± SD *p value ≥0.05. Abbreviations: TH: Thalamus, PTH: Prethalamus 3V: Third Ventricle

3.5 DISCUSSION

3.5.1 MATERNAL HYPOTHYRODISM VIA PHARMACOLOGICAL BLOCKADE LEADS TO DISRUPTION OF RORα EXPRESSION IN E16.5 MICE CEREBELLUM.

We explored the impact of transient maternal hypothyroidism on the development of cerebellar neurons, with a particular focus on Purkinje cell staining via RoRα. This nuclear receptor is important for Purkinje neuron survival and differentiation (Takeo, Kakegawa et al. 2015). Our findings are consistent with previous research on mice with disrupted RoRα, which resulted in abnormalities similar to those observed in animals with hypothyroidism (Doulazmi, Frederic et al. 2001, Morellini, Lohof et al. 2023).

Our semiquantitative analysis revealed a statistically significant decrease in the density of Purkinje cells in the brains of MMI-treated mice ($p = 0.0135$), underscoring the sensitivity of developing neurons to maternal thyroid dysfunction.

Although the F value did not reach statistical significance ($F=1.098$), it is crucial to note that the p value was significant. This finding suggests that the reduction in Rorα staining in Purkinje cells is unlikely to have occurred by chance alone, even though the effect size is not substantial. The diminished Rorα staining in the Purkinje cells may indicate disrupted Rorα activity within these cells. Previous research has demonstrated that such disruption results in abnormalities consistent with those observed in animals with hypothyroidism (see Figure 3.2) (Boukhtouche, Brugg et al. 2010).Furthermore, connections among thyroid hormones, RoRα, and early Purkinje cell dendritic differentiation in cases of congenital or perinatal hypothyroidism have been established (Fauquier, Chatonnet et al., 2014; Yu, Iwasaki et al., 2015). Given the known influence of RoRα on early Purkinje cell dendritic differentiation, further investigation into the functionality of these Purkinje cells with reduced Rorα

expression is warranted. This exploration will help determine whether their behaviour remains consistent with that of other hypothyroid models.

The implications of our study extend beyond embryonic stages, echoing the behavioural effects discussed in section 1.6. Here, it was established that the P30 mouse model exhibited behaviours such as ASD.

Purkinje cells, which are integral to cognitive function, have been found to have significant associations with ASD. Postmortem examinations of ASD brains have revealed a reduction in the population of Purkinje cells (Skefos, Cummings et al. 2014, Wegiel, Flory et al. 2014) Furthermore, impairments in social behaviour and vocalizations, as well as abnormalities in Purkinje cell function and structure, have been observed in mouse models in which the ASD-related genes *Tcs1*, *Shank2*, and *Auts2* have been conditionally knocked out in Purkinje cells (Yamashiro, Hori et al. 2020) (Tsai, Hull et al. 2012, Peter, Ten Brinke et al. 2016)

In addition to these genetic models, drug-induced models have also provided insights into the role of Purkinje cells in ASD. For example, the valproate model of autism has shown that anomalies in cerebrocerebellar circuits are correlated with the number of Purkinje cells. This model has demonstrated that the loss of function of ASD-causing genes, specifically in Purkinje cells, is sufficient to drive ASD-like behaviour and functional deficits in forebrain regions traditionally implicated in social and cognitive control (Spisák, Román et al. 2019)

Our findings suggest that understanding this endophenotype at the prenatal level could provide valuable insights into the behaviours observed in juvenile mice. The potential connection between maternal thyroid dysfunction and ASD-related behaviours becomes more concrete as we continue to unravel this complex relationship.

However, it is important to emphasize that additional studies are needed to fully understand the transition of the endophenotype from the prenatal stage to the late juvenile stage.

3.5.2 MATERNAL HYPOTHYROIDISM VIA PHARMACOLOGICAL BLOCKADE EFFECT ON THE RHOMBIC LIP LINEAGE

Our investigation yielded significant findings when staining for TBR1-positive cells (p=0.0255) F (295.1), a well-established marker for the fastigial or medial cerebellar nucleus (Figure 4.1). Intriguingly, the temporal expression pattern of TBR1 aligns with the early presence of the Thyroxine transport marker MCT8 during chick development. This correlation highlights TBR1 as a compelling candidate for further exploration into potential cerebellar abnormalities arising from maternal hypothyroidism, as noted previously (Delbaere, Van Herck et al. 2016).

Despite its traditional association with connections from the spinocerebellar cortex to the brainstem and its role in balance, posture, and motor control (Coffman, Dum et al. 2011), increasing evidence suggests a significant role for the fastigial nucleus in behavioural traits. Lesions directly affecting the fastigial nucleus have been linked to disruptions in social behaviour and anxiety, which aligns with the behavioural effects observed following MMI treatment in our previous study (Helgers, Al Krinawe et al. 2020, Helgers 2021). These findings suggest that the action of TH on elements involved in fastigial nucleus development or transportation from the NTZ may play a pivotal role in how maternal hypothyroidism contributes to these behavioural traits.

Given that there was a reduction in the number of observed TBR1^{+} cells, further investigation of the possible mechanism of action of the maternal hypothyroid condition during the development of the rhombic lip lineages is important. A reduction in TBR1+ cells during rhombic lip development has been observed in the Pax6 null Sey cerebellum mutant (Yeung, Ha et al. 2016). Therefore, our difference in Tbr1 cell count could have occurred early in rhombic formation during the Pax6-TBR2-TBR1 cascade. However, our IHC analysis of PAX6, with granule cell precursors, revealed no discernible reduction in granule cell density or count (as illustrated in Figure 3.2) p (0.6924) F (4.396). As a later expression of PAX6 is unaffected, this would initially suggest that the mechanism of action of the model occurs later, temporally, during TBR1 or Tbr2 expression. However, Pax6-null mice have been shown to have only minor defects involving granule cells; the granules themselves are still produced from the rhombic lip in the absence of Pax6, and their migration and terminal differentiation is disrupted (Engelkamp, Rashbass et al. 1999, Swanson, Tong et al. 2005, Yeung, Ha et al. 2016)). Therefore, to fully understand whether maternal hypothyroidism acts at an earlier time point in the PAX6-TBR2 cascade, it may be necessary to look at early embryos and investigate the nuclear transitory zone expression of PAX6 and TBR2.

Given the known projection of the initial cerebellar output to the thalamus via the cerebellum-thalamocortical pathway (Mosconi, Wang et al. 2015), an investigation was conducted to ascertain whether the disruptions observed in the fastigial nuclei had any adverse effects on Pax6 staining within the prethalamus. This investigation also aimed to determine whether other areas of the thalamus, known to receive projections from the dentate nucleus, the primary output of the cerebellar nuclei, exhibited any indications of being affected. The aberrant staining observed in the fastigial nuclei prompted particular interest in the lateral subregion of the Mediodorsal

thalamic (MD) nucleus, which is known to receive projections from the fastigial nucleus (Fujita, Kodama et al. 2020, Georgescu, Popa et al. 2020, Heck, Fox et al. 2023). Figure 3.4 presents the results of our immunohistochemical evaluation of Pax6 staining in the thalamus, shedding light on the interplay between disruptions in the fastigial nuclei and Pax6 expression.

The comparison between MMI-treated brains and control brains revealed no significant difference in Pax6 staining, with statistical analysis supporting this observation ($p = 0.6644$) ($F=23.77$). Although there does not appear to be a reduction in cell density within the prethalamus, a more precise future study should combine this staining with RORα staining in the embryonic thalamus at this stage, which will eventually form the thalamocortical nuclei. Initially, we planned to conduct this study; however, the preliminary RORα staining in the thalamus showed poor contrast against the background and could not be accurately quantified (Supplemental Figure 1).

We cannot then rule out that maternal hypothyroidism may be linked to ASD as a connectivity disorder, with the focus shifting from a reduction in cells in the thalamus to the impact of reduced connections received from the fastigial nuclei. In cats, fastigial electrolytic lesions lead to the degeneration of fibres that project into and through the midline thalamus towards the medial forebrain(Harper and Heath 1973). Therefore, future investigations would benefit from investigating the disruption of these fibres. A more accurate representation would expect us to see changes within Rorα within the embryonic thalamus which will proceed to form the thalamocortical nuclei

3.6 FUTURE DIRECTIONS

To fully understand the impact of maternal hypothyroidism on prenatal brain development, assessing the expression of the dentate nuclei during this stage is crucial. Unfortunately, owing to COVID-19 restrictions, we were unable to conduct these measurements in our initial study.

Furthermore, the acquisition of TBR2 will allow us to investigate potential changes in the interposed nucleus. This will provide insights into whether the observed effects are confined to the output from the dentate nuclei or if juvenile social behaviour is a result of combined effects from multiple nuclei.

While our initial study did not reveal any changes in the thalamic targets of the DCN efferent, it would be intriguing to measure other targets, such as the nucleus accumbens. Additionally, assessing any alterations in the output projections themselves could provide valuable information. Furthermore, owing to the resources used during the optimization period, we were not able to test for molecular reasons, such as the sexual dimorphism in behaviour within our models, so I would like to run more experiments to determine whether that trend continues molecularly.

Although cerebral cortical connections may not have fully formed at this stage, they would have begun to reach the thalamus. Therefore, investigating whether aberrant cerebellar dentate nuclei have influenced potential efferent projections into more cognitive areas of the brain would be interesting. This line of inquiry could shed light on the broader implications of maternal hypothyroidism on brain development and function.

While the changes in TBR1 and RoRα expression have provided valuable insights into the anatomical defects, particularly in terms of the number of stained deep cerebellar nuclei and Purkinje cells, we are still left with unanswered questions regarding the functional impact on these cerebellar structures.

To further investigate both the internal and external functionality of the cerebellum, it would first be of interest to use optogenetic methods through ChR2 expression in Purkinje cells. This would allow us to investigate whether there is any loss in functionality in the inhibitory axonal projections from the Purkinje cells to the deep cerebellar nuclei. This would then allow us to investigate the firing rate of these Purkinje cells through whole-cell patch recording as well as measure postsynaptic calcium levels within the deep cerebellar nuclei.

We would also like to investigate the change in functionality of the Deep cerebellar nuclei (DCNs) within cerebro-cerebello-cognitive loops. Optogenetic studies investigating the axonal projections from the deep cerebellar nuclei to the VTA of the thalamus have already shown success in measuring the output of the deep cerebellar nuclei. Based on this study, it will be required to measure both dopaminergic output and the projections to other regions of interest following up on the success of that study.

Chapter 4: MOLECULAR STUDIES IN P30 TRANSIENT HYPOTHYROID MOUSE

4.1 ABSTRACT

In Chapter 4 of this thesis, we delve into the enduring impact of early developmental disruptions on the juvenile brain, particularly in the context of ASD. Building on our established maternal hypothyroid model, we observed ASD-like behavioural traits in our juvenile model. Previous investigations have highlighted significant changes in the prenatal brain following MMI treatment, particularly in Purkinje cells and the fastigial nucleus.

However, the subsequent effects of these prenatal changes on the pathophysiology of juvenile brains remain unclear. While previous studies explored the impact on the white matter volume of the adult brain, the evidence was inconclusive.

To address this gap, we investigated protein distribution in a juvenile brain via Immunohistochemistry (IHC). We expanded our analysis to examine Pax6 expression in the juvenile granule cell layer and evaluated RoRα expression in Purkinje cells. We also quantified the development of deep cerebellar nuclei (DCNs), which are highly expressed in juvenile P30 brains, through both RoRα and PAX6 staining.

Contrary to our expectations, we did not observe any significant differences in any of our IHCs of the juvenile brains. This finding suggests a different underlying reason for the observed behavioural changes in our model.

This holistic approach enhances our understanding of ASD pathology and the long-term consequences of early developmental disruptions, thereby informing future therapeutic strategies.

4.2 INTRODUCTION

In Chapter 3, we established that changes in our E16.5 prenatal studies resulted in changes within the fastigial nucleus and the Purkinje cell layer in our E16.5 prenatal brains within the early stages of pregnancy. The fastigial nucleus has been found to play a significant role in social behaviour. Studies have shown that alterations in the fastigial nucleus can lead to less intense social interactions and more behaviours to prevent social interaction (Behnke, Stevenson et al. 2018, Al-Afif, Krauss et al. 2019). These findings suggest that changes within the fastigial nucleus could contribute to the behavioural changes observed in individuals with ASD and within our model. Furthermore, in ASD models, changes in Purkinje cells have been associated with system-wide ASD-like behavioural deficits, including in models of thyroid dysfunction (Heuer and Mason 2003, Sudarov 2013, Skefos, Cummings et al. 2014). These changes could represent early signs of ASD pathology, providing valuable insights into the disease's onset and progression.

However, to identify potential biomarkers that could be used in the clinical setting and to further understand the long-term impact of this change in the prenatal environment, we need to understand how these changes in prenatal brains affect juvenile brains. This is particularly important, as biomarkers should be able to account for late-stage diagnoses of the disorder.

In mice, the initial neurogenesis of Purkinje cells (PCs) and deep glutamatergic neurons occurs between E10 and E14 (Martí-Clua 2022). However, cerebellar development extends far beyond this embryonic period, encompassing significant growth during the perinatal and postnatal phases. Therefore, investigating how prenatal environmental alterations, such as maternal hypothyroidism, impact this process is important. A good example of single outside environmental effects within

the early prenatal cerebellum leading to lasting changes can be seen in the well-established valproic acid model of ASD. Prenatal valproic acid exposure results in abnormal structural changes in the cerebellum as well as dysregulation of several ASD-linked genes (Guerra, Medici et al. 2023).

Expanding on our research, it is important to highlight that while we initially observed molecular results in E16 brains, our interest transcended the neonatal and perinatal periods. We decided to conduct a comparison by examining the ages of P30 juveniles. This decision was guided by the finding of ASD-like behaviours in juveniles (see section 1.6), which prompted us to investigate how the changes we observed in the E16.5 models during the critical initial stage might carry over into the late juvenile stage.

It is well-documented that cerebellar development extends into the perinatal and postnatal periods. There is clear evidence that abnormalities caused at the perinatal stage of cerebellar development persist into the late juvenile stage (Wang, Kloth et al. 2014). However, it is unclear whether we will see a consistent change between our foetal and juvenile brains from a restricted window of hypothyroidism (E0-13.5). Postnatal development of the cerebellum is increasingly recognized as a highly sensitive phase for acquiring cognitive functions and represents a significant vulnerability linked to ASD. Therefore, investigating how prenatal environmental alterations such as maternal hypothyroidism impact this process is valuable.

To investigate the long-term pathophysiology of our prenatal changes, we will use our established staining protocols to provide deeper insight into the observed behavioural changes. This becomes especially important, as many studies linking hypothyroidism to ASD have focused primarily on thyroid levels during the neonatal stage and not the

adult brain. However, our treatment-induced transient maternal hypothyroidism concluded at E13.5, urging us to investigate whether any defects from this vulnerable early stage of pregnancy endure into adulthood.

We will further expand our analysis to include an examination of Pax6 expression in the juvenile granule cell layer. Additionally, we will evaluate RoRα expression in Purkinje cells and quantify DCN development in juvenile P30 brains through both RoRα and PAX6 staining, which are highly expressed in juvenile DCNs. This approach provides a more holistic understanding of the enduring impact of early developmental disruptions on the juvenile brain, thereby contributing to our understanding of ASD pathology and informing future therapeutic strategies.

4.3 METHODOLOGY

4.3.1 Tissue Handling:

The detailed procedures concerning tissue handling can be found in "2.1 Animal Tissue."

4.3.2 Embedding

The embedding process was executed in accordance with the methodology outlined in "Methods Chapter 3."

4.3.3 Sectioning:

For immunohistological analysis, tissue sections were obtained from Leica Microsystems via a microtome. The sections were sliced at a thickness of 6 µm, chosen because of the larger section size and the density of white matter observed in juvenile tissues. This specific thickness was found to increase the stability and decrease the susceptibility to tearing.

4.3.4 **Staining:**

Protocols for staining were meticulously followed, following the guidelines provided in "Methods Chapter 3."

4.3.5 **Statistics and Semiquantitative Analysis:**

Statistical analyses and semiquantitative assessments were performed via the methods described in "Methods Chapter 4."

Three juvenile brains from both the control and MMI-treated groups were selected for analysis. The selection criteria were as follows:

The cerebellum had to remain intact after previous experiments involving micro-CT scanning.

All the brains were from different mouse pairs to prevent bias toward a single litter.

Given the limited number of brains meeting both criteria, we did not separate them by sex to maintain a statistically relevant sample size. For immunohistochemistry (IHC) and quantification, each brain was sectioned at 6 µm, resulting in three sections per slide. To determine the rostrocaudal levels for analysis, we combined information from the Allen Brain Atlas with the cerebellar foliation as an anatomical landmark. Initially, structures were assessed based on the shape of the white matter in the cerebellum after sectioning. We subsequently compared these structures to slides within a similar range, ensuring the best alignment for analysis.

4.4 RESULTS

4.4.1 Changes in Purkinje density is not consistent between E16.5 and P30 brains.

To explore changes in Purkinje cell density over time, we examined both E16.5 (embryonic) and juvenile (P30) brains. Interestingly, our findings revealed that the alterations in Purkinje cell density observed at E16.5 were not consistent with the patterns observed in juvenile brains.

As previously described in section 3.4.2, induced transient maternal hypothyroidism led to a reduced density of RoRα-positive cells specifically at the E16.5 developmental stage (Figure 3.2).

As shown in Figure 4.1, we investigated the differences in Purkinje cell density between juvenile (P30) brains of the control group and those exposed to maternal hypothyroidism (MMI-treated). Statistical analysis revealed no significant difference in Purkinje cell density between the MMI-treated and control groups at the juvenile stage (P30) ($p=0.7505$, $F=2.4575$), indicating a comparable density of Purkinje cells in both treatment types.

4.4.2 Changes in DCN development are not carried to the P30 brain.

In addition to assessing Purkinje cell density, we conducted an immunohistochemical analysis using the RoRα marker to investigate potential changes in the deep cerebellar nuclei within the cerebellum of P30 brains.

Our analysis of P30 brains did not reveal significant alterations in the cerebellar nuclei. The data in Figure 4.2 revealed no statistically significant difference between the MMI-treated and control groups for interposed nuclei ($p=0.1174$, $F=11.61$) or fastigial nuclei ($p=0.1802$, $F=1.560$), suggesting that induced transient maternal hypothyroidism did not significantly impact the cerebellar nuclei at this stage.

4.4.3 There was no change in the granular cell layer in the P30 brain.

We investigated potential changes in the granular cell layer following induced transient maternal hypothyroidism. We conducted an immunohistochemical analysis and examined the data presented in Figure 4.3. Our analysis revealed that no significant changes were observed in the granular cell layer between the MMI-treated and control groups. The data from Figure 4.3 demonstrated consistent granular cell layer morphology and cellular density, with no statistically significant alterations ($p=0.5982$, $F=1.975$).

4.4.4 The dentate nucleus was not significantly different.

The dentate nucleus was examined to investigate potential differences between the control and MMI brains. Upon visual observation, there were notable differences between the two groups, as depicted in Figure 4.4. However, to confirm the significance of these observed changes, we conducted a thorough statistical analysis via Qupath software. The statistical analysis revealed that the observed differences in the dentate nucleus between the experimental (MMI-treated) and control groups did not reach statistical significance ($p=0.0851$, $F=13.44$).

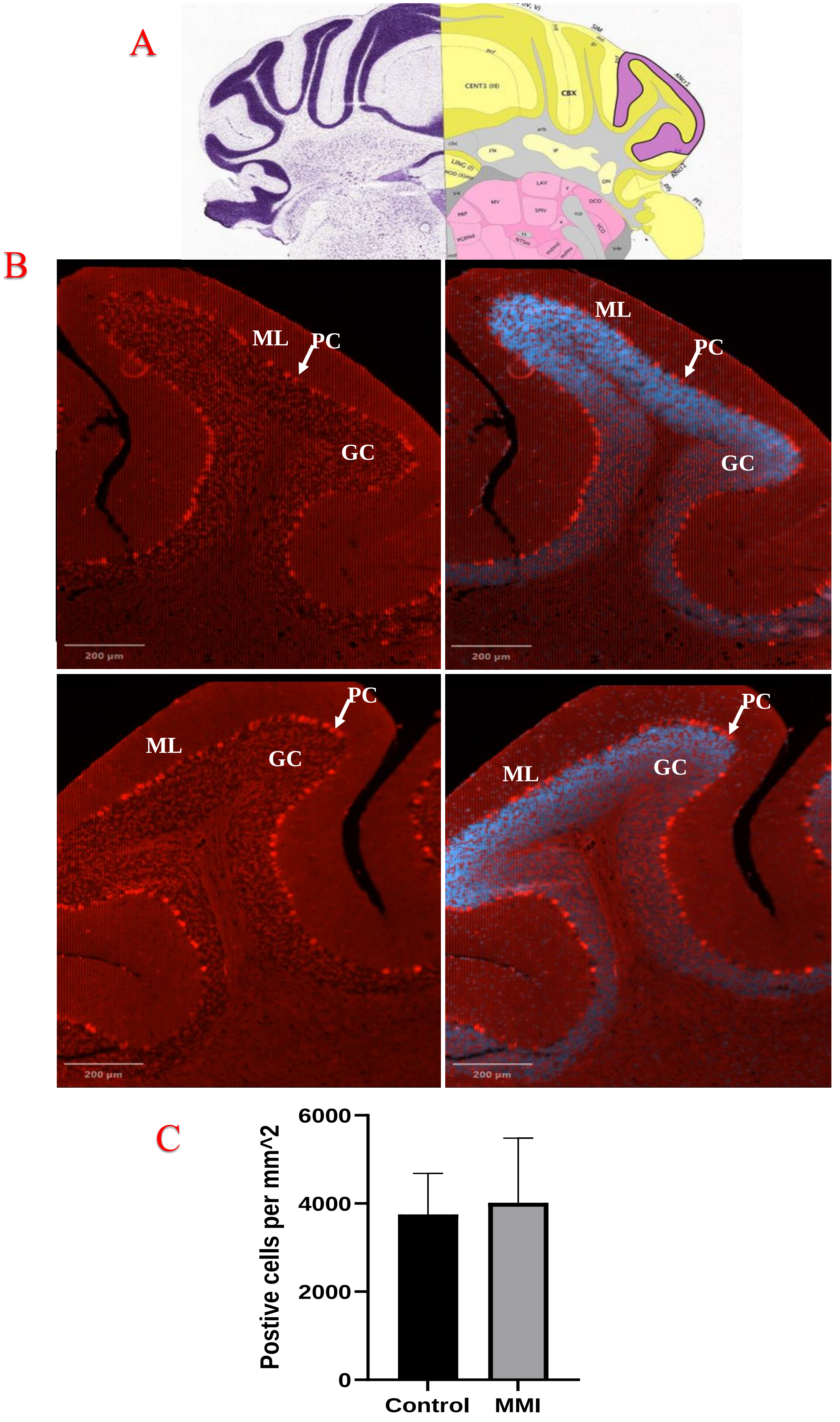
A
B
ML
PC
GC
200 µm
C
6000
4000
2000
0
Postive cells per mm^2
Control
MMI

Figure 4.1 RoRα staining of Purkinje cells in juvenile cerebellum. (a): Section position represented in Allen brain atlas http://atlas.brain-map.org/atlas?atlas=1&plate=100960520 (b) Representative images of RoRα staining in juvenile Purkinje cells in the Control and MMI groups, respectively N=3 mice per group, with n=3 sections per mouse Scale bars are 100 µm. (c) Quantification of Pax6 staining image analysis with the Qupath programme measuring the density of Pax6 expression in each group (quantitative analysis of the number of Pax6 positive cells in the cerebella) p=0.7505 F=2.4575 Data are expressed as mean ± SD *p value ≥0.05. Abbreviations: PC: Purkinje Cells ML: Molecular Layer, GCL: Granule Cell Layer.

A

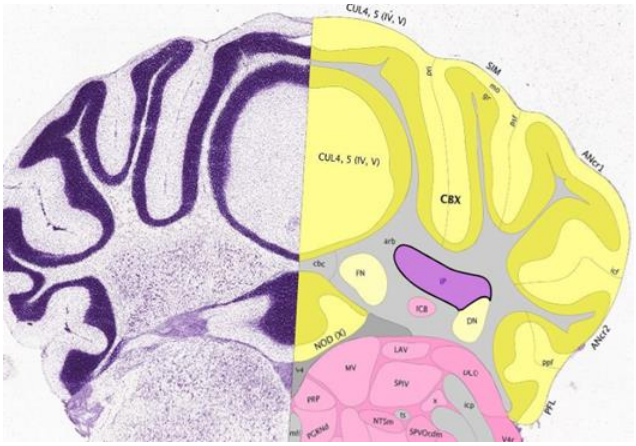
CUL4, 5 (IV, V)
CBX
FN
IP
ICB
DN
LAV
SPIV
PRP
NOD (X)
ANcr1
ANcr2
PFL

B

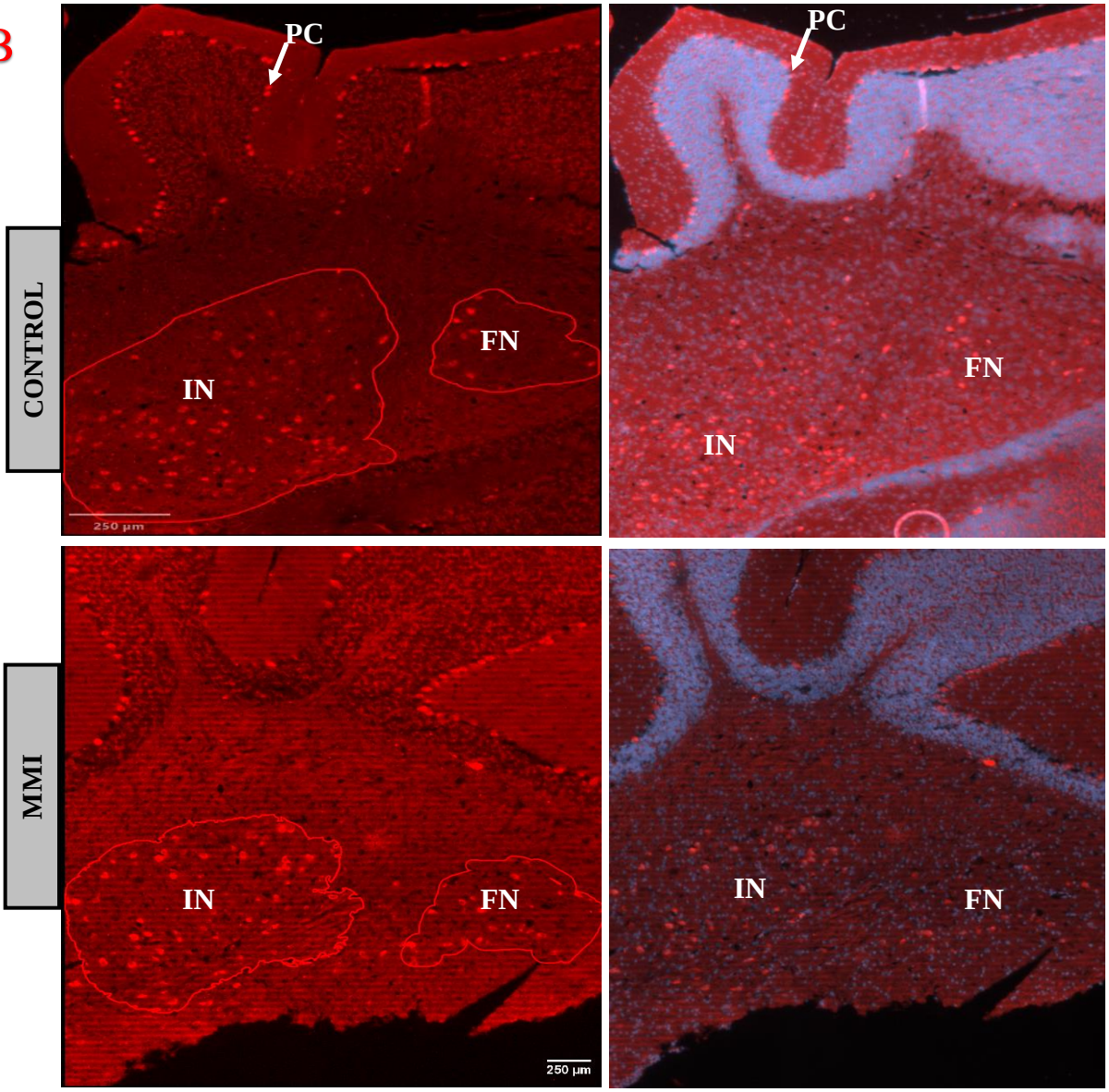
CONTROL
MMI
PC
IN
FN
250 µm

C

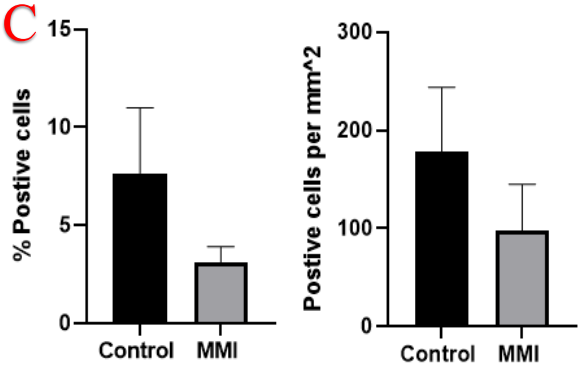
% Postive cells
Postive cells per mm^2
Control
MMI

D

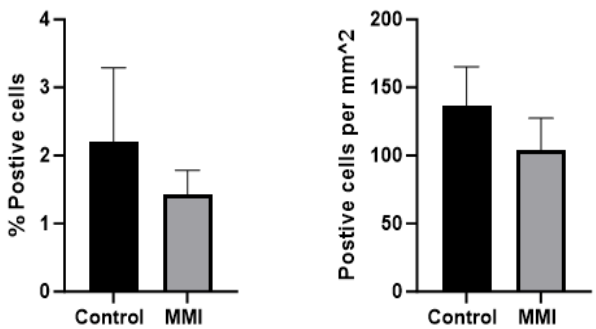
% Postive cells
Postive cells per mm^2
Control
MMI

Figure 4.2 RoRα staining in the juvenile interposed and fastigial nucleus. A: Section position represented in Allen brain atlas http://atlas.brain-map.org/atlas?atlas=1&plate=100960520. RoRα staining in the juvenile interposed and fastigial nucleus. (B) Representative images of RoRα- staining in the interposed and fastigial nucleus in the Control and Methimazole MMI groups respectively. N=3 mice per group, with n=3 sections per mouse Scale bars, 200 μm. Outlines of the cerebellar nuclei. The borders were determined using a mixture of brain atlases and by distinguishing the nuclei from the surrounding arbour vitae. This approach aimed to provide accurate identification and mapping of the cerebellar nuclei. In the interposed nucleus (C), the percentage of positive cells was p=0.0974 and the number of positive cells per mm² was p=0.1174 F=11.61. In the fastigial nucleus (D), the difference in the percentage of positive cells had a p score of 0.2194 and the number of positive cells per mm² was p=0.1802 F=1.560 Data are expressed as mean ± SD *p value ≥0.05. Abbreviations: FN: Fastigial Nucleus, IN: Interposed Nucleus PC: Purkinje Cell

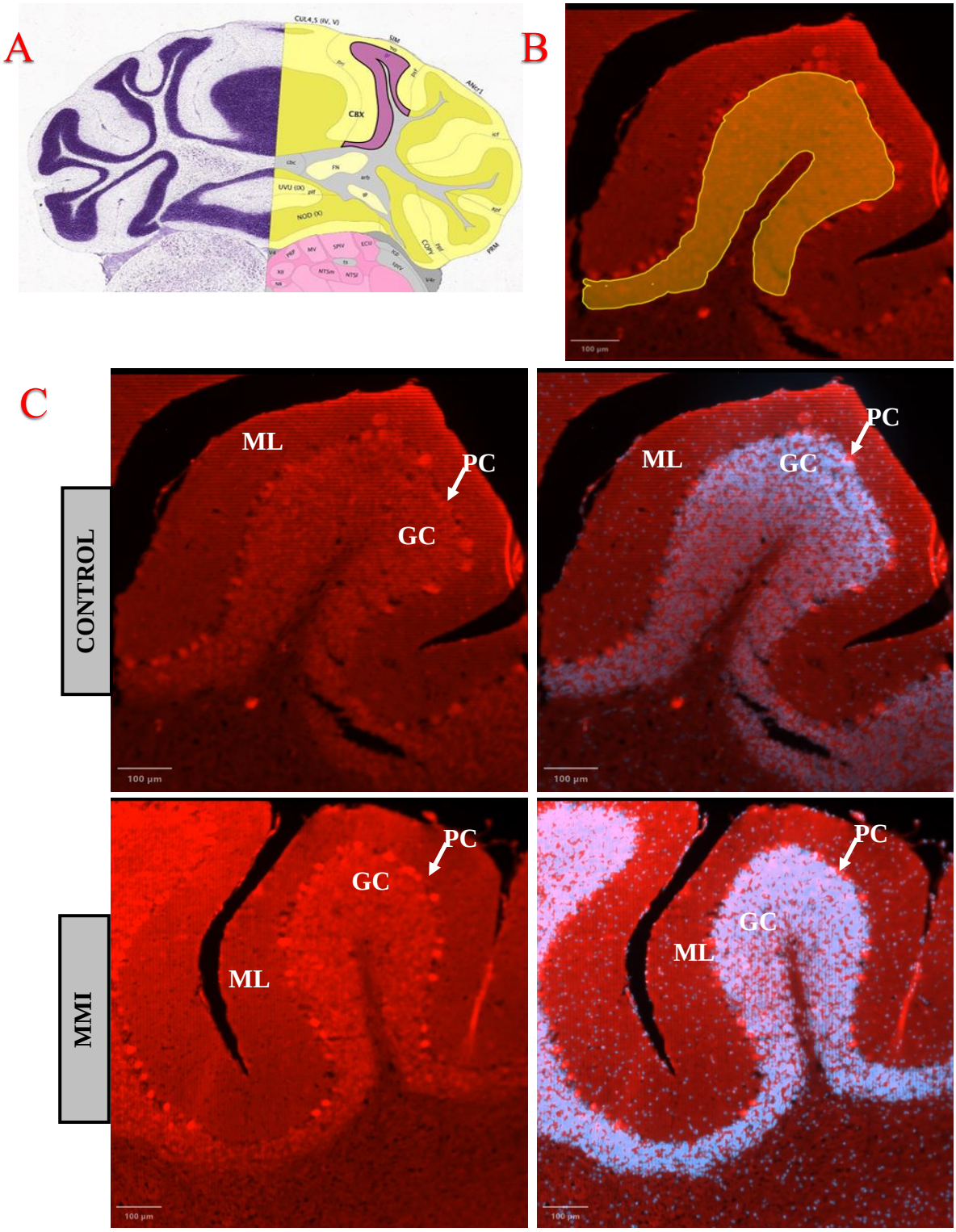
A
B
C
CONTROL
MMI
ML
PC
GC
100 µm
D
Postive cells per mm^2
6000
4000
2000
0
Control
MMI

Previous page Figure 4.3 Pax6 staining in Adult granule cell layer. (A) Section position represented in Allen brain atlas http://atlas.brain-map.org/atlas?atlas=1&plate=100960520. B. Image showing the mask created to define the region of interest (ROI), ensuring only granule cells were included, excluding Purkinje cells.

(C) Representative images of Pax6 staining in the granule cell layer in the Control and MMI groups respectively. N=3 mice per group, with n=3 sections per mouse Scale bars, 100 μm.D). Quantification of Pax6 staining image analysis with the Qupath programme measuring the density of Pax6 expression in each group .The p score for the quantification of Pax6 staining is 0.5982. This was determined through image analysis with the Qupath program, measuring the density of Pax6 expression in each group. The quantitative analysis of the number of Pax6 positive cells in the cerebella is also included.Data are expressed as: mean ± SD *p value ≥0.05; Abbreviations: PC: Purkinje Cells ML: Molecular Layer, GCL: Granule Cell Layer.

A

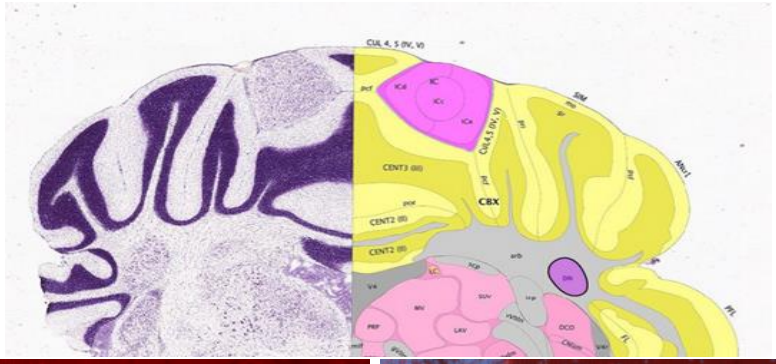
CBX

B

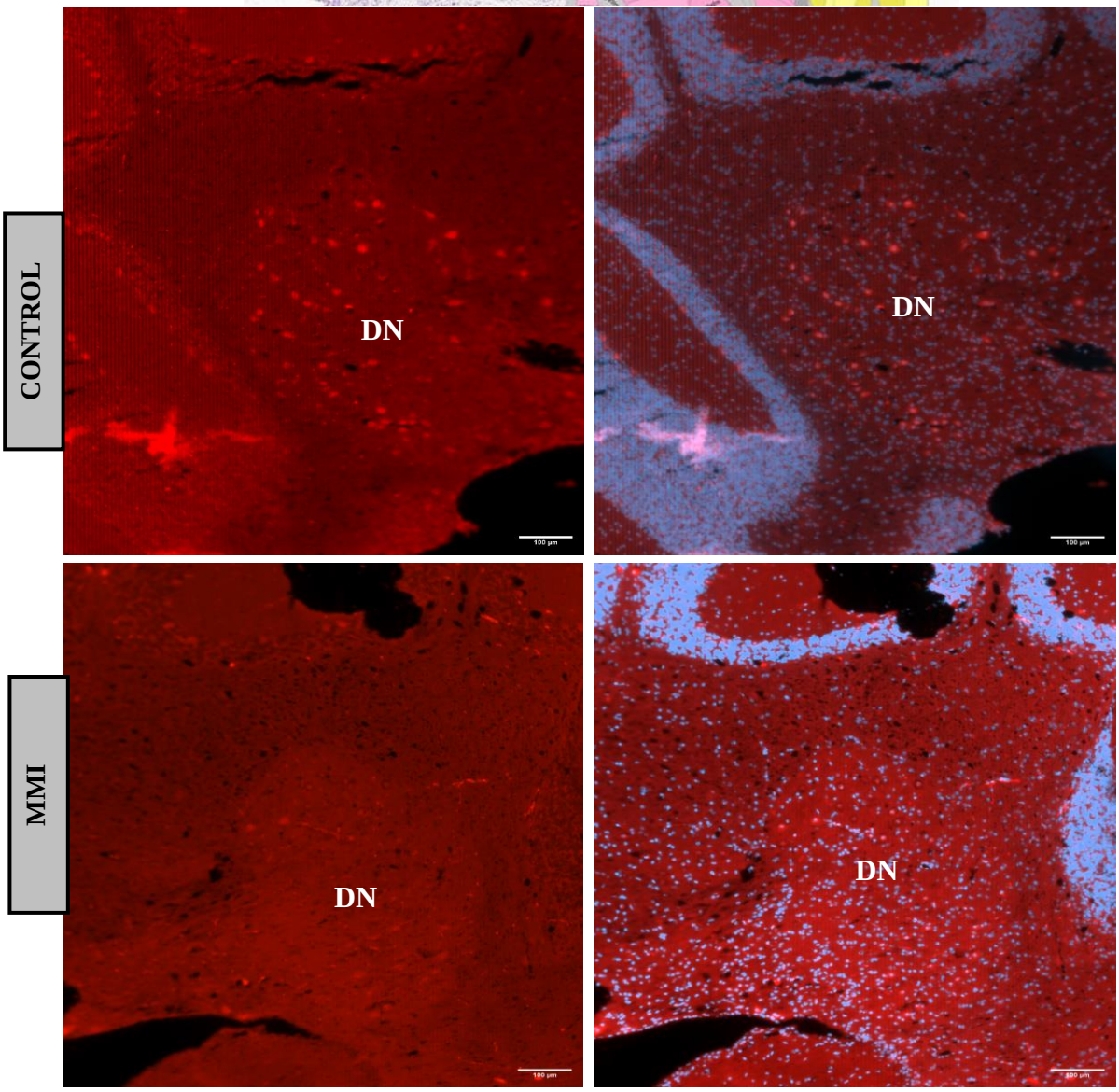
CONTROL
MMI
DN
DN
DN
DN

C

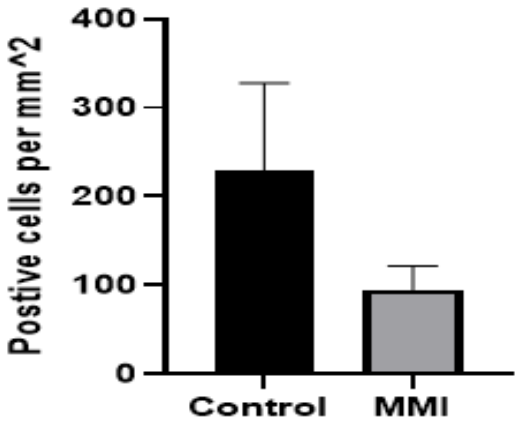
Postive cells per mm^2
400
300
200
100
0
Control
MMI

Figure 4.4 Pax6 staining in the dentate nucleus of the cerebellum. A) Section position represented in Allen brain atlas http://atlas.brain-map.org/atlas?atlas=1&plate=100960520. B) representative staining pattern of Pax6 in the dentate nucleus for both the Control and Methimazole MMI groups N=3 mice per group, with n=3 sections per mouse Scale bars are provided, indicating a length of 100 µm. C) Quantitative analysis is performed to assess the density of Pax6 expression in the dentate nucleus using the Qupath program. Additionally, the figure provides quantitative data analysis, indicating the number of Pax6 positive cells in the cerebella p=0.0851 F=13.44. Data are expressed as the mean ± standard deviation (SD). Abbreviations: DN: Dentate Nucleus

4.5 DISCUSSION

4.5.1 Purkinje and granule cells

In our study, we observed significant changes in the Purkinje cells and fastigial nuclei of E16.5 mice affected by maternal hypothyroidism. This led us to hypothesize that similar alterations might be present in juvenile mice, potentially linking these changes to ASD-like behaviours previously identified (see section 1.1 Aims). However, our examination of Purkinje cells in P30 MMI-treated and control brains (as depicted in Figure 4.1) did not reveal any statistically significant differences ($p = 0.7505$) ($F = 2.4575$). This finding is noteworthy given that previous research associated Purkinje cell loss in hypothyroid cases with ASD (Khan, Harney et al. 2014). Furthermore, we observed reduced Purkinje cell density in E16.5 brains exposed to the same environmental conditions. This finding diverges from prior research suggesting that abnormal Purkinje cell growth in response to hypothyroidism often results in poor dendritic outgrowth, particularly through the TH receptor Trα1 (Heuer and Mason 2003).

One key factor contributing to this discrepancy may be our experimental design. Many previous studies investigating the effects of hypothyroidism or thyroid knockout in mice maintained a hypothyroid state throughout the entire duration of their experiments. In contrast, our study focused on a specific timeframe, spanning from pregnancy to E13.5, which corresponds to a critical developmental window in the first trimester of pregnancy. This temporal limitation raises the possibility that intrinsic TH production by the foetus, rather than reliance on maternal TH, could mitigate these effects. This finding is supported by studies using longer exposure windows along with melatonin, which may play a paracrine role in the regulation of thyroid activity

and rescue of Purkinje cells (D'Angelo, Marseglia et al. 2016, Hidayat, Lail et al. 2020) I attribute our differences observed in other hypothyroid models to two key factors in our experimental design: first, the conclusion of our maternal treatment, and second, the reduced dependency of the foetus on maternal TH.

Considering this, we can perform a similar study involving maternal subclinical hypothyroidism induced by electrocauterization, which has shown similar behavioural effects (Hu, Wang et al. 2022). Our initial study revealed a potential reduction in the population of RORα-positive Purkinje cells within the prenatal mouse prepontine hindbrain. However, our subsequent observations in this study indicate that this reduction in cell density does not persist when it is measured in a juvenile model. These findings prompt us to question the assumption that once the foetus achieves independence in thyroid production or the cause of maternal hypothyroidism is resolved, it can completely mitigate the effects observed during the earlier developmental window. However, it is important to note that even when the foetus is not fully dependent on maternal THs after the first trimester, there is still a substantial degree of dependence, as foetus and maternal THs cooperate in various ways (Forhead and Fowden 2014).

Notably, Purkinje cells have demonstrated regenerative capacity in response to injury, particularly before postnatal day 5 (Bayin, Wojcinski et al. 2018). As our experimental intervention was limited to the E0--E13.5 period, this left a window for potential recovery from midgestation onwards. These findings suggest that studies where there was early intervention of T4 or T3 treatment in a hypothyroid model would show similar recoveries. An example of this can be seen in neocortical studies in which maternal hypothyroidism at the earliest onset of drug-induced maternal hypothyroidism, starting at e6, led to cortical changes; however, these changes could

be reversed by TH replacement (Mohan, Sinha et al. 2012). Therefore, once mouse brains regain access to the maternal thyroid, this may lead to recovery. The changes we observed prenatally are not preserved in juveniles. However, despite the absence of these initial changes in juveniles, we still see behavioural changes at P30. This suggests that the initial prenatal changes may trigger a downstream cascade of effects that lead to different but lasting impacts on juvenile behaviour.

4.5.2 DCN in Juveniles

Given the observed inconsistencies in changes between E16.5 and P30 brains, we investigated whether a similar trend would emerge when the DCN was assessed, with a particular emphasis on the fastigial nuclei, which exhibited significant differences in the E16.5 cohort. Within our examined cerebellar nuclei populations, we found no significant difference in cell density or cell number. (Figure 4.3, 4.4). Notably, however, the dentate nuclei trended toward significance, with a p-value of 0.0851 and an F value of 13.44. The interposed and fastigial nuclei did not show a similar trend, with p values of 0.1174 and 0.1802 and F values of 11.61 and 1.560, respectively. Despite this, visual differences were observed in the interposed and fastigial nuclei, suggesting potential variations that may not have been captured by the statistical analysis.

Therefore, while the dentate nuclei stood out as the most significant among them, the interposed and fastigial nuclei did not show a strong trend toward differences. Further research is needed to confirm these findings and explore their implications, particularly considering the observed visual differences in the interposed and fastigial nuclei.

The dentate nucleus has been strongly linked to the cerebellum's role in ASD cognition because of its role within cognitive circuits (Olivito, Clausi et al. 2017,

Anteraper, Guell et al. 2019). It has rarely been suggested that any of the other cerebellar nuclei are a target for hypothyroidism's links to cognitive disorders, with most of the focus on alterations within the Purkinje and Granule cell layers (Ishii, Amano et al. 2021) (Koibuchi 2008). However, studies have shown that the thyroid transporter MCT8 is heavily present within cerebellar neurons in chick models. (López-Espíndola, Morales-Bastos et al. 2014). Furthermore, a model of Allan–Herndon–Dudley syndrome, a disorder characterized by a deficiency in the thyroid transporter MCT8, was shown in an early clinical study to exhibit decreased myelination in the brain and impaired neuronal differentiation in the dentate nucleus.

If we consider that none of the cerebellar nuclei were significantly different in juveniles and that the fastigial nuclei were different at E16.5, it could be inferred that the early changes in cerebellar nuclei caused by maternal hypothyroidism may not have been fully maintained into the late juvenile stage. Despite this, we still observed significant changes in the behavioural studies of the model. These findings suggest that the early prenatal impact of maternal hypothyroidism results in non-structural changes that persist into the late juvenile stage. Therefore, understanding the pathophysiology of these changes is important for future research.

Considering the potential impact of sex differences in individuals with ASD on our findings is essential. Thus, having access to a substantial cohort to separate males and females, as in Chapter 2, and delving deeper into potential sexual dimorphism would be an ideal approach. Previous studies examining valproic acid exposure have revealed differences in DCN cell counts between males and females, underscoring the importance of this investigation (Mowery, Wilson et al. 2015). This is particularly interesting because of the sexual dimorphism observed in previous behavioural studies of the model.

4.6 FUTURE RESEARCH DIRECTIONS

While investigations into the DCN revealed notable trends, particularly within the dentate nuclei, but notably not the fastigial nuclei, which displayed significant differences at the E16.5 stage, our analysis, unfortunately, did not produce statistically significant results. As previously discussed in Chapter 3, the DCN has a well-established connection with social behaviour. Nevertheless, the absence of clear statistical significance in our findings leaves us with lingering questions about how the early prenatal changes observed in maternal hypothyroidism correlate with the later behavioural outcomes observed in the juvenile model.

Although our findings from juvenile brain studies have been largely inconclusive, they have opened new avenues for future research. Further investigations using larger sample sizes, or the identification of more specific juvenile markers are needed.

Our study, which focused on the morphology and count of cerebellar cell types, did not reveal changes in Purkinje cells or significant changes within the dentate nuclei. However, to gain deeper insights into our cerebellar nuclei, especially regarding synaptic activity, further investigations with larger sample sizes or the identification of specific juvenile markers—particularly glutamatergic markers—would be valuable. Glutamate, the primary neurotransmitter for excitatory neurons in the CNS, plays a crucial role. By examining these glutamatergic markers, such as Vesicular glutamate transporter 1 (VGLUT1) and Vesicular glutamate transporter 2 (VGLUT2), we can better understand the function and dysfunction of Deep cerebellar nucleus (DCN) neurons.

Interestingly, we noted an apparent change in Purkinje cell migration and differentiation during our prenatal studies. It would be prudent to determine at what stage these Purkinje cells recover. Research has suggested that Purkinje cells may retain regenerative potential until P5. Therefore, incorporating a perinatal group into our research could help ascertain whether our observed changes persist beyond this point. In the future, it could be beneficial to have a cohort that receives extended treatment. This group could then be compared to those who only receive treatment in the first trimester. Furthermore, another valuable comparison could be made between those who only receive treatment in the first trimester and those who receive extended treatment for MMI during pregnancy, paired with T4 after the first trimester. This could help to observe whether the rescue in Purkinje cells is similar to that seen in cases where the treatment is limited only to the first trimester. Such a study could provide further insights into the effectiveness of different treatment durations and methods on foetal development, particularly in relation to Purkinje cells. However, as we would expect to see behaviour changes in both cohorts, it would be interesting if the underlying pathophysiology remained consistent.

.

Chapter 5: General Discussion

This study aimed to explore the mechanism by which maternal hypothyroidism creates a behavioural model with changes in social behaviour akin to those in other models of ASD. (Figure 1.10). This goal was achieved through neuroanatomical studies of large white matter structures in late juvenile models as well as molecular investigations in both E16.5 models and late juvenile models to provide further information about any changes in structure and relevant protein expression in Purkinje cells and deep cerebellar nuclei.

The white matter studies were largely inconclusive, with no changes observed across either treatment or sex in the juvenile models. While the results of white matter studies in patients with ASD can contradict each other, our results are still unexpected compared with those of previous studies. While we can consider our results at facial value, there are many limitations to our anatomical study, which may account for errors or artefacts in the data. However, excellent contrast was observed at both the 9-micron and 4-micron levels. Most of the work has been performed at 19 microns, which is suitable for studying the area of the corpus callosum at the midline of each brain; however, this could have led to inconsistencies when moving to volumetric work. This was emphasized by the large cohort of the samples which had to be removed from the data when moving from area studies to volumetric studies, which decreased the sample size (Table 2.1). In the future, a larger cohort of brains scanned at higher resolutions could help us gain a better understanding of how neuroanatomy is affected in this maternal hypothyroid model.

In our exploration of staining for important markers in the embryonic and juvenile mouse brain, we observed significant changes in the staining for the marker TBR1, which has been traditionally associated with staining populations of fastigial cerebellar nuclei. We also observed data suggesting that there was a reduction in the number of Rorα-positive cells in the early Purkinje cell layer within these sections. These data

contrast with our findings from the stains of the juvenile tissue sections, which showed no difference in staining in either the Purkinje cell layer or the cerebellar nuclei. While we did observe differences in the embryonic brain for TBR1 and, to a lesser extent, Rorα, it is still unclear why we observed this reduction in staining. This could have occurred due to a complete absence of the cells themselves an issue with the cells specifying into the cerebellar nuclei or Purkinje precursors as they migrated from the rhombic lip or even just lost the ability to express TBR1 or RORα.

While the observed differences in staining in our embryonic model present a promising avenue for future research, several limitations of this study must be acknowledged. First, the small sample sizes across both embryonic and adult brains represent a significant limitation, potentially leading to an overestimation of the observed effects. Future studies should aim to reconfirm these findings through larger-scale investigations, which would help eliminate outliers and reduce the impact of errors. The limited scale of this study was due primarily to the restricted timeline imposed by the COVID-19 pandemic. Additionally, the small sample size hindered our ability to explore sex differences within the model, as previous experiments involving CT scans or optimization processes reduced the available cohort of undamaged, treatable brains.

Second, while we observed changes in protein expression, these findings do not provide insights into the functional roles of these proteins within the cerebellum, thereby obscuring potential links to the behavioural effects observed in MMI progeny. This issue is further compounded by the semiquantitative nature of the data acquisition. Despite efforts to ensure accurate data collection, it is important to acknowledge that certain aspects require human interpretation, such as the identification of regions of interest and threshold set within the measurement software. To more accurately clarify the observed trends and results, follow-up studies

employing more quantitative methods, such as planned in situ hybridization studies, would be beneficial in providing a more reliable foundation for our findings.

Within the constraints of this study, the significant alterations in the expression of key markers such as TBR1 and Rorα in the embryonic brain suggest potential disruptions in the development of the fastigial nucleus and Purkinje cells at this early stage.

More importantly, the changes in the expression of these markers are not conserved into the late juvenile stage, indicating that the initial disruptions may either resolve over time or lead to compensatory mechanisms that normalize marker expression. This discrepancy between the embryonic and juvenile stages underscores the complexity of neurodevelopmental processes and highlights the need for further investigation to understand the long-term implications of these early changes. Future studies should focus on longitudinal analyses to track these markers across different developmental stages and explore their functional consequences concerning behavioural outcomes.

These findings contribute to our understanding of the underlying mechanisms that may lead to the behavioural changes observed in ASD models. Furthermore, the data gathered from this study lay a foundation for future research, highlighting the need for larger-scale studies and more quantitative methods to validate and expand upon our results.

The Interaction of Environment and Genetics: Transient Gestational Hypothyroidism”

ASD is a set of neurodevelopmental conditions characterized by enduring impairments in social interaction and communication, along with repetitive patterns of behaviour, interest, and activities. Given the idiopathic nature of most cases, it has become important to deepen our understanding of the potential risk factors for ASD, the molecular and cellular mechanisms that influence brain development and how these mechanisms translate into observed behavioural changes.

The aetiology of ASD is multifactorial and involves intricate interactions between genetic and environmental factors. The clinical diversity and complex aetiology of this disorder have hindered the development of reliable biomarkers for early detection and have constrained our comprehension of the disorder. In recent years, the prevalence of ASD diagnosis has increased steadily, and we can probably attribute most of the increase to better public response and improved diagnosis of ASD; we cannot fully account for this increase in the prevalence of these factors (Presmanes Hill, Zuckerman et al. 2015). Hence, it is vital to understand how epidemiological studies associate environmental factors with ASD and how environmental triggers such as exposure to pollutants might account for the sporadic occurrence of ASD, especially when coupled with genetic risk factors. Transient gestational hypothyroidism presents a compelling example of the interaction between the environment and genetics in ASD. In early pregnancy, the embryonic brain relies entirely on the mother for thyroid hormone, which in turn is contingent on adequate dietary iodine intake. Pregnancy places a demand on thyroid status, making it vulnerable to environmental organic toxins such as PCBs, PBDEs, and PFASs, which are known as inhibitors of TH receptors and/or the thyroid synthesis pathway (Boesen, Long et al. 2020).

Our research confirmed that blocking thyroid hormone signals at the early stages of development distinctly affects a specific time-bound group from the rhombic lip lineage. This group is instrumental in the formation of the TBR1 fastigial cerebellar nucleus (Figure 3.1). We verified that a reduction in TBR1-positive cells within the fastigial cerebellar nucleus is a consequence of maternal hypothyroidism, although the exact mechanism of action remains unknown.

Our maternal hypothyroid treatment did not affect the development of Pax6-positive granule cells. Pax6, TBR2, and TBR1 are expressed sequentially from the rhombic lip to the NTZ (Fink, Englund et al. 2006). As previously mentioned, the role of PAX6 in ensuring the survival of TBR1+ glutamatergic CN neurons has been identified (Yeung, Ha et al. 2016). However, in the Sey cerebellum, there is only minor disorganization of the EGL with foliation defects and no apparent GC loss (Engelkamp, Rashbass et al. 1999, Swanson, Tong et al. 2005, Ha, Swanson et al. 2015).

The cells that leave the RL become cerebellar GCPs from E13.5 onwards, which coincides with the end of our treatment. This finding suggests that these later-born PAX6 populations could remain unaffected while disrupting their earlier rhombic lip lineages (Machold and Fishell 2005). Although no change in PAX6 cell density was observed, it may still be responsible for our observed reduction in TBR1-positive cells. As PAX6 affects both TBR1 and TBR2, we initially stained for TBR2 to confirm that both lineages were affected. We then used an earlier model to identify any disruption of Pax6 at the rhombic lip and of all three markers at the NTZ. To further explore the mechanism of action of maternal hypothyroidism, especially in a mouse model and for clinical transition into humans, we considered LHX9, a marker of the dentate

nucleus. LHX9 is an early-born derivative from the rhombic lip that is expressed earlier than the PAX6+ glutamatergic neuron population (Green and Wingate 2014).

We planned to investigate LHX9 through RNAscope in situ hybridization, but we were unable to complete this work due to COVID-19. Disruption of LHX9 populations, such as those in our TBR1 population, would suggest that TH disruption affects all rhombic lip lineages and may affect Atoh1/Math1. This finding aligns with Math-1 being regulated by thyroid hormones in other brain areas, such as the hippocampal neurogenic niche (Kapoor, Desouza et al. 2012). However, the lack of change in LHX9 further suggests that the thyroid acts at a later temporal point in development.

When we look at the function of thyroid hormones in various instances of hypothyroidism within the cerebellum, it seems that their primary role is in differentiation (Heuer and Mason 2003). Hypothyroidism, which occurs late in embryonic development or early after birth, leads to the failure of cerebellar granule cells to fully differentiate and migrate radially to form mature cells in the inner granule layer (Wang, Wang et al. 2014).

Following a deficiency in thyroid hormones, Purkinje cells exhibit a significant reduction in arborization and fail to establish mature connections with incoming climbing fibres (Yajima, Amano et al. 2021). GABAergic interneurons in the cerebellar cortex exhibit delayed differentiation and maturation, along with diminished connectivity (Patel, Smith et al. 1980, Bernal 2007). Although these effects are mostly observed during late cerebellar development, it is possible that the differentiation of cells in the nuclear transitory zone of the cerebellar nuclei could be similarly disrupted.

5.1 "P30 BRAIN TRENDS: TRENDING TOWARDS SIGNIFICANT PATTERNS OR JUST NOISE IN THE DATA?

Initial behavioural studies conducted on our models revealed significant changes in behaviour within the juvenile group (Figure 1.10). Male mice treated with MMI presented increased anxiety, and female mice treated with MMI presented impaired social approaches. These findings suggest that the abnormalities observed at the prenatal level could either persist into the late juvenile stage, thereby causing these behavioural phenotypes or lead to further downstream changes that become apparent upon examination of the juvenile brain.

However, contrary to these findings, we did not observe any significant changes in the cerebellum of these juveniles (Figure 4.1--4.4). Although several factors, such as our DCN, trended in the expected direction, indicating potential changes with a larger sample size or more quantitative methods would be needed in the future to fully ratify these results. Previous single-cell transcriptomics studies have shown a clear atlas of the molecular makeup of the cerebellar cortex at embryonic stages (Carter, Bihannic et al. 2018, Peng, Sheng et al. 2019, Kozareva, Martin et al. 2021). Single-cell RNA sequencing has already provided a detailed breakdown of the mechanistic differences in Purkinje cells between embryonic and adult stages. To begin, it would be beneficial to compare our models to this work to gain greater insight into the discrepancies between our juvenile and embryonic results (Apsley and Becker 2022). There is ample research showing differences in the transcriptome of Purkinje cells in cases of ASD with changes in targets such as CHD8 (Clifford, Dulneva et al. 2019) (Brandenburg, Griswold et al. 2022). There are by comparison few studies to show of the change in

the transcriptome in the DCN both glutamatergic CN and GABAergic within adult models. This is largely hindered by the lack of cell-specific markers for adult CNs within the cerebellum outside of PCs and GCs (Tam, Wang et al. 2021). Therefore, it would be necessary to have clear spatial analysis for any cohort of genes we are looking at by either paring single-cell transcriptomics with an in situ hybridization or using a method such as in situ single-cell transcriptomics for targets such as VGLUT1 or GABRA1 for glutamatergic and GABAergic cerebellar neurons along with a cross-section of genes known to be involved in both ASD and TH function such as *RELN* *TBR1*, *NEUROD2*. *RORα* and *MECP2* (Navarro, Alvarado et al. 2015, Lenart, Augustyniak et al. 2020).

Therefore, we should proceed with the assumption that prenatal changes do not persist in the same manner in juveniles. Instead, these changes may cause further downstream effects during development, leading to the observed behavioural phenotype.

While there are potential arguments for changes in DCN, the complete absence of any alterations within Purkinje cells and granule cells contradicts the findings observed in other hypothyroid models (Boukhtouche, Brugg et al. 2010, López-Espíndola, Morales-Bastos et al. 2014, Yu, Iwasaki et al. 2015). This discrepancy is particularly notable in models in which hypothyroidism is present during perinatal stages(Boukhtouche, Brugg et al. 2010, Fauquier, Chatonnet et al. 2014). Considering that thyroid hormone is instrumental in the differentiation of Purkinje cells within this stage, the lack of observed change suggests that the changes observed prenatally concerning the prenatal Purkinje cell layer may be from variance, as indicated by its F score. The difference in results between perinatal hypothyroidism and our treatment, which was limited to a treatment window of E0--13.5, could be due

to the varied expression of the thyroid receptor THRα1. This receptor is expressed only in postmitotic Purkinje neurons around E15.5 (Bradley, Towle et al. 1992). The mechanism of action of thyroid hormones is believed to involve THRα1 receptors (Heuer and Mason 2003, Fauquier, Chatonnet et al. 2014). This could account for the observed discrepancy in Purkinje neurons in our model compared with those where hypothyroidism was present from a later stage.

For each cerebellar nucleus, it was clear that there were trends and visual indicators toward differences (Figure 4.4), but none of these results were significant. While we can argue that larger sample sizes or the use of higher-throughput quantitative methods could lead to significant changes in these trends in the future, it is just as likely that in a small sample size, these changes are caused by variance between the samples. One hypothesis suggests that early disruption may not lead to a total loss of DCN in adults, but it could influence the formation of cortical–thalamic–cerebellar loops and, by altering the timing of CN development, disrupt their connectivity, thereby causing dysfunction in the corresponding cortical targets (Kelly, Meng et al. 2020).

The primary method of identifying connectivity defects in ASD has been through the examination of changes in white matter and the identification of structural biomarkers (Jiang, Shou et al. 2021, Nisar and Haris 2023). This is typically achieved through MRI data, but in our case, we used µCT data to analyse large sets of volumetric white matter data in regions commonly associated with ASD.

Despite our expectations, we did not find any significant changes in our volumetric studies. This could be due to the need for a more powerful scanner or a larger sample size. We anticipated that the gene Reelin, which we expected to affect both the cerebellum and white matter, would tie our findings together. However, the molecular

results were not substantial enough to publish. There were traces of what could be dentate nuclei neuroblasts, but this could merely be a minor difference in time between samples and did not pass initial screening during quantification.

With no clear significance in our set of connectivity data, we must consider what kind of connectivity data we would expect to see differently moving forward. The first step is to look at what changed prenatally and what historically changed prenatally in cases of maternal hypothyroidism, such as a lack of TBR1 staining in the fastigial nuclei.

In cases where lesions are made to the fastigial nucleus, effects are observed due to its efferent projections to the thalamus and the subsequent changes made to the medial prefrontal cortex (Behnke, Stevenson et al. 2018, Helgers 2021, Frontera, Sala et al. 2023). Therefore, I hypothesize that these prenatal insults may affect the formation of these efferent connections to cortical areas of the brain later in development, impacting the connectivity and cognitive activity of the cerebellum.

While the lateral/dentate nucleus has been strongly associated with the cognitive effects of the cerebellum, increasing evidence supports the role of other DCNs, such as the fastigial nucleus, as potential contributors to neuropsychiatric disorders. The fastigial nucleus sends fibres to the forebrain, including the limbic system and prefrontal regions, highlighting its importance for higher-order functions such as emotions, social behaviour, and cognition (Watson, Becker et al. 2014, Zhang, Wang et al. 2016, Carta, Chen et al. 2019). In addition to this indirect input via the Ventral tegmental area (VTA) and the thalamus, several other limbic and mesolimbic structures, such as the amygdala, the septum, and the hippocampus, are directly targeted by the fastigial nucleus (Carta, Chen et al. 2019). These widespread connections, confirmed in electrophysiological studies, suggest a broader and more

complex role for the cerebellum in cognitive and emotional processes (Watson, Becker et al. 2014, Carta, Chen et al. 2019, Helgers 2021).

The formation of connections between the cerebral nuclei and the thalamus begins between 14.5 and 15.5 days, with these fibres invading the thalamus at 16.5 days. This timeline directly aligns with the observed change in staining in the fastigial nuclei, as we observed a reduction in TBR1-positive cells at 16.5 (Dumas, Gornati et al. 2022).

Prenatal damage to the fastigial nucleus may be linked to the long-term behavioural changes observed in our model, as it alters thalamo-cortical connections. In adult models, restricting the activity of the fastigial nucleus through either lesions or chemogenetic alterations results in the modulation of the thalamic–prefrontal cortex circuitry (Helgers, Al Krinawe et al. 2020, Frontera, Sala et al. 2023). An observed behavioural change resulting from this modulation is increased fear and anxiety behaviours, as observed in male mice treated with MMI. This finding suggests that future research with this model should not only investigate modulation in these areas but also consider the sexual dimorphism of our initially observed behaviours. Importantly, owing to time constraints and the sample size caused by the COVID-19 pandemic and damage to tissues from previous tests, a comprehensive examination of sexual dimorphisms was not feasible in this study.

Consequently, could disruptions in the development of the fastigial nucleus potentially impair its connectivity, leading to dysfunction in the associated cortical targets? However, this hypothesis might be questioned by initial cerebellar experiments involving TBR1 knockouts. These studies suggest that TBR1 might not be essential for the early development of DCN axon pathways (Fink, Englund et al. 2006).

Therefore, if there is a change in DCN output, it might need to be attributed to a different source. However, this study examined only efferent connections to the red nuclei and pons, suggesting that pathways related to more cognitive functions, such as the mediodorsal thalamus or the mesolimbic system, are involved (Bohne, Schwarz et al. 2019, Carta, Chen et al. 2019).

Another explanation for the long-term behavioural effects we are observing may be that the aberrant environment of maternal hypothyroidism in the first trimester results in delayed formation of the fastigial nucleus, leading to long-term epigenetic effects. Lesions of the fastigial nucleus in juvenile rats have been shown to affect significant DNA methylation and protein expression changes in GAD1 and OXTR in the Prefrontal cortex (PFC) and Nucleus accumbens (NaC) (Helgers, Angelov et al. 2021). This hypothesis gains additional support through the observed association of cerebellar-related ASD with the epigenetic dysregulation of GAD1 and OXTRs (Waye and Cheng 2018). This finding is also in line with previous studies showing that pharmacological intervention with maternal hormones during pregnancy during the first trimester can lead to epigenetic effects with TH-mediated epigenetic programming of GFAP in the neocortex through increased expression of the epigenetic regulator Mecp2 (Kumar, Godbole et al. 2018). Interestingly, OXTR and MECP2 are dysregulated in response to maternal environmental factors such as folic acid deficiency, suggesting that these epigenetic changes in response to changes in the prenatal environment may be key in the sporadic nature of idiopathic ASD (Gallo, Stoccoro et al. 2022).

In the future, a study using functional MRI or EEG electrophysiological studies could help us gain further insight into the aetiology of the disorder and how these initial insults caused by maternal hypothyroidism led to the behavioural effects we observed

later in juvenile mice. recent studies have demonstrated that cerebellar stimulation can entrain prefrontal cortex activity in a frequency-dependent manner, with effects varying based on the initial EEG state (Tremblay, Chapman et al. 2019). By investigating stimulation at different frequencies (1-50 Hz), we can observe distinct effects on oscillatory power and coherence in both cerebellar and cortical regions. This approach could help us understand how maternal hypothyroidism leads to the behavioural effects observed in juvenile mice.

Additionally, transcranial magnetic stimulation of the cerebellum has been used to assess cerebello-cortical connectivity, revealing specific EEG responses in prefrontal and parietal areas, including a high-beta frequency power increase in the left prefrontal region (Gassmann, Gordon et al. 2022). These findings highlight the cerebellum's role in modulating cortical networks across various frequencies, which could be crucial for our study.

Further research has explored cerebellar connectivity and functionality using various techniques. In vitro assessments have revealed frequency-dependent modulation of cerebellar slice excitability and functional connectivity in response to repetitive transcranial magnetic stimulation (Tang, Zhang et al. 2016). These studies emphasize the importance of considering frequency-dependent factors in understanding cerebellar function and dysfunction, which will be integral to our investigation.

Electrophysiological measurements of the cerebellum have provided valuable insights into its functional mechanisms. Intracranial recordings in humans have revealed cerebellar rhythms up to 250 Hz with task-related modulations lasting 100-200 ms (Dalal, Osipova et al. 2013).These findings align with rodent studies and human

magnetoencephalography results, suggesting that similar frequency ranges could be informative in our study.

By focusing on these frequency ranges, our experiment can build on past research to gain a deeper understanding of the cerebellum's role in modulating cortical networks and the underlying mechanisms of the observed behavioural effects.

5.2 FUTURE OF ASD DIAGNOSIS AND LIMITATIONS IN BIOMARKER TESTING

In contrast, significant progress has been made in the conceptualization of ASD and the molecular and cellular mechanisms underlying its pathology. Despite this, the role and contribution of environmental factors to how genotype and phenotype are related in terms of differing genotypes and differing factors in heterogeneous disorders and how they are related still need to be fully understood. The small barrier may be understanding how to faithfully recreate the complex events of human development with the limitations of in vivo work and models given differences in brain morphology and functionality. This is a particular challenge regarding both cerebellar development and environmental factors, which may have a specific window of influence during pregnancy. The protracted development of the cerebellum differs across different timelines between rodents and humans (Westerhuis, Dudink et al. 2023). In the case of maternal hypothyroidism in both rodents and humans, there is a dependency on maternal thyroid hormones during pregnancy. However, this dependency extends longer into gestation for rodents than it does for humans. The models would be most accurate if they consider this difference and restrict hypothyroidism to the period where each species is completely dependent on maternal thyroid hormones (Ghanbari and Ghasemi 2017). However, even when the foetus is not fully dependent on maternal thyroid hormones, there is still a substantial degree of dependence, as

foetal and maternal thyroid hormones cooperate in various ways (Forhead and Fowden 2014). Animal models such as rat studies, which can extend the effect beyond the early stages of pregnancy, may become worse models, as development can deviate from that of a human embryo, as common animal models such as rats do not complete the development of a fully follicular thyroid gland until 3 weeks postnatally (Forhead and Fowden 2014). There is a difference in the availability of maternal T3 after the onset of foetal thyroid hormone, even between rodent species. The availability of maternal T3 varies after the onset of foetal thyroid hormone, even among different rodent species. In mice, the maternal T4 contribution at term is greater than that in rats, with 60% of the total TH content in peripheral tissues coming directly from the mother. In contrast, in rats, only approximately 17.5% of the foetal extrathyroidal T4 and 47% of the foetal pool of T3 originate from the mother (Bárez-López, Obregon et al. 2017). This finding suggests a greater reliance on the local conversion of T4 into T3 via D2 within the mouse's later foetal stages. This finding suggests that studies that investigate maternal hypothyroidism with windows that extend far past foetal thyroid onset should be aware of any differences that a model may bring.

Therefore, models should create hypothyroidism when an overlap between the foetus and the mother's THs is at its minimum and when the two stages of development are most comparable. To address the constraints associated with interspecies variations in brain morphology and functionality observed in vivo rodent models, exploring in vitro screening methods for endocrine-induced developmental neurotoxicity could be advantageous. One promising approach is currently being developed by the ENDpoiNT consortium. Given the heterogeneity of the disorder, a viable solution would likely involve patient-specific approaches. This finding implies that the use of patient-derived induced pluripotent stem cells could be the most effective strategy.

However, this approach is not without significant limitations, particularly in terms of screening and testing. (Villa, Combi et al. 2021). In 2D cultures, there appears to be a disruption in morphology, the environmental stress response, and cellular regulation compared with 3D cultures (Forsberg, Ilieva et al. 2018).

Comparisons were made at the intersection of genes and the environment. This discrepancy could pose a challenge to the use of 2D cell culture for investigating epigenetic regulation in ASD. Organoids represent a promising method of modelling moving forward for ASD with cerebral organoids that are already able to show an epigenomic state very similar to that of the human fetal brain (Luo, Lancaster et al. 2016). Organoids have shown promise in elucidating responses to environmental factors, a key aspect in identifying disrupted gene targets in idiopathic ASD. Valproate exposure in human forebrain organoids has been shown to modify the expression of genes involved in neural development, synaptic transmission, and oxytocin signalling, which are all significant factors in ASD (Meng, Zhang et al. 2022). This study further revealed that such exposure disrupted genes within ASD risk-associated gene coexpression modules. This highlights the utility of organoids in decoding the complex gene-environment interplay in ASD. However, progress has been made in understanding the role of organoids, such as vascularization, and the absence of microglia in these models hinders the accurate representation of synaptic defects within ASDs (Chan, Griffiths et al. 2020). Notably, modelling ASD cases in which the pathophysiology is related to the cerebellum in organoids may be difficult. Although early cerebellar organoid models have shown the ability to express cerebellar progenitors, such as those in the PCS and DCNS, they are only partially able to recapitulate the complexity of the human cerebellum, are heavily restricted to the early stages of development and fail to show the full neuronal connectivity of the cerebellum

(Muguruma, Nishiyama et al. 2015). More recent developments in the formation of cerebellar organoids, such as those recently created by Altman et al., have allowed for longer periods of organoid differentiation, maturation, and network formation. Recent advancements in cerebellar organoid formation, exemplified by Altman et al.'s work, have extended the duration of organoid differentiation, maturation, and network development. Notably, these in vitro differentiated Purkinje cells (PCs) closely resemble late midgestational in vivo neurons. These findings suggest that cerebellar organoids hold promise for exploring neurophysiological aspects of ASD. Additionally, expression analysis revealed an enrichment of ASD risk genes across various neuronal cell types within these organoids, including progenitor and mature molecular layer interneurons, immature and mature inhibitory neurons of the cerebellar nuclei, and especially immature and differentiated PCs.

As we rapidly approach solutions for critical challenges related to cerebellar organoids—such as addressing cellular diversity and internal connectivity—we must also anticipate the next set of hurdles facing in vitro cerebellar disease modelling. A pivotal aspect of cerebellar disorders, and their impact on cognitive function, lies in their intricate connections with other brain regions via cerebellocortical pathways. These connections play crucial roles, as research suggests that early developmental changes in the cerebellum, triggered by environmental factors such as prenatal hypothyroidism, may later manifest through cerebral connections rather than direct cerebellar defects. Consequently, the next phase of modelling involves advancing cerebellar assembloids—brain organoids that allow the combination of multiple brain regions in a three-dimensional culture. Ultimately, this progress will enable us to closely observe the interactions between these interconnected brain areas

5.3 HETEROGENEITY CLUSTERING AND STRATIFICATION

Biomarkers are objective measures of biological or pathophysiological processes or pharmacologic responses to therapeutic interventions (Group, Atkinson Jr et al. 2001). Identifying biomarkers for ASD presents a significant challenge due to the heterogeneity of the disorder. While the same behavioural phenotypes are observed across multiple different insults or effectors, whether genetic or lesion-based, many of these tend to have differing or even contradictory effects (Patel, Lukkes et al. 2018). The issue of heterogeneity was further complicated by the DSM-5's decision to group all disorders under one umbrella (DSM-5 2013). While current stratifications of the disorder are limited, further stratifying ASD into more homogeneous groups may be beneficial for research and biomarker discovery. There are three potential interpretations for the observed diversity in ASD. The first interpretation suggests that we might be observing multiple distinct conditions that exhibit similar behavioural traits but lack biological connections. This implies that ASD might not be a single entity, at least not a single entity biologically (Waterhouse, London et al. 2016). The second interpretation considers this diversity as an inherent characteristic of ASD. This suggests that the path to personalized medicine and improved therapeutic interventions necessitates better stratification of relevant subgroups (Mottron and Bzdok 2020, Molloy and Gallagher 2022). The third interpretation is that the diversity is due to the absence of a comprehensive framework and understanding of the underlying mechanisms. This creates a circular problem where diversity makes the underlying mechanisms less discernible, and the absence of a clear model contributes to perceived diversity. If we can identify the mechanisms contributing to the diversity, we could separate their effects, resulting in a more uniform phenotype. Research in

animals shows that certain effects create the social behaviours associated with ASD (Li, Zhu et al. 2021). However, it might be more effective to group disorders on the basis of their pathophysiology or endophenotypes. This approach could help us converge on singular biomarkers or find specific biomarkers for each stratification, thereby enhancing our understanding of ASD and improving diagnostic accuracy.

The concept of categorizing ASD based on its underlying mechanisms and creating clusters of endophenotypes is not a novel approach. Previous attempts have been made to group ASD-associated genes according to their corresponding phenotypes. The pathophysiology of ASD has been classified in various ways, including changes in white matter, alterations in functional connectivity, and the roles of genes identified through Genome-wide association studies (GWASs) (Ellegood, Anagnostou et al. 2015, Narita, Nagai et al. 2020, Zerbi, Pagani et al. 2021). However, the application of these research concepts to the actual diagnosis of ASD remains unexplored.

5.4 POTENTIAL OF PRECISION MEDICINES FOR ASD

The heterogeneity of ASD necessitates a shift towards precision or personalized medicine. This transformation is driven by the recognition of the phenotypic and etiological variability among individuals on the ASD spectrum and the current lack of effective treatments. The future of ASD biomarkers may lie in the development of personalized medicine, as highlighted by (Mesleh, Abdulla et al. 2021). This approach is supported by the potential of multiomics and clinical data integration to identify distinct disease subtypes, as discussed by (Higdon, Earl et al. 2015). A recent investigation highlighted the effectiveness of a method that combines various data sources, such as healthcare claims, electronic health records, whole-exome sequencing, and transcriptome profiles. This method was used to pinpoint a subset of dyslipidemia-associated ASD (Luo, Eran et al. 2020). However, it is important to note that relying solely on this big data approach may not overcome all the challenges. Detailed genotype-phenotype studies, along with quantitative in vitro and in vivo ASD models, are essential for the discovery of new treatments or the repurposing of existing treatments.

Given the importance of subphenotype-dependent disease markers for the diagnosis and personalized treatment of ASD (Hu 2012), personalized technology may play a key role in providing individuals with ASD with the means to access the world (Farr, Yuill et al. 2010). These studies collectively highlight the need for a personalized approach to the development of ASD biomarkers, considering the heterogeneity of the disorder and the unique needs of individuals. Precision medicine aims to tailor treatments by understanding the underlying pathophysiology and combining the drug or intervention with a companion diagnostic, such as a stratification biomarker. Given the diverse etiologies and mechanisms in ASD, precision medicine offers a promising approach to effective treatments. For instance, in Cystic fibrosis (CF), understanding

genetic mutations allows for patient stratification into six classes based on the mutations and their effects, aiding in the development of optimal therapy plans. The development of CFTR modulator drugs based on these genetic mutations exemplifies the success of precision medicine, showing significant clinical benefits (Haq et al., 2022). This approach highlights how genotype-phenotype correlations and pharmacogenetic therapies can address the primary defects of genetic disorders (Chang & Zabner, 2015).

In ASD, the heterogeneous nature of the condition necessitates a precision medicine approach to identify effective treatments (Loth, Spooren et al. 2016). Research is increasingly focusing on genetic and molecular data to identify biomarkers and subgroups that respond to specific treatments (Stojanovska 2024). Both ASD and CF underscore the potential of precision medicine to improve patient outcomes through tailored treatments. (Chang and Zabner 2015). The National Academy of Sciences Precision Medicine Report proposes that 'when multiple molecular indicators are used in combination with conventional clinical, histological, and laboratory findings, they offer the opportunity for a more accurate and precise description and classification of disease'(Luo, Eran et al. 2020). These findings underscore the potential of precision medicine in transforming the treatment landscape for ASD.

Chapter 6: Conclusions

This thesis has detailed the current challenges facing ASD diagnosis and underscored the need for a deeper understanding of how environmental effects contribute to its sporadic nature. The following key achievements have been made in advancing this field:

1. No large gross white matter changes were observed in cases of maternal hypothyroidism in a mammalian model. This finding provides insights into the potential limitations of neuroimaging in identifying consistent structural biomarkers across ASD).

2. Transient maternal hypothyroidism was found to lead to significant changes in the expression of TBR1 within the fastigial medial nuclei in a prenatal murine model. These changes, conserved from chick models, suggest potential clinical relevance and interest in human targets.

3. It was observed that prenatal changes leading to ASD behavioural effects in adult mice may not be fully conserved into adulthood. This implies that the initial cause may not be obvious for late-stage diagnoses, especially in tight windows of environmental exposure such as PCBs or PBDEs. This could explain some of the sporadic nature of ASD.

Each of these findings contributes to our growing understanding of ASD and offers new avenues for future research. We hope that my work here helps increase the overall understanding of the pathophysiology of the disorder.

Chapter 7: References

Abdallah, M. W., N. Larsen, J. Grove, B. Nørgaard-Pedersen, P. Thorsen, E. L. Mortensen and D. M. Hougaard (2013). "Amniotic fluid inflammatory cytokines: potential markers of immunologic dysfunction in autism spectrum disorders." The World Journal of Biological Psychiatry **14**(7): 528-538.

Achkova, M. and H. Manolova (2014). "Diagnosis “autism”–from Kanner and Asperger to DSM-5." Journal of Intellectual Disability-Diagnosis and Treatment **2**(2): 112-118.

Ahmed, R. (2018). "Is there a connection between maternal hypothyroidism and developing autism spectrum disorders." ARC Journal of Neuroscience **3**(1): 5-8.

Al-Afif, S., J. K. Krauss, F. Helms, S. Angelov, N. John, K. Schwabe and E. J. Hermann (2019). "Long-term impairment of social behavior, vocalizations and motor activity induced by bilateral lesions of the fastigial nucleus in juvenile rats." Brain Structure and Function **224**(5): 1739-1751.

Ameis, S. H. and M. Catani (2015). "Altered white matter connectivity as a neural substrate for social impairment in Autism Spectrum Disorder." Cortex **62**: 158-181.

Anagnostou, E. (2018). "Clinical trials in autism spectrum disorder: evidence, challenges and future directions." Current opinion in neurology **31**(2): 119-125.

Andersen, S. L., S. Andersen, P. Vestergaard and J. Olsen (2018). "Maternal thyroid function in early pregnancy and child neurodevelopmental disorders: a Danish nationwide case-cohort study." Thyroid **28**(4): 537-546.

Anderson, G. M. (2015). "Autism biomarkers: challenges, pitfalls and possibilities." Journal of Autism and Developmental Disorders **45**: 1103-1113.

Anderson, R. and A. M. Maga (2015). "A novel procedure for rapid imaging of adult mouse brains with microCT using iodine-based contrast." PloS one **10**(11): e0142974.

Anteraper, S. A., X. Guell, H. P. Taylor, A. D'Mello, S. Whitfield-Gabrieli and G. Joshi (2019). "Intrinsic functional connectivity of dentate nuclei in autism spectrum disorder." Brain Connectivity **9**(9): 692-702.

Apsley, E. J. and E. B. Becker (2022). "Purkinje cell patterning—insights from single-cell sequencing." Cells **11**(18): 2918.

Auyeung, B., M. V. Lombardo and S. Baron-Cohen (2013). "Prenatal and postnatal hormone effects on the human brain and cognition." Pflügers Archiv-European Journal of Physiology **465**: 557-571.

Bankhead, P., M. B. Loughrey, J. A. Fernández, Y. Dombrowski, D. G. McArt, P. D. Dunne, S. McQuaid, R. T. Gray, L. J. Murray and H. G. Coleman (2017). "QuPath: Open source software for digital pathology image analysis." Scientific reports **7**(1): 1-7.

Barez-Lopez, S., D. Bosch-García, D. Gomez-Andres, I. Pulido-Valdeolivas, A. Montero-Pedrazuela, M. J. Obregon and A. Guadano-Ferraz (2014). "Abnormal motor phenotype at adult stages in mice lacking type 2 deiodinase." PloS one **9**(8): e103857.

Bárez-López, S., M. J. Obregon, J. Bernal and A. Guadaño-Ferraz (2017). "Thyroid Hormone Economy in the Perinatal Mouse Brain: Implications for Cerebral Cortex Development." Cerebral Cortex **28**(5): 1783-1793.

Barnard, R. A., J. N. Jahncke, S. Grindstaff, L. M. Fedorov, A. C. Adey, K. M. Wright and B. J. O'Roak (2022). "Shared and distinct functional effects of patient-specific Tbr1 mutations on cortical development." Journal of Neuroscience **42**(37): 7166-7181.

Baron-Cohen, S., B. Auyeung, B. Nørgaard-Pedersen, D. M. Hougaard, M. W. Abdallah, L. Melgaard, A. S. Cohen, B. Chakrabarti, L. Ruta and M. V. Lombardo (2015). "Elevated fetal steroidogenic activity in autism." Molecular psychiatry **20**(3): 369-376.

Barra, G. B., L. F. Velasco, R. P. Pessanha, A. M. Campos, F. N. Moura, S. M. Dias, I. Polikarpov, R. C. Ribeiro, L. A. Simeoni and F. A. Neves (2004). "Molecular mechanism of thyroid hormone action." Arquivos Brasileiros de Endocrinologia & Metabologia **48**: 25-39.

Basson, M. A. and R. J. Wingate (2013). "Congenital hypoplasia of the cerebellum: developmental causes and behavioral consequences." Frontiers in neuroanatomy **7**: 29.

Bauman, M. and T. L. Kemper (1985). "Histoanatomic observations of the brain in early infantile autism." Neurology **35**(6): 866-866.

Bayin, N. S., A. Wojcinski, A. Mourton, H. Saito, N. Suzuki and A. L. Joyner (2018). "Age-dependent dormant resident progenitors are stimulated by injury to regenerate Purkinje neurons." Elife **7**.

Beck, D. B., A. Petracovici, C. He, H. W. Moore, R. J. Louie, M. Ansar, S. Douzgou, S. Sithambaram, T. Cottrell and R. L. P. Santos-Cortez (2020). "Delineation of a human Mendelian disorder of the DNA demethylation machinery: TET3 deficiency." The American Journal of Human Genetics **106**(2): 234-245.

Behnke, V. K., M. E. Stevenson and R. A. Swain (2018). "Inactivation of the cerebellar fastigial nuclei alters social behavior in the rat." Behavioral neuroscience **132**(6): 552.

Bernal, J. (2007). "Thyroid hormone receptors in brain development and function." Nature clinical practice Endocrinology & metabolism **3**(3): 249-259.

Bianco, A. C. and P. R. Larsen (2005). "Cellular and structural biology of the deiodinases." Thyroid **15**(8): 777-786.

Bilbo, S. D., C. L. Block, J. L. Bolton, R. Hanamsagar and P. K. Tran (2018). "Beyond infection-Maternal immune activation by environmental factors, microglial

development, and relevance for autism spectrum disorders." Experimental neurology **299**: 241-251.

Björnholm, L., O. Orell, M. Kerkelä, U. Honka, S. Laasonen, T. Riekki, H.-M. Surcel, E. Suvanto and J. Veijola (2023). "Maternal thyroid function during pregnancy and offspring white matter microstructure in early adulthood: A prospective birth cohort study." Thyroid **33**(10): 1245-1254.

Björnholm, L., O. Orell, M. Kerkelä, U. Honka, S. Laasonen, T. Riekki, H. M. Surcel, E. Suvanto and J. Veijola (2023). "Maternal Thyroid Function During Pregnancy and Offspring White Matter Microstructure in Early Adulthood: A Prospective Birth Cohort Study." Thyroid **33**(10): 1245-1254.

Boerckel, J. D., D. E. Mason, A. M. McDermott and E. Alsberg (2014). "Microcomputed tomography: approaches and applications in bioengineering." Stem cell research & therapy **5**(6): 1-12.

Boesen, S. A., M. Long, M. Wielsøe, V. Mustieles, M. F. Fernandez and E. C. Bonefeld-Jørgensen (2020). "Exposure to Perflouroalkyl acids and foetal and maternal thyroid status: a review." Environmental Health **19**(1): 1-28.

Bohne, P., M. K. Schwarz, S. Herlitze and M. D. Mark (2019). "A New Projection From the Deep Cerebellar Nuclei to the Hippocampus via the Ventrolateral and Laterodorsal Thalamus in Mice." Frontiers in Neural Circuits **13**.

Bölte, S., S. Girdler and P. B. Marschik (2019). "The contribution of environmental exposure to the etiology of autism spectrum disorder." Cellular and Molecular Life Sciences **76**: 1275-1297.

Bonora, E., K. Beyer, J. Lamb, J. Parr, S. Klauck, A. Benner, M. Paolucci, A. Abbott, I. Ragoussis and A. Poustka (2003). "Analysis of reelin as a candidate gene for autism." Molecular psychiatry **8**(10): 885-892.

Boukhtouche, F., B. Brugg, R. Wehrlé, B. Bois-Joyeux, J. L. Danan, I. Dusart and J. Mariani (2010). "Induction of early Purkinje cell dendritic differentiation by thyroid hormone requires RORα." Neural Dev **5**: 18.

Bradley, D. J., H. Towle and W. r. Young (1992). "Spatial and temporal expression of alpha-and beta-thyroid hormone receptor mRNAs, including the beta 2-subtype, in the developing mammalian nervous system." Journal of Neuroscience **12**(6): 2288-2302.

Brandenburg, C., A. J. Griswold, D. J. Van Booven, M. B. Kilander, J. A. Frei, M. W. Nestor, D. M. Dykxhoorn, M. A. Pericak-Vance and G. J. Blatt (2022). "Transcriptomic analysis of isolated and pooled human postmortem cerebellar Purkinje cells in autism spectrum disorders." Frontiers in genetics **13**: 944837.

Buffo, A. and F. Rossi (2013). "Origin, lineage and function of cerebellar glia." Progress in neurobiology **109**: 42-63.

Cao, J., C. Chen, T. Zhang, Y. Han, R. Qin, W. Su, J. Tian, F. Liang, Q. Shi and H. Zhang (2023). "Segmental Abnormalities of White Matter Microstructure in Primary Hypothyroidism Identified by Automated Fiber Quantification." Neuroendocrinology **113**(6): 589-605.

Carta, I., C. H. Chen, A. L. Schott, S. Dorizan and K. Khodakhah (2019). "Cerebellar modulation of the reward circuitry and social behavior." Science **363**(6424): eaav0581.

Carter, R. A., L. Bihannic, C. Rosencrance, J. L. Hadley, Y. Tong, T. N. Phoenix, S. Natarajan, J. Easton, P. A. Northcott and C. Gawad (2018). "A single-cell transcriptional atlas of the developing murine cerebellum." Current Biology **28**(18): 2910-2920. e2912.

Cerrato, V. and A. Buffo (2021). Gliogenesis. Handbook of the cerebellum and cerebellar disorders, Springer**:** 121-138.

Cerrato, V., E. Parmigiani, M. Figueres-Oñate, M. Betizeau, J. Aprato, I. Nanavaty, P. Berchialla, F. Luzzati, C. De'Sperati and L. López-Mascaraque (2018). "Multiple origins and modularity in the spatiotemporal emergence of cerebellar astrocyte heterogeneity." PLoS biology **16**(9): e2005513.

Cesh, L. S., K. H. Elliott, S. Quade, M. A. McKinney, F. Maisoneuve, D. K. Garcelon, C. D. Sandau, R. J. Letcher, T. D. Williams and J. E. Elliott (2010). "Polyhalogenated aromatic hydrocarbons and metabolites: Relation to circulating thyroid hormone and retinol in nestling bald eagles (Haliaeetus leucocephalus)." Environmental toxicology and chemistry **29**(6): 1301-1310.

Chan, W. K., R. Griffiths, D. J. Price and J. O. Mason (2020). "Cerebral organoids as tools to identify the developmental roots of autism." Molecular Autism **11**(1): 1-14.

Chang, E. H. and J. Zabner (2015). "Precision genomic medicine in cystic fibrosis." Clinical and translational science **8**(5): 606-610.

Chaste, P. and M. Leboyer (2012). "Autism risk factors: genes, environment, and gene-environment interactions." Dialogues in clinical neuroscience **14**(3): 281-292.

Chen, K. C., A. Arad, Z. M. Song and D. Croaker (2018). "High-definition neural visualization of rodent brain using micro-CT scanning and non-local-means processing." BMC Med Imaging **18**(1): 38.

Cheng, S.-Y., J. L. Leonard and P. J. Davis (2010). "Molecular aspects of thyroid hormone actions." Endocrine reviews **31**(2): 139-170.

Cheroni, C., N. Caporale and G. Testa (2020). "Autism spectrum disorder at the crossroad between genes and environment: contributions, convergences, and interactions in ASD developmental pathophysiology." Molecular autism **11**(1): 69.

Chiurazzi, P., A. K. Kiani, J. Miertus, S. Barati, E. Manara, S. Paolacci, L. Stuppia, F. Gurrieri and M. Bertelli (2020). "Genetic analysis of intellectual disability and autism." Acta Bio Medica: Atenei Parmensis **91**(Suppl 13).

Christensen, J., T. K. Grønborg, M. J. Sørensen, D. Schendel, E. T. Parner, L. H. Pedersen and M. Vestergaard (2013). "Prenatal valproate exposure and risk of autism spectrum disorders and childhood autism." Jama **309**(16): 1696-1703.

Chuang, H. C., T. N. Huang and Y. P. Hsueh (2015). "T-Brain-1–A Potential Master Regulator in Autism Spectrum Disorders." Autism Research **8**(4): 412-426.

Clifford, H., A. Dulneva, C. P. Ponting, W. Haerty and E. B. Becker (2019). "A gene expression signature in developing Purkinje cells predicts autism and intellectual disability co-morbidity status." Scientific reports **9**(1): 485.

Clos, J., C. Legrand and J. Legrand (1980). "Effects of thyroid state on the formation and early morphological development of Bergmann glia in the developing rat cerebellum." Dev Neurosci **3**(4-6): 199-208.

Coffman, K. A., R. P. Dum and P. L. Strick (2011). "Cerebellar vermis is a target of projections from the motor areas in the cerebral cortex." Proceedings of the National Academy of Sciences **108**(38): 16068-16073.

Cooper, H. E., E. Kaden, L. F. Halliday, D.-E. Bamiou, K. Mankad, C. Peters and C. A. Clark (2019). "White matter microstructural abnormalities in children with severe congenital hypothyroidism." NeuroImage: Clinical **24**: 101980.

Coperchini, F., L. Croce, G. Ricci, F. Magri, M. Rotondi, M. Imbriani and L. Chiovato (2021). "Thyroid disrupting effects of old and new generation PFAS." Frontiers in Endocrinology **11**: 612320.

Cranston, J. S., S. F. Tiene, K. Nielsen-Saines, Z. Vasconcelos, M. V. Pone, S. Pone, A. Zin, T. S. Salles, J. P. Pereira and D. Orofino (2020). "Association between antenatal exposure to Zika virus and anatomical and neurodevelopmental abnormalities in children." JAMA network open **3**(7): e209303-e209303.

Crawley, J. N. (2007). "Mouse behavioral assays relevant to the symptoms of autism." Brain pathology **17**(4): 448-459.

D'Angelo, E. (2018). "Physiology of the cerebellum." Handbook of clinical neurology **154**: 85-108.

D'Angelo, G., L. Marseglia, S. Manti, L. Colavita, C. Cuppari, P. Impellizzeri, S. Arena, T. Arrigo, C. Salpietro and E. Gitto (2016). "Atopy and autoimmune thyroid diseases: melatonin can be useful?" Italian Journal of Pediatrics **42**: 1-6.

Dalal, S. S., D. Osipova, O. Bertrand and K. Jerbi (2013). "Oscillatory activity of the human cerebellum: the intracranial electrocerebellogram revisited." Neuroscience & Biobehavioral Reviews **37**(4): 585-593.

Dalvand, A., S. C. da Silva Rosa, S. Ghavami and H. Marzban (2022). "Potential role of TGFB and autophagy in early cerebellum development." Biochemistry and Biophysics Reports **32**: 101358.

Davis, P. J., F. Goglia and J. L. Leonard (2016). "Nongenomic actions of thyroid hormone." Nature Reviews Endocrinology **12**(2): 111-121.

de Escobar, G. M., M. a. J. Obregón and F. E. del Rey (2004). "Maternal thyroid hormones early in pregnancy and fetal brain development." Best practice & research Clinical endocrinology & metabolism **18**(2): 225-248.

De Rubeis, S., X. He, A. P. Goldberg, C. S. Poultney, K. Samocha, A. Ercument Cicek, Y. Kou, L. Liu, M. Fromer and S. Walker (2014). "Synaptic, transcriptional and chromatin genes disrupted in autism." Nature **515**(7526): 209-215.

Delbaere, J., S. L. Van Herck, N. Bourgeois, P. Vancamp, S. Yang, R. J. Wingate and V. M. Darras (2016). "Mosaic expression of thyroid hormone regulatory genes defines cell type-specific dependency in the developing chicken cerebellum." The Cerebellum **15**(6): 710-725.

Delbaere, J., S. L. Van Herck, N. M. Bourgeois, P. Vancamp, S. Yang, R. J. Wingate and V. M. Darras (2016). "Mosaic expression of thyroid hormone regulatory genes defines cell type-specific dependency in the developing chicken cerebellum." The Cerebellum **15**: 710-725.

Delbaere, J., P. Vancamp, S. Van Herck, N. Bourgeois, M. J. Green, R. Wingate and V. M. Darras (2017). "MCT8 deficiency in Purkinje cells disrupts embryonic chicken cerebellar development." J Endocrinol **232**(2): 259-272.

Den Hoed, J., E. Sollis, H. Venselaar, S. B. Estruch, P. Deriziotis and S. E. Fisher (2018). "Functional characterization of TBR1 variants in neurodevelopmental disorder." Scientific Reports **8**(1): 14279.

Desouza, L. A., M. Sathanoori, R. Kapoor, N. Rajadhyaksha, L. E. Gonzalez, A. H. Kottmann, S. Tole and V. A. Vaidya (2011). "Thyroid hormone regulates the expression of the sonic hedgehog signaling pathway in the embryonic and adult Mammalian brain." Endocrinology **152**(5): 1989-2000.

Di Giovanni, D., R. Enea, V. Di Micco, A. Benvenuto, P. Curatolo and L. Emberti Gialloreti (2023). "Using machine learning to explore shared genetic pathways and possible endophenotypes in autism spectrum disorder." Genes **14**(2): 313.

Diamanti-Kandarakis, E., J.-P. Bourguignon, L. C. Giudice, R. Hauser, G. S. Prins, A. M. Soto, R. T. Zoeller and A. C. Gore (2009). "Endocrine-disrupting chemicals: an Endocrine Society scientific statement." Endocrine reviews **30**(4): 293-342.

Divya, T. S., S. Lalitha, S. Parvathy, C. Subashini, R. Sanalkumar, S. B. Dhanesh, V. A. Rasheed, M. S. Divya, S. Tole and J. James (2016). "Regulation of Tlx3 by Pax6 is required for the restricted expression of Chrnα3 in Cerebellar Granule Neuron progenitors during development." Scientific Reports **6**(1): 30337.

Doulazmi, M., F. Frederic, F. Capone, M. Becker-Andre, N. Delhaye-Bouchaud and J. Mariani (2001). "A comparative study of Purkinje cells in two RORα gene mutant mice: staggerer and RORα−/−." Developmental Brain Research **127**(2): 165-174.

DSM-5 (2013). ""Autism spectrum disorder." Diagnostic and Statistical Manual of Mental Disorders (The American Psychiatric Association): 50-59.

Duan, D., Y. Fu, G. Paxinos and C. Watson (2013). "Spatiotemporal expression patterns of Pax6 in the brain of embryonic, newborn, and adult mice." Brain Structure and Function **218**: 353-372.

Dumas, D. B., S. V. Gornati, Y. Adolfs, T. Shimogori, R. J. Pasterkamp and F. E. Hoebeek (2022). "Anatomical development of the cerebellothalamic tract in embryonic mice." Cells **11**(23): 3800.

Ebert, D. H. and M. E. Greenberg (2013). "Activity-dependent neuronal signalling and autism spectrum disorder." Nature **493**(7432): 327-337.

Edmonson, C., M. N. Ziats and O. M. Rennert (2014). "Altered glial marker expression in autistic post-mortem prefrontal cortex and cerebellum." Mol Autism **5**(1): 3.

Ellegood, J., E. Anagnostou, B. Babineau, J. Crawley, L. Lin, M. Genestine, E. DiCicco-Bloom, J. Lai, J. Foster and O. Peñagarikano (2015). "Clustering autism: using neuroanatomical differences in 26 mouse models to gain insight into the heterogeneity." Molecular psychiatry **20**(1): 118-125.

Ellegood, J., L. K. Pacey, D. R. Hampson, J. P. Lerch and R. M. Henkelman (2010). "Anatomical phenotyping in a mouse model of fragile X syndrome with magnetic resonance imaging." Neuroimage **53**(3): 1023-1029.

Engelkamp, D., P. Rashbass, A. Seawright and V. v. Heyningen (1999). "Role of Pax6 in development of the cerebellar system." Development **126**(16): 3585-3596.

Englund, C., A. Fink, C. Lau, D. Pham, R. A. Daza, A. Bulfone, T. Kowalczyk and R. F. Hevner (2005). "Pax6, Tbr2, and Tbr1 are expressed sequentially by radial glia, intermediate progenitor cells, and postmitotic neurons in developing neocortex." Journal of Neuroscience **25**(1): 247-251.

Escher, J., W. Yan, E. F. Rissman, H.-L. V. Wang, A. Hernandez and V. G. Corces (2022). "Beyond genes: germline disruption in the etiology of autism spectrum disorders." Journal of autism and developmental disorders **52**(10): 4608-4624.

Farr, W., N. Yuill and H. Raffle (2010). "Social benefits of a tangible user interface for children with autistic spectrum conditions." Autism **14**(3): 237-252.

Fatemi, S. H., K. A. Aldinger, P. Ashwood, M. L. Bauman, C. D. Blaha, G. J. Blatt, A. Chauhan, V. Chauhan, S. R. Dager and P. E. Dickson (2012). "Consensus paper: pathological role of the cerebellum in autism." The Cerebellum **11**: 777-807.

Fauquier, T., F. Chatonnet, F. Picou, S. Richard, N. Fossat, N. Aguilera, T. Lamonerie and F. Flamant (2014). "Purkinje cells and Bergmann glia are primary targets of the TRα1 thyroid hormone receptor during mouse cerebellum postnatal development." Development **141**(1): 166-175.

Feldt-Rasmussen, U., M. Klose and S. Benvenga (2018). "Interactions between hypothalamic pituitary thyroid axis and other pituitary dysfunctions." Endocrine **62**(3): 519-527.

Fernández, L. P., A. López-Márquez and P. Santisteban (2015). "Thyroid transcription factors in development, differentiation and disease." Nat Rev Endocrinol **11**(1): 29-42.

Ferreira, A., M. Pereira, A. Manhaes and P. Barradas (2007). "Ultrastructural identification of oligodendrocyte/myelin proteins in corpus callosum of hypothyroid animals." International journal of developmental neuroscience **25**(2): 87-94.

Fink, A. J., C. Englund, R. A. Daza, D. Pham, C. Lau, M. Nivison, T. Kowalczyk and R. F. Hevner (2006). "Development of the deep cerebellar nuclei: transcription factors and cell migration from the rhombic lip." Journal of Neuroscience **26**(11): 3066-3076.

Flamant, F., J. D. Baxter, D. Forrest, S. Refetoff, H. Samuels, T. S. Scanlan, B. Vennström and J. Samarut (2006). "International Union of Pharmacology. LIX. The pharmacology and classification of the nuclear receptor superfamily: thyroid hormone receptors." Pharmacological reviews **58**(4): 705-711.

Flamant, F., K. Gauthier and S. Richard (2017). "Genetic investigation of thyroid hormone receptor function in the developing and adult brain." Current topics in developmental biology **125**: 303-335.

Forhead, A. J. and A. L. Fowden (2014). "Thyroid hormones in fetal growth and prepartum maturation." J Endocrinol **221**(3): R87-R103.

Forsberg, S. L., M. Ilieva and T. Maria Michel (2018). "Epigenetics and cerebral organoids: promising directions in autism spectrum disorders." Transl Psychiatry **8**(1): 14.

Fransson, P., K.-D. Merboldt, K. M. Petersson, M. Ingvar and J. Frahm (2002). "On the effects of spatial filtering—A comparative fMRI study of episodic memory encoding at high and low resolution." NeuroImage **16**(4): 977-984.

Frontera, J. L., R. W. Sala, I. A. Georgescu, H. Baba Aissa, M. N. d'Almeida, D. Popa and C. Léna (2023). "The cerebellum regulates fear extinction through thalamo-prefrontal cortex interactions in male mice." Nat Commun **14**(1): 1508.

Frontera, J. L., R. W. Sala, I. A. Georgescu, H. Baba Aissa, M. N. d'Almeida, D. Popa and C. Léna (2023). "The cerebellum regulates fear extinction through thalamo-prefrontal cortex interactions in male mice." Nature Communications **14**(1): 1508.

Frye, R. E., S. Vassall, G. Kaur, C. Lewis, M. Karim and D. Rossignol (2019). "Emerging biomarkers in autism spectrum disorder: a systematic review." Annals of translational medicine **7**(23).

Fujita, H., T. Kodama and S. Du Lac (2020). "Modular output circuits of the fastigial nucleus for diverse motor and nonmotor functions of the cerebellar vermis." Elife **9**: e58613.

Gallo, R., A. Stoccoro, R. Cagiano, V. Nicolì, R. Ricciardi, R. Tancredi, R. Trovato, F. M. Santorelli, S. Calderoni and F. Muratori (2022). "Correlation among maternal risk factors, gene methylation and disease severity in females with autism spectrum disorder." Epigenomics **14**(4): 175-185.

Gassmann, L., P. C. Gordon and U. Ziemann (2022). "Assessing effective connectivity of the cerebellum with cerebral cortex using TMS-EEG." Brain Stimulation **15**(6): 1354-1369.

Georgescu, I. A., D. Popa and L. Zagrean (2020). "The anatomical and functional heterogeneity of the mediodorsal thalamus." Brain Sciences **10**(9): 624.

Gereben, B., A. M. Zavacki, S. Ribich, B. W. Kim, S. A. Huang, W. S. Simonides, A. Zeold and A. C. Bianco (2008). "Cellular and molecular basis of deiodinase-regulated thyroid hormone signaling." Endocrine reviews **29**(7): 898-938.

Ghanbari, M. and A. Ghasemi (2017). "Maternal hypothyroidism: An overview of current experimental models." Life Sciences **187**: 1-8.

Gill, P. S., J. L. Clothier, A. Veerapandiyan, H. Dweep, P. A. Porter-Gill and G. B. Schaefer (2021). "Molecular dysregulation in autism spectrum disorder." Journal of Personalized Medicine **11**(9): 848.

Gold, D. A., S. H. Baek, N. J. Schork, D. W. Rose, D. D. Larsen, B. D. Sachs, M. G. Rosenfeld and B. A. Hamilton (2003). "RORα coordinates reciprocal signaling in cerebellar development through sonic hedgehog and calcium-dependent pathways." Neuron **40**(6): 1119-1131.

Gravel, C., R. Sasseville and R. Hawkes (1990). "Maturation of the corpus callosum of the rat: II. Influence of thyroid hormones on the number and maturation of axons." Journal of Comparative Neurology **291**(1): 147-161.

Greco, M., D. Bell, L. Woolnough, S. Laycock, N. Corps, D. Mortimore and D. Hudson (2014). "3-D visualisation, printing, and volume determination of the tracheal respiratory system in the adult desert locust, S chistocerca gregaria." Entomologia Experimentalis et Applicata **152**(1): 42-51.

Green, M. J. and R. J. Wingate (2014). "Developmental origins of diversity in cerebellar output nuclei." Neural development **9**(1): 1-8.

Grøntved, L., J. J. Waterfall, D. W. Kim, S. Baek, M.-H. Sung, L. Zhao, J. W. Park, R. Nielsen, R. L. Walker, Y. J. Zhu, P. S. Meltzer, G. L. Hager and S.-y. Cheng (2015). "Transcriptional activation by the thyroid hormone receptor through ligand-dependent receptor recruitment and chromatin remodelling." Nature Communications **6**(1): 7048.

Group, B. D. W., A. J. Atkinson Jr, W. A. Colburn, V. G. DeGruttola, D. L. DeMets, G. J. Downing, D. F. Hoth, J. A. Oates, C. C. Peck and R. T. Schooley (2001). "Biomarkers and surrogate endpoints: preferred definitions and conceptual framework." Clinical pharmacology & therapeutics **69**(3): 89-95.

Grove, J., S. Ripke, T. D. Als, M. Mattheisen, R. K. Walters, H. Won, J. Pallesen, E. Agerbo, O. A. Andreassen and R. Anney (2019). "Identification of common genetic risk variants for autism spectrum disorder." Nature genetics **51**(3): 431-444.

Guerra, M., V. Medici, R. Weatheritt, V. Corvino, D. Palacios, M. C. Geloso, D. Farini and C. Sette (2023). "Fetal exposure to valproic acid dysregulates the expression of autism-linked genes in the developing cerebellum." Translational Psychiatry **13**(1): 114.

Guidotti, A., D. R. Grayson and H. J. Caruncho (2016). "Epigenetic RELN dysfunction in schizophrenia and related neuropsychiatric disorders." Frontiers in cellular neuroscience **10**: 89.

Guissart, C., X. Latypova, P. Rollier, T. N. Khan, H. Stamberger, K. McWalter, M. T. Cho, S. Kjaergaard, S. Weckhuysen and G. Lesca (2018). "Dual molecular effects of dominant RORA mutations cause two variants of syndromic intellectual disability with either autism or cerebellar ataxia." The American Journal of Human Genetics **102**(5): 744-759.

Ha, T., D. Swanson, M. Larouche, R. Glenn, D. Weeden, P. Zhang, K. Hamre, M. Langston, C. Phillips and M. Song (2015). "CbGRiTS: cerebellar gene regulation in time and space." Developmental biology **397**(1): 18-30.

Ha, T. J., D. J. Swanson, R. Kirova, J. Yeung, K. Choi, Y. Tong, E. J. Chesler and D. Goldowitz (2012). "Genome-wide microarray comparison reveals downstream genes

of Pax6 in the developing mouse cerebellum." European Journal of Neuroscience **36**(7): 2888-2898.

Hardan, A., N. Minshew and M. Keshavan (2000). "Corpus callosum size in autism." Neurology **55**(7): 1033-1036.

Harper, J. W. and R. G. Heath (1973). "Anatomic connections of the fastigial nucleus to the rostral forebrain in the cat." Experimental neurology **39**(2): 285-292.

Hashimoto, M. and K. Mikoshiba (2003). "Mediolateral compartmentalization of the cerebellum is determined on the “birth date” of Purkinje cells." Journal of Neuroscience **23**(36): 11342-11351.

Hashimoto, R., K. Hori, T. Owa, S. Miyashita, K. Dewa, N. Masuyama, K. Sakai, Y. Hayase, Y. Seto and Y. U. Inoue (2016). "Origins of oligodendrocytes in the cerebellum, whose development is controlled by the transcription factor, Sox9." Mechanisms of development **140**: 25-40.

Havdahl, A., M. Niarchou, A. Starnawska, M. Uddin, C. van der Merwe and V. Warrier (2021). "Genetic contributions to autism spectrum disorder." Psychological medicine **51**(13): 2260-2273.

Hawkes, R. and G. G. Consalez (2023). Cerebellar Neurogenesis. Essentials of Cerebellum and Cerebellar Disorders: A Primer For Graduate Students, Springer**:** 93-98.

Heck, D. H., M. B. Fox, B. Correia Chapman, S. S. McAfee and Y. Liu (2023). "Cerebellar control of thalamocortical circuits for cognitive function: A review of pathways and a proposed mechanism." Frontiers in Systems Neuroscience **17**: 1126508.

Helgers, S. (2021). Long-term effects of fastigial nucleus lesions in juvenile rats: behavioral, electrophysiological, and molecular biological analysis, Dissertation, Hannover, Tierärztliche Hochschule Hannover, 2021.

Helgers, S. O., Y. Al Krinawe, M. Alam, J. K. Krauss, K. Schwabe, E. J. Hermann and S. Al-Afif (2020). "Lesion of the fastigial nucleus in juvenile rats deteriorates rat behavior in adulthood, accompanied by altered neuronal activity in the medial prefrontal cortex." Neuroscience **442**: 29-40.

Helgers, S. O., S. Angelov, M. A. Muschler, A. Glahn, S. Al-Afif, Y. Al Krinawe, E. J. Hermann, J. K. Krauss, H. Frieling and K. Schwabe (2021). "Epigenetic regulation of neural transmission after cerebellar fastigial nucleus lesions in juvenile rats." The Cerebellum: 1-9.

Heuer, H. and C. A. Mason (2003). "Thyroid hormone induces cerebellar Purkinje cell dendritic development via the thyroid hormone receptor α1." Journal of Neuroscience **23**(33): 10604-10612.

Heuer, H. and T. J. Visser (2009). "Pathophysiological importance of thyroid hormone transporters." Endocrinology **150**(3): 1078-1083.

Hidayat, M., R. A. Lail and K. P. Lone (2020). "Melatonin Protects the Purkinje Neurons of Cerebellum of Neonates from Apoptosis Induced by Maternal Hypothyroidism in Wistar Rats." Journal of Medical and Biological Science Research **6**(4): 42-50.

Higdon, R., R. K. Earl, L. Stanberry, C. M. Hudac, E. Montague, E. Stewart, I. Janko, J. Choiniere, W. Broomall, N. Kolker, R. A. Bernier and E. Kolker (2015). "The promise of multi-omics and clinical data integration to identify and target personalized healthcare approaches in autism spectrum disorders." Omics **19**(4): 197-208.

Holroyd, S., A. L. Reiss and R. N. Bryan (1991). "Autistic features in Joubert syndrome: a genetic disorder with agenesis of the cerebellar vermis." Biological psychiatry **29**(3): 287-294.

Hoshino, M., S. Nakamura, K. Mori, T. Kawauchi, M. Terao, Y. V. Nishimura, A. Fukuda, T. Fuse, N. Matsuo and M. Sone (2005). "Ptf1a, a bHLH transcriptional gene, defines GABAergic neuronal fates in cerebellum." Neuron **47**(2): 201-213.

Hu, C., S. Wang, D. Wu, C. Yan and M. Wu (2022). "Subclinical hypothyroidism in pregnancy rats impaired offspring's spatial learning and memory and the cerebellar development." Biochem Biophys Res Commun **602**: 63-69.

Hu, V. W. (2012). "Subphenotype-dependent disease markers for diagnosis and personalized treatment of autism spectrum disorders." Disease Markers **33**(5): 277-288.

Hu, V. W., T. Sarachana, R. M. Sherrard and K. M. Kocher (2015). "Investigation of sex differences in the expression of RORA and its transcriptional targets in the brain as a potential contributor to the sex bias in autism." Molecular autism **6**(1): 1-19.

Huang, T.-N. and Y.-P. Hsueh (2015). "Brain-specific transcriptional regulator T-brain-1 controls brain wiring and neuronal activity in autism spectrum disorders." Frontiers in neuroscience **9**: 406.

Ino, H. (2004). "Immunohistochemical characterization of the orphan nuclear receptor RORα in the mouse nervous system." Journal of Histochemistry & Cytochemistry **52**(3): 311-323.

Ishii, S., I. Amano and N. Koibuchi (2021). "The Role of Thyroid Hormone in the Regulation of Cerebellar Development." Endocrinol Metab (Seoul) **36**(4): 703-716.

Iskaros, J., M. Pickard, I. Evans, A. Sinha, P. Hardiman and R. Ekins (2000). "Thyroid hormone receptor gene expression in first trimester human fetal brain." The Journal of Clinical Endocrinology & Metabolism **85**(7): 2620-2623.

Jeon, S. J., J.-W. Kim, K. C. Kim, S. M. Han, H. S. Go, J. E. Seo, C. S. Choi, J. H. Ryu, C. Y. Shin and M.-R. Song (2014). "Translational regulation of NeuroD1 expression by FMRP: involvement in glutamatergic neuronal differentiation of cultured rat primary neural progenitor cells." Cellular and molecular neurobiology **34**: 297-305.

Jetten, A. M. (2009). "Retinoid-related orphan receptors (RORs): critical roles in development, immunity, circadian rhythm, and cellular metabolism." Nucl Recept Signal **7**: e003.

Jiang, X., X.-J. Shou, Z. Zhao, F. Meng, J. Le, T. Song, X. Xu, X. Ke, Y. Chen and X. Cai (2021). "A brain structural connectivity biomarker for diagnosis of autism spectrum disorder in early childhood." medRxiv: 2021.2011. 2003.21265845.

Judd, E. N., S. M. Lewis and A. L. Person (2021). "Diverse inhibitory projections from the cerebellar interposed nucleus." Elife **10**: e66231.

Kalkbrenner, A. E., R. J. Schmidt and A. C. Penlesky (2014). "Environmental chemical exposures and autism spectrum disorders: a review of the epidemiological evidence." Current problems in pediatric and adolescent health care **44**(10): 277-318.

Kanner, L. (1943). "Autistic disturbances of affective contact." Nervous child **2**(3): 217-250.

Kapoor, R., L. A. Desouza, I. N. Nanavaty, S. G. Kernie and V. A. Vaidya (2012). "Thyroid hormone accelerates the differentiation of adult hippocampal progenitors." J Neuroendocrinol **24**(9): 1259-1271.

Keil-Stietz, K. and P. J. Lein (2023). "Gene× environment interactions in autism spectrum disorders." Current topics in developmental biology **152**: 221-284.

Kelly, E., F. Meng, H. Fujita, F. Morgado, Y. Kazemi, L. C. Rice, C. Ren, C. O. Escamilla, J. M. Gibson and S. Sajadi (2020). "Regulation of autism-relevant behaviors by cerebellar–prefrontal cortical circuits." Nature neuroscience **23**(9): 1102-1110.

Kelly, R. M. and P. L. Strick (2003). "Cerebellar loops with motor cortex and prefrontal cortex of a nonhuman primate." Journal of neuroscience **23**(23): 8432-8444.

Kemper, T. L. and M. L. Bauman (1993). "The contribution of neuropathologic studies to the understanding of autism." Neurologic clinics **11**(1): 175-187.

Kersseboom, S., G.-J. Kremers, E. C. Friesema, W. E. Visser, W. Klootwijk, R. P. Peeters and T. J. Visser (2013). "Mutations in MCT8 in patients with Allan-Herndon-Dudley-syndrome affecting its cellular distribution." Molecular endocrinology **27**(5): 801-813.

Khan, A., J. Harney, A. Zavacki and E. Sajdel-Sulkowska (2014). "Disrupted brain thyroid hormone homeostasis and altered thyroid hormone-dependent brain gene expression in autism spectrum disorders." J Physiol Pharmacol **65**(2): 257-272.

Khan, A. J., A. Nair, C. L. Keown, M. C. Datko, A. J. Lincoln and R.-A. Müller (2015). "Cerebro-cerebellar resting-state functional connectivity in children and adolescents with autism spectrum disorder." Biological psychiatry **78**(9): 625-634.

Kikkawa, T., C. R. Casingal, S. H. Chun, H. Shinohara, K. Hiraoka and N. Osumi (2019). "The role of Pax6 in brain development and its impact on pathogenesis of autism spectrum disorder." Brain research **1705**: 95-103.

Kim, K. C., P. Kim, H. S. Go, C. S. Choi, S.-I. Yang, J. H. Cheong, C. Y. Shin and K. H. Ko (2011). "The critical period of valproate exposure to induce autistic symptoms in Sprague–Dawley rats." Toxicology letters **201**(2): 137-142.

Kim, K. C., D.-K. Lee, H. S. Go, P. Kim, C. S. Choi, J.-W. Kim, S. J. Jeon, M.-R. Song and C. Y. Shin (2014). "Pax6-Dependent Cortical Glutamatergic Neuronal Differentiation Regulates Autism-Like Behavior in Prenatally Valproic Acid-Exposed Rat Offspring." Molecular Neurobiology **49**(1): 512-528.

Kircher, M. F. and J. K. Willmann (2012). "Molecular body imaging: MR imaging, CT, and US. part I. principles." Radiology **263**(3): 633-643.

Koibuchi, N. "Cerebellum Development & Thyroid Hormone." Save the Dates!

Koibuchi, N. and P. M. Yen (2016). Thyroid Hormone Disruption and Neurodevelopment, Springer.

Kozareva, V., C. Martin, T. Osorno, S. Rudolph, C. Guo, C. Vanderburg, N. Nadaf, A. Regev, W. G. Regehr and E. Macosko (2021). "A transcriptomic atlas of mouse cerebellar cortex comprehensively defines cell types." Nature **598**(7879): 214-219.

Krishnan, A., R. Zhang, V. Yao, C. L. Theesfeld, A. K. Wong, A. Tadych, N. Volfovsky, A. Packer, A. Lash and O. G. Troyanskaya (2016). "Genome-wide prediction and functional characterization of the genetic basis of autism spectrum disorder." Nature neuroscience **19**(11): 1454-1462.

Koibuchi, N. and P. M. Yen (2016). Thyroid Hormone Disruption and Neurodevelopment, Springer.

Kumar, P., N. M. Godbole, C. P. Chaturvedi, R. S. Singh, N. George, A. Upadhyay, B. Anjum, M. M. Godbole and R. A. Sinha (2018). "Mechanisms involved in epigenetic down-regulation of Gfap under maternal hypothyroidism." Biochemical and biophysical research communications **502**(3): 375-381.

Lai, M. C., M. V. Lombardo and S. Baron-Cohen (2014). "Autism." Lancet **383**(9920): 896-910.

LaSalle, J. M. (2023). "Epigenomic signatures reveal mechanistic clues and predictive markers for autism spectrum disorder." Molecular Psychiatry: 1-12.

Lax, E., S. Do Carmo, Y. Enuka, D. M. Sapozhnikov, L. A. Welikovitch, N. Mahmood, S. A. Rabbani, L. Wang, J. P. Britt, W. W. Hancock, Y. Yarden and M. Szyf (2023). "Methyl-CpG binding domain 2 (Mbd2) is an epigenetic regulator of autism-risk genes and cognition." Translational Psychiatry **13**(1): 259.

Lazar, M. A. (2003). "Thyroid hormone action: a binding contract." The Journal of clinical investigation **112**(4): 497-499.

Legué, E., J. L. Gottshall, E. Jaumouillé, A. Roselló-Díez, W. Shi, L. H. Barraza, S. Washington, R. L. Grant and A. L. Joyner (2016). "Differential timing of granule cell production during cerebellum development underlies generation of the foliation pattern." Neural Development **11**(1): 17.

Legué, E., E. Riedel and A. L. Joyner (2015). "Clonal analysis reveals granule cell behaviors and compartmentalization that determine the folded morphology of the cerebellum." Development **142**(9): 1661-1671.

Leijs, M. M., G. W. t. Tusscher, K. Olie, T. v. Teunenbroek, W. M. C. v. Aalderen, P. d. Voogt, T. Vulsma, A. Bartonova, M. K. v. Krauss, C. Mosoiu, H. Riojas-Rodriguez, G. Calamandrei and J. G. Koppe (2012). "Thyroid hormone metabolism and environmental chemical exposure." Environmental Health **11**(1): S10.

Lejeune, E., A. Javili, J. Weickenmeier, E. Kuhl and C. Linder (2016). "Tri-layer wrinkling as a mechanism for anchoring center initiation in the developing cerebellum." Soft Matter **12**(25): 5613-5620.

Lenart, J., J. Augustyniak, J. W. Lazarewicz and E. Zieminska (2020). "Altered expression of glutamatergic and GABAergic genes in the valproic acid-induced rat model of autism: A screening test." Toxicology **440**: 152500.

Leto, K., M. Arancillo, E. B. Becker, A. Buffo, C. Chiang, B. Ding, W. B. Dobyns, I. Dusart, P. Haldipur and M. E. Hatten (2016). "Consensus paper: cerebellar development." The Cerebellum **15**: 789-828.

Leto, K., M. Arancillo, E. B. E. Becker, A. Buffo, C. Chiang, B. Ding, W. B. Dobyns, I. Dusart, P. Haldipur, M. E. Hatten, M. Hoshino, A. L. Joyner, M. Kano, D. L. Kilpatrick, N. Koibuchi, S. Marino, S. Martinez, K. J. Millen, T. O. Millner, T. Miyata, E. Parmigiani, K. Schilling, G. Sekerková, R. V. Sillitoe, C. Sotelo, N. Uesaka, A. Wefers, R. J. T. Wingate and R. Hawkes (2016). "Consensus Paper: Cerebellar Development." The Cerebellum **15**(6): 789-828.

Li, C., N. B. Saliba, H. Martin, N. A. Losurdo, K. Kolahdouzan, R. Siddiqui, D. Medeiros and W. Li (2023). "Purkinje cell dopaminergic inputs to astrocytes regulate cerebellar-dependent behavior." Nature Communications **14**(1): 1613.

Li, M., M. D. Fallin, A. Riley, R. Landa, S. O. Walker, M. Silverstein, D. Caruso, C. Pearson, S. Kiang and J. L. Dahm (2016). "The association of maternal obesity and diabetes with autism and other developmental disabilities." Pediatrics **137**(2).

Li, Z., Y. X. Zhu, L. J. Gu and Y. Cheng (2021). "Understanding autism spectrum disorders with animal models: applications, insights, and perspectives." Zool Res **42**(6): 800-824.

Lischinsky, J. E., J. Skocic, H. Clairman and J. Rovet (2016). "Preliminary findings show maternal hypothyroidism may contribute to abnormal cortical morphology in offspring." Frontiers in Endocrinology **7**: 16.

Lombardo, M. V., M.-C. Lai and S. Baron-Cohen (2019). "Big data approaches to decomposing heterogeneity across the autism spectrum." Molecular psychiatry **24**(10): 1435-1450.

López-Espíndola, D., C. Morales-Bastos, C. Grijota-Martínez, X.-H. Liao, D. Lev, E. Sugo, C. F. Verge, S. Refetoff, J. Bernal and A. Guadaño-Ferraz (2014). "Mutations of the Thyroid Hormone Transporter MCT8 Cause Prenatal Brain Damage and Persistent Hypomyelination." The Journal of Clinical Endocrinology & Metabolism **99**(12): E2799-E2804.

Loth, E., W. Spooren, L. M. Ham, M. B. Isaac, C. Auriche-Benichou, T. Banaschewski, S. Baron-Cohen, K. Broich, S. Bölte, T. Bourgeron, T. Charman, D. Collier, F. de Andres-Trelles, S. Durston, C. Ecker, A. Elferink, M. Haberkamp, R. Hemmings, M. H. Johnson, E. J. Jones, O. S. Khwaja, S. Lenton, L. Mason, V. Mantua, A. Meyer-Lindenberg, M. V. Lombardo, L. O'Dwyer, K. Okamoto, G. J. Pandina, L. Pani, A. M. Persico, E. Simonoff, S. Tauscher-Wisniewski, J. Llinares-Garcia, S. Vamvakas, S. Williams, J. K. Buitelaar and D. G. Murphy (2016). "Identification and validation of biomarkers for autism spectrum disorders." Nat Rev Drug Discov **15**(1): 70-73.

Lu, Z., Z. Liu, W. Mao, X. Wang, X. Zheng, S. Chen, B. Cao, S. Huang, X. Zhang, T. Zhou, Y. Zhang, X. Huang, Q. Sun and J.-D. Li (2020). "Locus-specific DNA methylation of Mecp2 promoter leads to autism-like phenotypes in mice." Cell Death & Disease **11**(2): 85.

Luo, C., M. A. Lancaster, R. Castanon, J. R. Nery, J. A. Knoblich and J. R. Ecker (2016). "Cerebral Organoids Recapitulate Epigenomic Signatures of the Human Fetal Brain." Cell Rep **17**(12): 3369-3384.

Luo, Y., A. Eran, N. Palmer, P. Avillach, A. Levy-Moonshine, P. Szolovits and I. S. Kohane (2020). "A multidimensional precision medicine approach identifies an autism subtype characterized by dyslipidemia." Nature medicine **26**(9): 1375-1379.

Luongo, C., M. Dentice and D. Salvatore (2019). "Deiodinases and their intricate role in thyroid hormone homeostasis." Nature Reviews Endocrinology **15**(8): 479-488.

Machold, R. and G. Fishell (2005). "Math1 is expressed in temporally discrete pools of cerebellar rhombic-lip neural progenitors." Neuron **48**(1): 17-24.

Magnusson, C., K. Kosidou, C. Dalman, M. Lundberg, B. K. Lee, D. Rai, H. Karlsson, R. Gardner and S. Arver (2016). "Maternal vitamin D deficiency and the risk of autism spectrum disorders: population-based study." BJPsych open **2**(2): 170-172.

Manuel, M. N., D. Mi, J. O. Mason and D. J. Price (2015). "Regulation of cerebral cortical neurogenesis by the Pax6 transcription factor." Frontiers in cellular neuroscience **9**: 70.

Martí-Clua, J. (2022). "Times of neuron origin and neurogenetic gradients in mice Purkinje cells and deep cerebellar nuclei neurons during the development of the cerebellum. A review." Tissue and Cell: 101897.

Martinez, R., C. Eller, N. B. Viana and F. C. Gomes (2011). "Thyroid hormone induces cerebellar neuronal migration and Bergmann glia differentiation through epidermal growth factor/mitogen-activated protein kinase pathway." Eur J Neurosci **33**(1): 26-35.

Mayerl, S., J. Müller, R. Bauer, S. Richert, C. M. Kassmann, V. M. Darras, K. Buder, A. Boelen, T. J. Visser and H. Heuer (2014). "Transporters MCT8 and OATP1C1 maintain murine brain thyroid hormone homeostasis." The Journal of clinical investigation **124**(5): 1987-1999.

McLean, T. R., M. M. Rank, P. M. Smooker and S. J. Richardson (2017). "Evolution of thyroid hormone distributor proteins." Molecular and Cellular Endocrinology **459**: 43-52.

Mecklenburg, N., R. Garcia-López, E. Puelles, C. Sotelo and S. Martinez (2011). "Cerebellar oligodendroglial cells have a mesencephalic origin." Glia **59**(12): 1946-1957.

Meng, Q., W. Zhang, X. Wang, C. Jiao, S. Xu, C. Liu, B. Tang and C. Chen (2022). "Human forebrain organoids reveal connections between valproic acid exposure and autism risk." Translational Psychiatry **12**(1): 130.

Mesleh, A. G., S. A. Abdulla and O. El-Agnaf (2021). "Paving the way toward personalized medicine: current advances and challenges in multi-OMICS approach in autism spectrum disorder for biomarkers discovery and patient stratification." Journal of personalized medicine **11**(1): 41.

Miki, A., Y. Sakuma, H. Ohzawa, A. Saito, Y. Meguro, J. Watanabe, K. Morishima, K. Endo, H. Sasanuma and A. Shimizu (2022). "Clearance of the liver remnant predicts short-term outcome in patients undergoing resection of hepatocellular carcinoma." World Journal of Gastroenterology **28**(38): 5614.

Mohan, V., R. A. Sinha, A. Pathak, L. Rastogi, P. Kumar, A. Pal and M. M. Godbole (2012). "Maternal thyroid hormone deficiency affects the fetal neocorticogenesis by reducing the proliferating pool, rate of neurogenesis and indirect neurogenesis." Experimental neurology **237**(2): 477-488.

Molloy, C. and L. Gallagher (2022). "Can stratification biomarkers address the heterogeneity of autism spectrum disorder?" Irish Journal of Psychological Medicine **39**(3): 305-311.

Moog, N. K., S. Entringer, C. Heim, P. D. Wadhwa, N. Kathmann and C. Buss (2017). "Influence of maternal thyroid hormones during gestation on fetal brain development." Neuroscience **342**: 68-100.

Morellini, N., A. M. Lohof, J. Mariani and R. M. Sherrard (2023). The Staggerer Mouse: RORα Deficiency Induces Cerebellar Neurodegeneration. Essentials of Cerebellum and Cerebellar Disorders: A Primer For Graduate Students, Springer**:** 425-429.

Mosconi, M. W., Z. Wang, L. M. Schmitt, P. Tsai and J. A. Sweeney (2015). "The role of cerebellar circuitry alterations in the pathophysiology of autism spectrum disorders." Frontiers in neuroscience **9**: 296.

Mottron, L. and D. Bzdok (2020). "Autism spectrum heterogeneity: fact or artifact?" Molecular psychiatry **25**(12): 3178-3185.

Mowery, T. M., S. M. Wilson, P. V. Kostylev, B. Dina, J. B. Buchholz, A. L. Prieto and P. E. Garraghty (2015). "Embryological exposure to valproic acid disrupts morphology of the deep cerebellar nuclei in a sexually dimorphic way." International Journal of Developmental Neuroscience **40**: 15-23.

Muguruma, K., A. Nishiyama, H. Kawakami, K. Hashimoto and Y. Sasai (2015). "Self-organization of polarized cerebellar tissue in 3D culture of human pluripotent stem cells." Cell Rep **10**(4): 537-550.

Narita, A., M. Nagai, S. Mizuno, S. Ogishima, G. Tamiya, M. Ueki, R. Sakurai, S. Makino, T. Obara and M. Ishikuro (2020). "Clustering by phenotype and genome-wide association study in autism." Translational psychiatry **10**(1): 290.

Navarro, D., M. Alvarado, F. Navarrete, M. Giner, M. J. Obregon, J. Manzanares and P. Berbel (2015). "Gestational and early postnatal hypothyroidism alters VGluT1 and VGAT bouton distribution in the neocortex and hippocampus, and behavior in rats." Frontiers in neuroanatomy **9**: 9.

Nisar, S. and M. Haris (2023). "Neuroimaging genetics approaches to identify new biomarkers for the early diagnosis of autism spectrum disorder." Molecular Psychiatry.

O'Shaughnessy, K. L., S. E. Thomas, S. R. Spring, J. L. Ford, R. L. Ford and M. E. Gilbert (2019). "A transient window of hypothyroidism alters neural progenitor cells and results in abnormal brain development." Scientific reports **9**(1): 4662.

Oh, J., D. H. Bennett, A. M. Calafat, D. Tancredi, D. L. Roa, R. J. Schmidt, I. Hertz-Picciotto and H. M. Shin (2021). "Prenatal exposure to per- and polyfluoroalkyl substances in association with autism spectrum disorder in the MARBLES study." Environ Int **147**: 106328.

Olivito, G., S. Clausi, F. Laghi, A. M. Tedesco, R. Baiocco, C. Mastropasqua, M. Molinari, M. Cercignani, M. Bozzali and M. Leggio (2017). "Resting-State Functional Connectivity Changes Between Dentate Nucleus and Cortical Social Brain Regions in Autism Spectrum Disorders." The Cerebellum **16**(2): 283-292.

Päkkilä, F., T. Männistö, A. Pouta, A.-L. Hartikainen, A. Ruokonen, H.-M. Surcel, A. Bloigu, M. Vääräsmäki, M.-R. Järvelin and I. Moilanen (2014). "The impact of gestational thyroid hormone concentrations on ADHD symptoms of the child." The Journal of Clinical Endocrinology & Metabolism **99**(1): E1-E8.

Panesar, H. K., C. L. Kennedy, K. P. Keil Stietz and P. J. Lein (2020). "Polychlorinated Biphenyls (PCBs): Risk Factors for Autism Spectrum Disorder?" Toxics **8**(3): 70.

Patel, A., R. Smith, A. Kingsbury, A. Hunt and R. Bala (1980). "Effects of thyroid state on brain development: muscarinic acetylcholine and GABA receptors." Brain Research **198**(2): 389-402.

Patel, J., K. Landers, H. Li, R. Mortimer and K. Richard (2011). "Thyroid hormones and fetal neurological development." Journal of Endocrinology **209**(1): 1.

Patel, J., J. L. Lukkes and A. Shekhar (2018). "Overview of genetic models of autism spectrum disorders." Progress in brain research **241**: 1-36.

Pathak, A., R. A. Sinha, V. Mohan, K. Mitra and M. M. Godbole (2011). "Maternal thyroid hormone before the onset of fetal thyroid function regulates reelin and downstream signaling cascade affecting neocortical neuronal migration." Cereb Cortex **21**(1): 11-21.

Paxinos, G. and K. B. Franklin (2019). Paxinos and Franklin's the mouse brain in stereotaxic coordinates, Academic press.

Peng, J., A.-l. Sheng, Q. Xiao, L. Shen, X.-C. Ju, M. Zhang, S.-T. He, C. Wu and Z.-G. Luo (2019). "Single-cell transcriptomes reveal molecular specializations of neuronal cell types in the developing cerebellum." Journal of molecular cell biology **11**(8): 636-648.

Perri, K., L. De Mori, D. Tortora, M. G. Calevo, A. E. Allegri, F. Napoli, G. Patti, D. Fava, M. Crocco and M. Schiavone (2021). "Cognitive and white matter microstructure development in congenital hypothyroidism and familial thyroid disorders." The Journal of Clinical Endocrinology & Metabolism **106**(10): e3990-e4006.

Peter, S., M. M. Ten Brinke, J. Stedehouder, C. M. Reinelt, B. Wu, H. Zhou, K. Zhou, H.-J. Boele, S. A. Kushner and M. G. Lee (2016). "Dysfunctional cerebellar Purkinje cells contribute to autism-like behaviour in Shank2-deficient mice." Nature communications **7**(1): 12627.

Pieper, A., S. Rudolph, G. L. Wieser, T. Götze, H. Mießner, T. Yonemasu, K. Yan, I. Tzvetanova, B. D. Castillo and U. Bode (2019). "NeuroD2 controls inhibitory circuit formation in the molecular layer of the cerebellum." Scientific reports **9**(1): 1448.

Pina-Camacho, L., S. Villero, L. Boada, D. Fraguas, J. Janssen, M. Mayoral, C. Llorente, C. Arango and M. Parellada (2013). "Structural magnetic resonance imaging data do not help support DSM-5 autism spectrum disorder category." Research in Autism Spectrum Disorders **7**(2): 333-343.

Pinto, R., J. Matula, M. Gomez-Lazaro, M. Sousa, A. Lobo, T. Zikmund, J. Kaiser and J. R. Gomes (2022). "High-resolution micro-CT for 3D infarct characterization and segmentation in mice stroke models." Scientific Reports **12**(1): 17471.

Piven, J., J. Bailey, B. J. Ranson and S. Arndt (1997). "An MRI study of the corpus callosum in autism." American Journal of Psychiatry **154**(8): 1051-1056.

Pohl, A., W. R. Jones, N. Marrus, Y. Zhang, A. Klin and J. N. Constantino (2019). "Behavioral predictors of autism recurrence are genetically independent and influence social reciprocity: evidence that polygenic ASD risk is mediated by separable elements of developmental liability." Translational psychiatry **9**(1): 202.

Prekop, H.-T., A. Delogu and R. J. T. Wingate (2023). Cerebellar Developmental Disorders and Cerebellar Nuclei. Development of the Cerebellum from Molecular Aspects to Diseases. H. Marzban. Cham, Springer International Publishing**:** 91-109.

Presmanes Hill, A., K. Zuckerman and E. Fombonne (2015). "Epidemiology of autism spectrum disorders." Translational approaches to autism spectrum disorder: 13-38.

Pua, E. P. K., S. C. Bowden and M. L. Seal (2017). "Autism spectrum disorders: Neuroimaging findings from systematic reviews." Research in Autism Spectrum Disorders **34**: 28-33.

Purves, D., G. Augustine, D. Fitzpatrick, L. Katz, A. LaMantia, J. McNamara and S. Williams (2001). "Circuits within the Cerebellum." 2nd ed.

Ramadoss, P., B. J. Abraham, L. T. Tsai, Y. Zhou, R. H. Costa-e-Sousa, F. D. Ye, M. Bilban, K. Zhao and A. N. Hollenberg (2013). "Novel Mechanism of Positive versus Negative Regulation by Thyroid Hormone Receptor β1 (TRβ1) Identified by Genome-wide Profiling of Binding Sites in Mouse Liver*." The Journal of Biological Chemistry **289**: 1313 - 1328.

Ramos, T. C., J. B. Balardin, J. R. Sato and A. Fujita (2019). "Abnormal cortico-cerebellar functional connectivity in autism spectrum disorder." Frontiers in systems neuroscience **12**: 74.

Román, G. C., A. Ghassabian, J. J. Bongers-Schokking, V. W. Jaddoe, A. Hofman, Y. B. De Rijke, F. C. Verhulst and H. Tiemeier (2013). "Association of gestational maternal hypothyroxinemia and increased autism risk." Annals of neurology **74**(5): 733-742.

Rotem, R. S., G. Chodick, V. Shalev, M. Davidovitch, G. Koren, R. Hauser, B. A. Coull, E. W. Seely, V. T. Nguyen and M. G. Weisskopf (2020). "Maternal thyroid disorders and risk of autism spectrum disorder in progeny." Epidemiology **31**(3): 409-417.

Saito, S. and K. Murase (2012). "Ex vivo imaging of mouse brain using micro-CT with non-ionic iodinated contrast agent: a comparison with myelin staining." The British journal of radiology **85**(1019): e973-e978.

Samadi, A., J. Skocic and J. F. Rovet (2015). "Children born to women treated for hypothyroidism during pregnancy show abnormal corpus callosum development." Thyroid **25**(5): 494-502.

Sandin, S., P. Lichtenstein, R. Kuja-Halkola, C. Hultman, H. Larsson and A. Reichenberg (2017). "The heritability of autism spectrum disorder." Jama **318**(12): 1182-1184.

Sandin, S., P. Lichtenstein, R. Kuja-Halkola, H. Larsson, C. M. Hultman and A. Reichenberg (2014). "The familial risk of autism." Jama **311**(17): 1770-1777.

Sarachana, T., M. Xu, R.-C. Wu and V. W. Hu (2011). "Sex hormones in autism: androgens and estrogens differentially and reciprocally regulate RORA, a novel candidate gene for autism." PloS one **6**(2): e17116.

Saxena, R., M. Babadi, H. Namvarhaghighi and F. I. Roullet (2020). "Role of environmental factors and epigenetics in autism spectrum disorders." Progress in molecular biology and translational science **173**: 35-60.

Schmahmann, J. D., X. Guell, C. J. Stoodley and M. A. Halko (2019). "The theory and neuroscience of cerebellar cognition." Annual review of neuroscience **42**: 337-364.

Schmahmann, J. D. and J. C. Sherman (1998). "The cerebellar cognitive affective syndrome." Brain: a journal of neurology **121**(4): 561-579.

Seress, L. (1978). "Pyramid-like basket cells in the granular layer of the dentate gyrus in the rat." J Anat **127**(Pt 1): 163-168.

Sethi, S., K. P. Keil Stietz, A. E. Valenzuela, C. R. Klocke, J. L. Silverman, B. Puschner, I. N. Pessah and P. J. Lein (2021). "Developmental exposure to a human-relevant polychlorinated biphenyl mixture causes behavioral phenotypes that vary by

sex and genotype in juvenile mice expressing human mutations that modulate neuronal calcium." Frontiers in Neuroscience **15**: 766826.

Shahid, M. A., M. A. Ashraf and S. Sharma (2018). "Physiology, thyroid hormone."

Shen, L., X. Liu, H. Zhang, J. Lin, C. Feng and J. Iqbal (2020). "Biomarkers in autism spectrum disorders: Current progress." Clinica Chimica Acta **502**: 41-54.

Shuid, A. N., P. A. Jayusman, N. Shuid, J. Ismail, N. Kamal Nor and I. N. Mohamed (2021). "Association between viral infections and risk of autistic disorder: an overview." International journal of environmental research and public health **18**(6): 2817.

Skefos, J., C. Cummings, K. Enzer, J. Holiday, K. Weed, E. Levy, T. Yuce, T. Kemper and M. Bauman (2014). "Regional alterations in purkinje cell density in patients with autism." PloS one **9**(2): e81255.

Spisák, T., V. Román, E. Papp, R. Kedves, K. Sághy, C. K. Csölle, A. Varga, D. Gajári, G. Nyitrai and Z. Spisák (2019). "Purkinje cell number-correlated cerebrocerebellar circuit anomaly in the valproate model of autism." Scientific Reports **9**(1): 9225.

Steadman, P. E., J. Ellegood, K. U. Szulc, D. H. Turnbull, A. L. Joyner, R. M. Henkelman and J. P. Lerch (2014). "Genetic effects on cerebellar structure across mouse models of autism using a magnetic resonance imaging atlas." Autism research **7**(1): 124-137.

Stoccoro, A., E. Conti, E. Scaffei, S. Calderoni, F. Coppedè, L. Migliore and R. Battini (2023). "DNA Methylation Biomarkers for Young Children with Idiopathic Autism Spectrum Disorder: A Systematic Review." International Journal of Molecular Sciences **24**(11): 9138.

Stoccoro, A., R. Gallo, S. Calderoni, R. Cagiano, F. Muratori, L. Migliore, E. Grossi and F. Coppede (2022). "Artificial neural networks reveal sex differences in gene methylation, and connections between maternal risk factors and symptom severity in autism spectrum disorder." Epigenomics **14**(19): 1181-1195.

Stojanovska, I. (2024). "Drug discovery and development and precision medicine for Autism Spectrum Disorder–current state." Journal of Health and Rehabilitation Sciences **3**(1): 1-9.

Stoodley, C. J., A. M. D'Mello, J. Ellegood, V. Jakkamsetti, P. Liu, M. B. Nebel, J. M. Gibson, E. Kelly, F. Meng and C. A. Cano (2017). "Altered cerebellar connectivity in autism and cerebellar-mediated rescue of autism-related behaviors in mice." Nature neuroscience **20**(12): 1744-1751.

Su, L.-D., F.-X. Xu, X.-T. Wang, X.-Y. Cai and Y. Shen (2021). "Cerebellar dysfunction, cerebro-cerebellar connectivity and autism spectrum disorders." Neuroscience **462**: 320-327.

Su, Y., X. Yang, L. Yang, X. Liu, Z. She, Y. Zhang and Z. Dong (2022). "Thyroid hormones regulate reelin expression in neuropsychiatric disorders." Canadian Journal of Physiology and Pharmacology **100**(11): 1033-1044.

Sudarov, A. (2013). "Defining the Role of Cerebellar Purkinje Cells in Autism Spectrum Disorders." The Cerebellum **12**(6): 950-955.

Sudarov, A. and A. L. Joyner (2007). "Cerebellum morphogenesis: the foliation pattern is orchestrated by multi-cellular anchoring centers." Neural Development **2**(1): 26.

Swanson, D. J., Y. Tong and D. Goldowitz (2005). "Disruption of cerebellar granule cell development in the Pax6 mutant, Sey mouse." Developmental Brain Research **160**(2): 176-193.

Takeo, Y. H., W. Kakegawa, E. Miura and M. Yuzaki (2015). "RORα regulates multiple aspects of dendrite development in cerebellar Purkinje cells in vivo." Journal of Neuroscience **35**(36): 12518-12534.

Tam, W. Y., X. Wang, A. S. Cheng and K.-K. Cheung (2021). "In search of molecular markers for cerebellar neurons." International journal of molecular sciences **22**(4): 1850.

Tang, R., G. Zhang, X. Weng, Y. Han, Y. Lang, Y. Zhao, X. Zhao, K. Wang, Q. Lin and C. Wang (2016). "In vitro assessment reveals parameters-dependent modulation on excitability and functional connectivity of cerebellar slice by repetitive transcranial magnetic stimulation." Scientific Reports **6**(1): 23420.

Tarplee, M. F. and N. Corps (2008). "Acquiring optimal quality X-ray µCT scans." Appl note **1**: 93-99.

Teng, X., Y.-Y. Liu, W. Teng and G. A. Brent (2018). "COUP-TF1 modulates thyroid hormone action in an embryonic stem-cell model of cortical pyramidal neuronal differentiation." Thyroid **28**(5): 667-678.

Tremblay, S. A., C. A. Chapman and R. Courtemanche (2019). "State-dependent entrainment of prefrontal cortex local field potential activity following patterned stimulation of the cerebellar vermis." Frontiers in Systems Neuroscience **13**: 60.

Tsai, P. T., C. Hull, Y. Chu, E. Greene-Colozzi, A. R. Sadowski, J. M. Leech, J. Steinberg, J. N. Crawley, W. G. Regehr and M. Sahin (2012). "Autistic-like behaviour and cerebellar dysfunction in Purkinje cell Tsc1 mutant mice." Nature **488**(7413): 647-651.

Umeda, T., N. Takashima, R. Nakagawa, M. Maekawa, S. Ikegami, T. Yoshikawa, K. Kobayashi, K. Okanoya, K. Inokuchi and N. Osumi (2010). "Evaluation of Pax6 mutant rat as a model for autism." PLoS One **5**(12): e15500.

van Essen, M. J., S. Nayler, E. B. Becker and J. Jacob (2020). "Deconstructing cerebellar development cell by cell." PLoS Genetics **16**(4): e1008630.

Villa, C., R. Combi, D. Conconi and M. Lavitrano (2021). "Patient-derived induced pluripotent stem cells (iPSCs) and cerebral organoids for drug screening and development in autism spectrum disorder: opportunities and challenges." Pharmaceutics **13**(2): 280.

Vitalis, T. and J. Mariani (2018). "Retinoid receptor-related orphan receptor alpha: a key gene setting brain circuits." Neural Regen Res **13**(5): 791-794.

Vitalis, T. and J. Mariani (2018). "Retinoid receptor-related orphan receptor alpha: a key gene setting brain circuits." Neural Regeneration Research **13**(5): 791.

Voogd, J. and M. Glickstein (1998). "The anatomy of the cerebellum." Trends in cognitive sciences **2**(9): 307-313.

Wang, S. S.-H., A. D. Kloth and A. Badura (2014). "The cerebellum, sensitive periods, and autism." Neuron **83**(3): 518-532.

Wang, V. Y., M. F. Rose and H. Y. Zoghbi (2005). "Math1 expression redefines the rhombic lip derivatives and reveals novel lineages within the brainstem and cerebellum." Neuron **48**(1): 31-43.

Wang, Y., Y. Wang, J. Dong, W. Wei, B. Song, H. Min, Y. Yu, X. Lei, M. Zhao and W. Teng (2014). "Developmental hypothyroxinemia and hypothyroidism reduce proliferation of cerebellar granule neuron precursors in rat offspring by downregulation of the sonic hedgehog signaling pathway." Molecular neurobiology **49**: 1143-1152.

Waterhouse, L., E. London and C. Gillberg (2016). "ASD validity." Review Journal of Autism and Developmental Disorders **3**: 302-329.

Watson, T. C., N. Becker, R. Apps and M. W. Jones (2014). "Back to front: cerebellar connections and interactions with the prefrontal cortex." Frontiers in systems neuroscience **8**: 4.

Waye, M. M. and H. Y. Cheng (2018). "Genetics and epigenetics of autism: A Review." Psychiatry and clinical neurosciences **72**(4): 228-244.

Wegiel, J., M. Flory, I. Kuchna, K. Nowicki, S. Y. Ma, H. Imaki, J. Wegiel, I. L. Cohen, E. London and T. Wisniewski (2014). "Stereological study of the neuronal number and volume of 38 brain subdivisions of subjects diagnosed with autism reveals significant alterations restricted to the striatum, amygdala and cerebellum." Acta neuropathologica communications **2**(1): 1-18.

Wegiel, J., I. Kuchna, K. Nowicki, H. Imaki, J. Wegiel, S. Y. Ma, E. C. Azmitia, P. Banerjee, M. Flory, I. L. Cohen, E. London, W. T. Brown, C. Komich Hare and T. Wisniewski (2013). "Contribution of olivofloccular circuitry developmental defects to atypical gaze in autism." Brain Res **1512**: 106-122.

Westerhuis, J., J. Dudink, C. I. De Zeeuw and C. B. Canto (2023). "Critical Periods and Vulnerability of Cerebellar Development in Human and Rodent."

Williams, G. R. (2008). "Neurodevelopmental and neurophysiological actions of thyroid hormone." Journal of neuroendocrinology **20**(6): 784-794.

Wilson, L. J. and R. J. Wingate (2006). "Temporal identity transition in the avian cerebellar rhombic lip." Developmental biology **297**(2): 508-521.

Wu, S., F. Wu, Y. Ding, J. Hou, J. Bi and Z. Zhang (2017). "Advanced parental age and autism risk in children: a systematic review and meta-analysis." Acta Psychiatrica Scandinavica **135**(1): 29-41.

Yajima, H., I. Amano, S. Ishii, T. Sadakata, W. Miyazaki, Y. Takatsuru and N. Koibuchi (2021). "Absence of thyroid hormone induced delayed dendritic arborization in mouse primary hippocampal neurons through insufficient expression of brain-derived neurotrophic factor." Frontiers in Endocrinology **12**: 629100.

Yamashiro, K., K. Hori, E. S. K. Lai, R. Aoki, K. Shimaoka, N. Arimura, S. F. Egusa, A. Sakamoto, M. Abe, K. Sakimura, T. Watanabe, N. Uesaka, M. Kano and M. Hoshino (2020). "AUTS2 Governs Cerebellar Development, Purkinje Cell Maturation, Motor Function and Social Communication." iScience **23**(12).

Yeung, J., T. J. Ha, D. J. Swanson and D. Goldowitz (2016). "A novel and multivalent role of Pax6 in cerebellar development." Journal of Neuroscience **36**(35): 9057-9069.

Ypsilanti, A. R. and J. L. Rubenstein (2016). "Transcriptional and epigenetic mechanisms of early cortical development: An examination of how Pax6 coordinates cortical development." J Comp Neurol **524**(3): 609-629.

Yu, L., T. Iwasaki, M. Xu, R. Lesmana, Y. Xiong, N. Shimokawa, W. W. Chin and N. Koibuchi (2015). "Aberrant cerebellar development of transgenic mice expressing dominant-negative thyroid hormone receptor in cerebellar Purkinje cells." Endocrinology **156**(4): 1565-1576.

Zaqout, S., L.-L. Becker and A. M. Kaindl (2020). "Immunofluorescence staining of paraffin sections step by step." Frontiers in Neuroanatomy **14**: 83.

Zaslavsky, K., W.-B. Zhang, F. P. McCready, D. C. Rodrigues, E. Deneault, C. Loo, M. Zhao, P. J. Ross, J. El Hajjar and A. Romm (2019). "SHANK2 mutations associated with autism spectrum disorder cause hyperconnectivity of human neurons." Nature neuroscience **22**(4): 556-564.

Zerbi, V., M. Pagani, M. Markicevic, M. Matteoli, D. Pozzi, M. Fagiolini, Y. Bozzi, A. Galbusera, M. L. Scattoni, G. Provenzano, A. Banerjee, F. Helmchen, M. A. Basson, J. Ellegood, J. P. Lerch, M. Rudin, A. Gozzi and N. Wenderoth (2021). "Brain mapping across 16 autism mouse models reveals a spectrum of functional connectivity subtypes." Molecular Psychiatry **26**(12): 7610-7620.

Zhang, X. Y., J. J. Wang and J. N. Zhu (2016). "Cerebellar fastigial nucleus: from anatomic construction to physiological functions." Cerebellum Ataxias **3**: 9.

Zhubi, A., Y. Chen, E. Dong, E. H. Cook, A. Guidotti and D. R. Grayson (2014). "Increased binding of MeCP2 to the GAD1 and RELN promoters may be mediated by an enrichment of 5-hmC in autism spectrum disorder (ASD) cerebellum." Translational Psychiatry **4**(1): e349-e349.

Zoeller, R. T., S. W. Tan and R. W. Tyl (2007). "General background on the hypothalamic-pituitary-thyroid (HPT) axis." Critical reviews in toxicology **37**(1-2): 11-53.

Chapter 8: Supplementary Material

Table S.1 P56 Mouse cohort assessed prior to experimentation.

Mouse ID	Sex	Treatment	Brain Weight(mg)
MP2-1-M	Male	Control	x
MP19-2-M (2)	Male	Control	367.8
MP9-2-M	Male	Control	x
MP2-3-M (10th March 2017)	Male	Control	262.2
MP14-2-M (3rd April 2017)	Male	Control	357
MP13-4-M (29th April 2017)	Male	Control	341.33
MP13-5-M (23rd May 2017)	Male	Control	x
MP16-1-M (23rd May 2017)	Male	Control	348.7
MP 13-1 (26th June 2017)	Male	Control	353.8
MP 11-2 (26th June 2017)	Male	Control	326
MP7-1 (3/10/2017)	Male	Control	394.6
MP20-2-M	Male	MMI 14	x
MP6-1-M (10th March 2017)	Male	MMI 14	270
MP1-M (3rd April 2017)	Male	MMI 14	319.4
MP12-1-M (29th April 2017)	Male	MMI 14	338
MP5-2-M (5th May 2017)	Male	MMI 14	298.4
MP17-2-M (23rd May 2017)	Male	MMI 14	348.7
MP20-1 (26th June 2017)	Male	MMI 14	341.6
MP 6-3 (26th June 2017)	Male	MMI 14	341.7
MP 5 2 (4th July 2017)	Male	MMI 14	323.2
MP 2-2 (19th July 2017)	Male	MMI 14	345.5
MP18_L (21/9/2017)	Male	MMI 14	376.4

MP5_2 (23/9/2017)	Male	MMI 14	323.2
MP17-2 (3/10/2017)	Male	MMI 14	348.7
MP9-2-F	Female	Control	x
MP9-4-F (10th March 2017)	Female	Control	324.8
MP14-2-F (3rd April 2017)	Female	Control	354.5
MP9-2-F (29th April 2017)	Female	Control	351.5
MP9-5-F (5th May 2017)	Female	Control	344.3
MP9-3-F (23rd May 2017)	Female	Control	353.1
MP4-1 (26th June 2017)	Female	Control	400
MP 13-4 12th July 2017	Female	Control	371.4
MP13_LF (19th July 2017)	Female	Control	371.4
MP16-1 (2/10/2017)	Female	Control	396.9
MP16-2 (3/10/2017)	Female	Control	408.3
MP11-1 (11/10/2017)	Female	Control	389.6
MP1-1-F	Female	MMI 14	x
MP12-2-F (10th March 2017)	Female	MMI 14	306.7
MP6-2-F (3rd April 2017)	Female	MMI 14	340.2
MP20-1-F (29th April 2017)	Female	MMI 14	403
MP5-4-F (5th May 2017)	Female	MMI 14	321
MP18-1-F (23rd May 2017)	Female	MMI 14	371.3
MP 20-2 (26th June 2017)	Female	MMI 14	391.8
MP5_1 (21/9/2017)	Female	MMI 14	355.6
MP5_3(21/9/17)	Female	MMI 14	339.8
MP1-2 (3/10/2017	Female	MMI 14	442.5

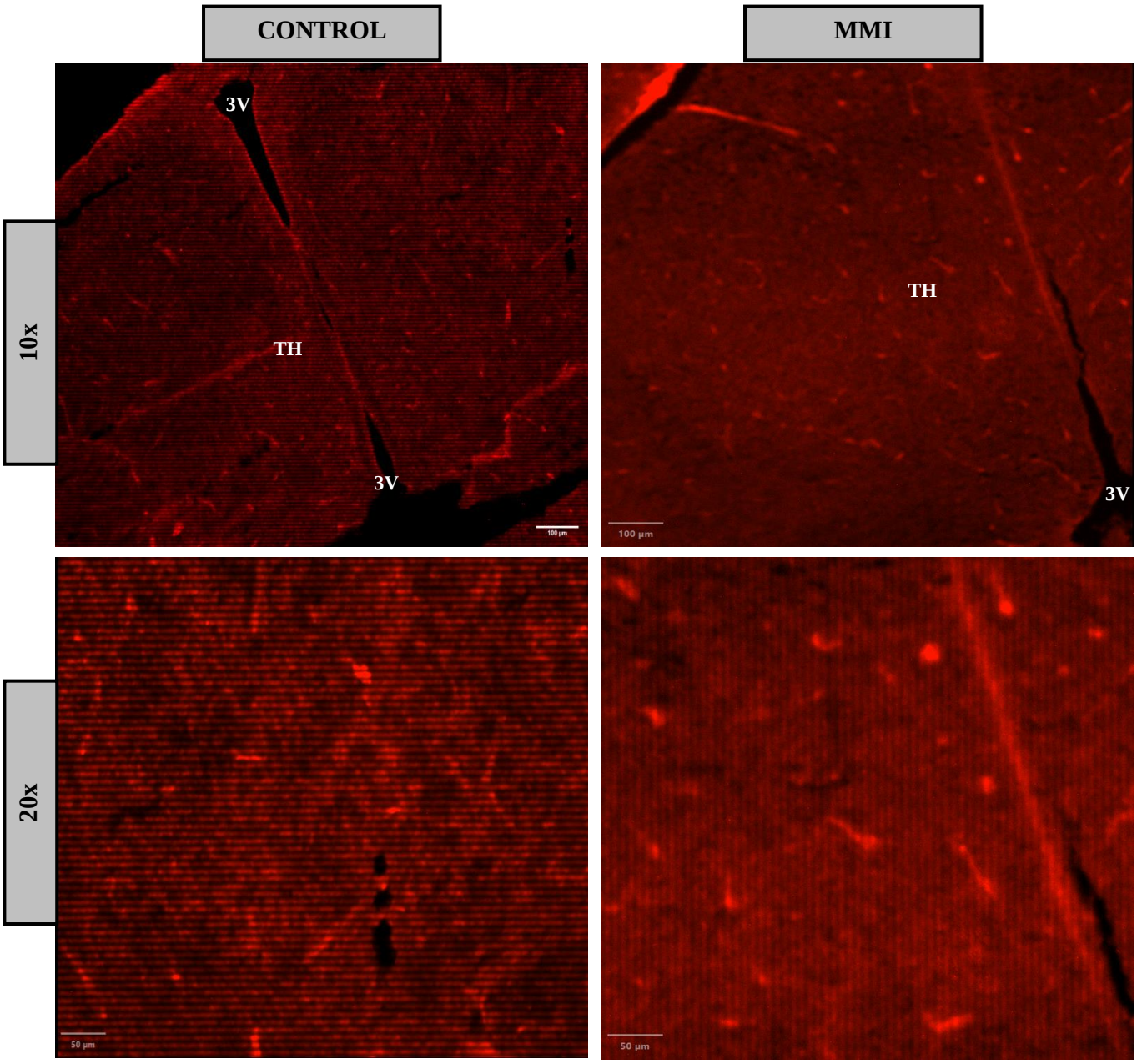

Supplemental Figure 1 RoRα staining in the E16.5 Thalamus. image exhibits the representative staining pattern of RoRα the thalamus for both the Control and Methimazole MMI groups *N* = 1 *n* = 3. Scale bars are provided, indicating a length of 100 µm.

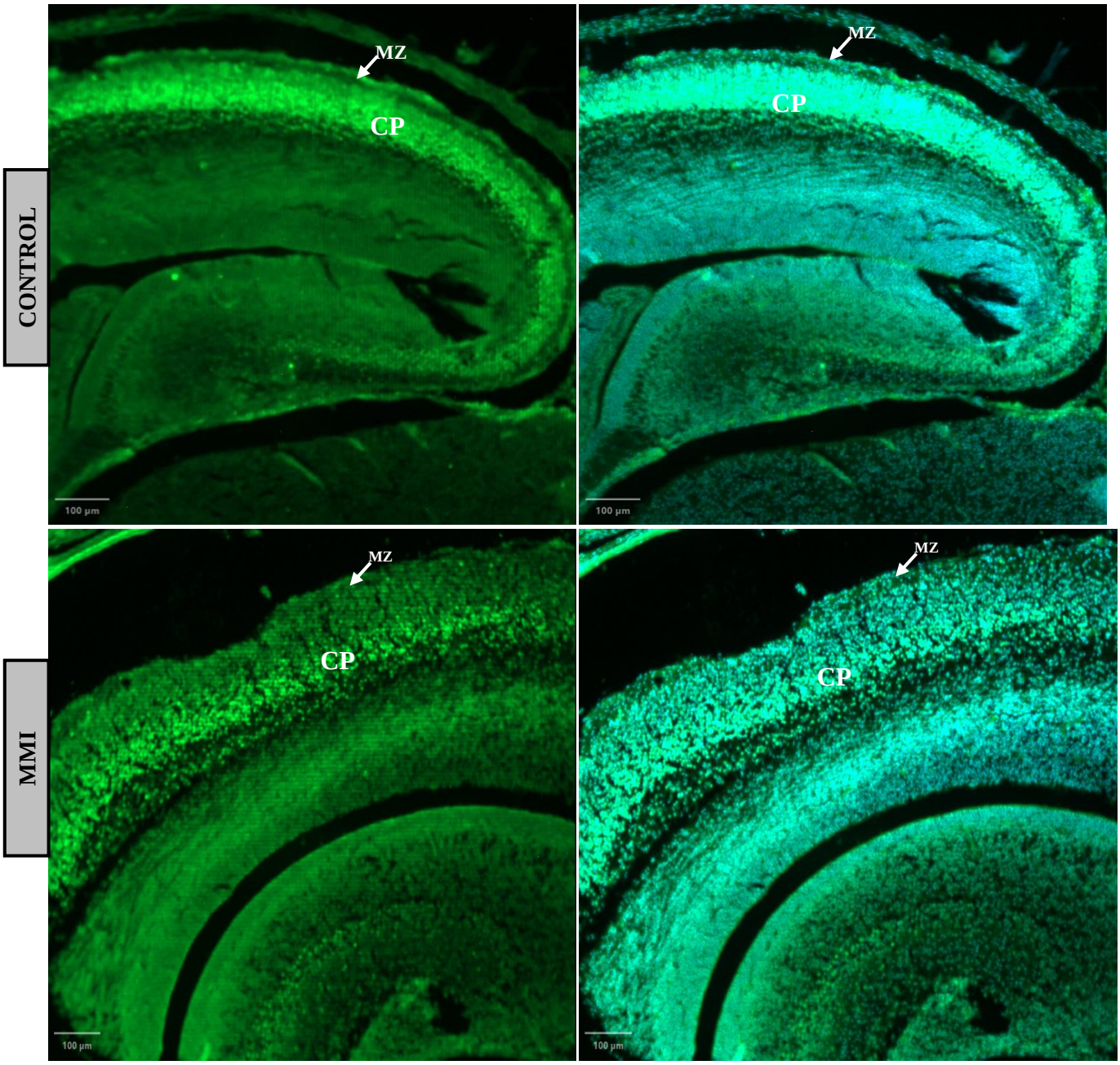

Supplemental Figure 2 TBR1 staining in the embryonic telencephalon The image exhibits the representative staining pattern of TBR1 in the Telecephalon of E16.5 mouse brain for both the Control and Methimazole MMI groups $N = 2$ $n = 3$. Scale bars are provided, indicating a length of 100 µm. Abbreviations: MZ: Marginal Zone ,

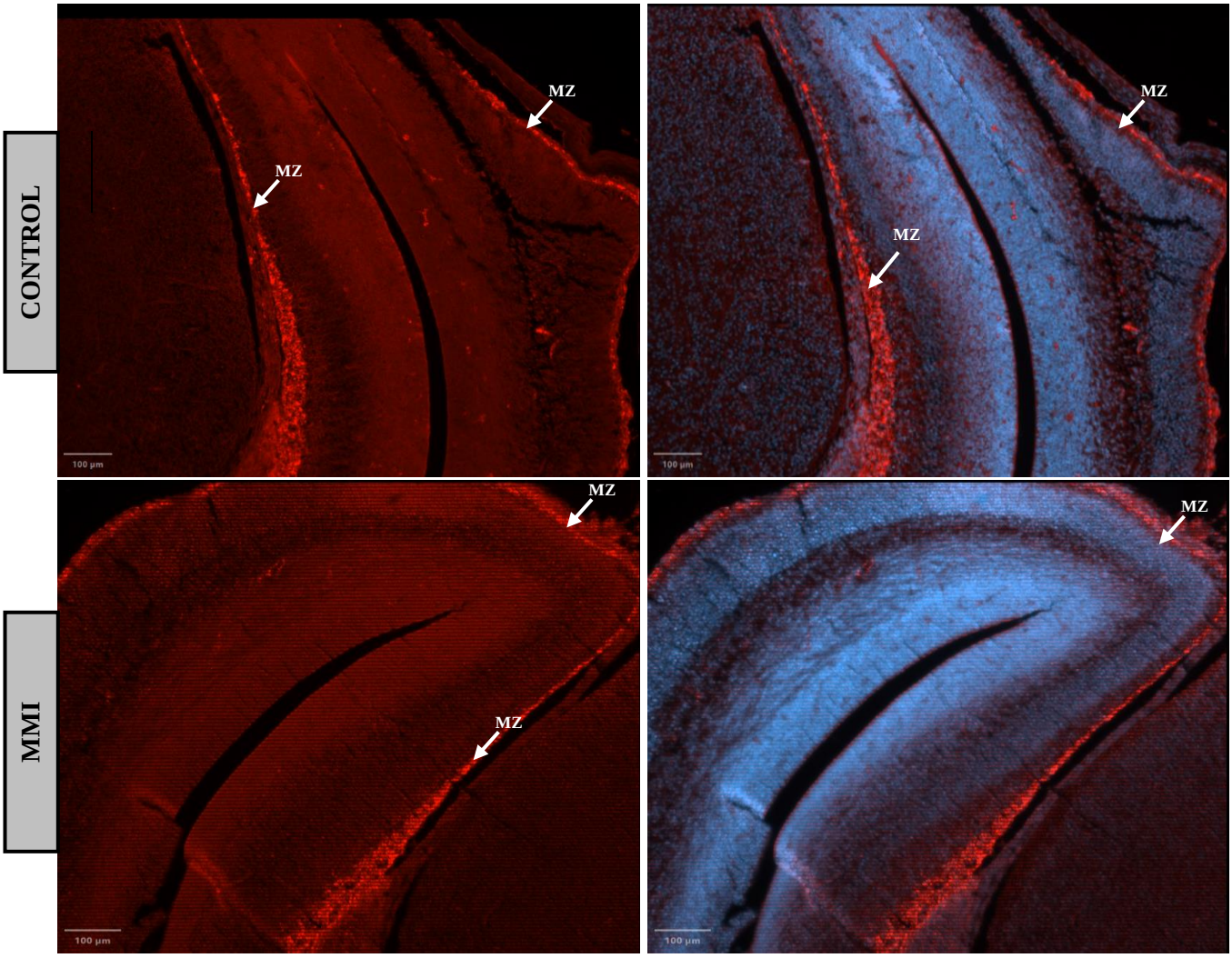

Supplemental Figure 3 **RELN staining in the embryonic telencephalon** Above: Section position represented i.The image exhibits the representative staining pattern of RELN staining in the MZ of the Telecephalon of E16.5 mouse brain for both the Control and Methimazole MMI groups *N* = 2 *n* = 3. Scale bars are provided, indicating a length of 100 µm.